Net Exchanges of carbon dioxide, methane, and nitrous oxide between Terrestrial Ecosystems and the Atmosphere in Tropical Asia during 1901–2010

by

Kamaljit Banger

A dissertation submitted to the Graduate Faculty of
Auburn University
in partial fulfillment of the
requirements for the Degree of
Doctor of Philosophy

Auburn, Alabama
August 1, 2015

Key words: Global Changes, Wildfire, Carbon fluxes,
Terrestrial ecosystem, process-based model, fire emissions

To be approved by
Hanqin Tian, Chair, Solon Dixon Professor of School of Forestry and Wildlife Sciences
Yucheng Feng, Professor Agronomy and Soils
Latif Kalin, Professor of School of Forestry and Wildlife Sciences
Graeme Lockaby, Professor, School of Forestry & Wildlife Sciences

Abstract

Terrestrial ecosystems act as important sources of the greenhouse gases (GHGs) such as carbon dioxide (CO_2), methane (CH_4), and nitrous oxide (N_2O), which cause climate warming. Therefore, understanding and quantification of the GHGs emissions has become an urgent task for accurately predicting climate change. Across the globe, several GHGs emission sources are well understood in North America, Europe, and China. However the magnitude and driving factors of GHGs emissions are uncertain in tropical Asia due to several constraints such as lack of reliable land cover and land use (LCLUC) datasets (Banger et al., 2013). Unlike temperate, tropical ecosystems are limited by phosphorus (P); however the C-N-P coupling mechanism is often lacking in the ecosystem models (Yang et al., 2014; Goll et al., 2012), producing uncertainties in GHGs emissions estimates.

In this study, I generated the new LCLUC datasets by combining high resolution remote sensing from Indian satellite (Resourcesat-1; 56-m resolution) with multiple inventory archives existing in India (covers 40% area of tropical Asia) during 1880–2010. Our newly developed LCLUC datasets in India were integrated with existing land use datasets at 0.25 degree resolution for other regions in the tropical Asia. In the second step, I have coupled the P cycle with carbon and nitrogen cycles in the DLEM modeling framework and applied it in conjunction with a series of spatial dataset including climate variability, atmospheric carbon dioxide (CO_2) concentration,

atmospheric nitrogen deposition (NDEP), and land cover and land use change (LCLUC), to quantify the GHGs emissions over the tropical Asia during 1901–2010.

The DLEM simulations results have shown that tropical Asia was a net carbon source (13±12 Tg C $year^{-1}$), with South Asia was a net source (61±7Tg C $year^{-1}$) while South-East Asia being a net sink (47±9 Tg C $year^{-1}$) during 1901–2010. Net carbon uptake showed significant increasing trend due to stimulation of plant growth by elevated CO_2 concentration, atmospheric nitrogen deposition (NDEP), and cropland management practices, and tropical Asia became a net carbon sink after 1950s. Among the factors, P limitation was the reduced carbon sink by 430±130 Tg C $year^{-1}$, while the effects of P limitation in reducing carbon uptake was 3-5 folds greater in the South-East Asia than South Asia.

Over the study period, CH_4 and N_2O emissions, with significant increasing trends ($p<0.001$), and ranged 20.4± 3.6 Tg C $year^{-1}$ and 0.70 ±0.09 Tg N $year^{-1}$, respectively. LCLUC was the dominant factor in stimulating CH_4 (8.7 TgC $year^{-1}$) and N_2O (0.29 TgC $year^{-1}$) emissions due to cropland expansion and increase in the nitrogen fertilizer use in tropical Asia. Interestingly, elevated CO_2 concentration has stimulated CH_4 (2.9 TgC $year^{-1}$) by increasing plant growth, which however has decreased N_2O (0.05TgN $year^{-1}$) emissions due to progressive nitrogen limitation. By accounting the effects of three GHGs (CO_2, CH_4, and N_2O) together, terrestrial ecosystems of tropical Asia have provided significant warming feedbacks (1063 ± 43Tg CO_2 equivalents $year^{-1}$) to global climate. Though net carbon uptake has increased, global warming potential (GWP) remained similar (*p<0.82*) due to stimulation of CH_4 and N_2O emissions, thereby

suggesting that benefits from increase in the carbon uptake were offset by stimulation of CH_4 and N_2O emissions during the study period.

This study has generated new LCLUC datasets for India, improved an ecosystem model for P limitation, and provides useful and valuable information to both scientific community and policy makers such as magnitude, spatiotemporal and underlying mechanisms of GHGs emissions in the tropical Asia.

Acknowledgements

My gratitude goes to Dr. Hanqin Tian, the chair of my Supervisory Committee, for his intellectual guidance, consistent support, and endless efforts to accomplish this project. His insightful visions for the academic research guided me and inspired me to pursue my lifelong dream to become a great scientist. I would sincerely appreciate all support from my advisory committee: Drs. Yucheng Feng, Latif Kalin, and Graeme Lockaby. I would like to thank Drs. Shufen Pan and Kelley Alley for providing critical review on my research work.

My gratitude goes to Drs. Wei Ren, Tao Bo, Chaoqun Lu, and Qichun Yang, who helped me on both research work and daily life. I thank Jia Yang, Bowen Zhang, Shree Sharma for helping me with programing during the course of my studies. My special gratitude goes to Audrey Grindle and Patti Staudenmaier for helping me with the administrative works.

I am deeply grateful to my mother, sister, my brother and his wife, who have been constantly supporting me for all the time. My wife, Aparna remained the source of happiness in my life; I enjoy their love and express my love all the way to the end.

Thanks to all who love me and care about me, and I shall dedicate this dissertation to them.

Table of Contents

List of Tables

List of Figures

List of Abbreviations

DES	Department of Economics & Statistics
C	Carbon
CH_4	Methane
CO_2	Carbon dioxide
DLEM	Dynamic Land Ecosystem Model
DOC	Dissolved Organic Carbon
FAO	Food and Agriculture Organization
GPP	Gross Primary Productivity
HYDE	History Database of the Global Environment
N	Nitrogen
N_2O	Nitrous oxide
NOAA	National Oceanic and Atmospheric Administration
NPP	Net Primary Productivity
O3	Ozone
PFT	Plant Function Type
P	Phosphorus
SOC	Soil Organic Carbon

Chapter 1. Introduction

The unprecedented increase in the atmospheric concentrations of greenhouse gases (GHGs) such as carbon dioxide (CO_2), methane (CH_4), and nitrous oxide (N_2O) are major drivers of climate warming (Forster et al., 2007). Among three GHGs, CO_2 is primarily emitted from fossil fuel burning and land use changes which contributes to 65% of the anthropogenic global warming effect. Though ambient concentrations of CH_4 and N_2O are much lower than CO_2; however contribute to one quarter of global warming due to 25–298 times higher global warming potential (GWP) than CO_2 at a 100-year time horizon. Terrestrial ecosystems can act as either sources or sinks of the GHGs, which vary significantly across different regions (Heimann and Reichstein, 2008; Tian et al., 2013; Peylin et al., 2013). In the past several decades, CO_2 flux estimation was the focus for ecosystem studies; however fewer have been made to quantify CH_4 and N_2O emissions along with CO_2 emissions (Rigby et al., 2008; Forster et al., 2007; Potter, 1996; Ridgwell et al., 1999; Chapuis-Lardy et al., 2007; Xu et al., 2008). Quantification of three GHGs emissions together from terrestrial ecosystems not only provide net cooling or warming feedbacks to climate changes but also will help to understand interactions between the global climate change, human activities, and ecosystem sustainability (Tian et al., 2014; Tian et al., 2011a).

The source or sink strength for GHGs emissions by terrestrial ecosystems is controlled by multiple complex biogeochemical processes. Firstly, plants convert atmospheric CO_2 into biological carbon via photosynthesis process and net amount of carbon captured by plants per unit space and time is known as net primary productivity (NPP). In the second step, terrestrial NPP act as a carbon source for soil biota, where it

undergoes several physical fragmentations and microbial transformations and becomes a part of soil organic carbon (SOC) with a turnover time of several hundreds to thousands of years. In aerobic conditions, SOC is decomposed by soil microorganisms, which is released as CO_2 into atmosphere. In the anaerobic conditions, group of fermentative and Methanogenic archaea convert a fraction of the SOC into CH_4. In terrestrial ecosystems, carbon transformations are interlinked to nutrient cycles (nitrogen and phosphorus) depending upon nutrient stoichiometric ratios (Yang et al., 2014). The production of N_2O is from the nitrification and denitrification processes occurring in the soils.

Several factors can alter GHGs emissions in terrestrial ecosystems such as elevated atmospheric CO_2 concentration (Bala et al., 2013; Hutchin et al., 1995), tropospheric ozone (O_3) pollution (Morsky et al., 2008), climate change (Goldberg and Gebauer, 2009), atmospheric nitrogen deposition (NDEP), and nitrogen fertilizer input (Ding et al., 2004), as well as land cover and land use change (Willison et al., 1995; Huang et al., 2010). These environmental factors will vary both in time and space thereby suggesting the need to quantify GHGs emission estimations using reliable regional datasets.

Tropical Asia, including South and Southeast Asia, plays a critical role in the global GHGs budgets (Richards and Flint, 1994; Tian et al., 2003; Tao et al., 2013; Houghton, 2002). South Asia, which includes the countries of Afghanistan, Bangladesh, Bhutan, India, Nepal, Sri Lanka, and Pakistan while Southeast Asia covers the countries of Brunei, Burma, Indonesia, Cambodia, Laos, Malaysia, the Philippines, Thailand, and Vietnam (Figure 1.1). Currently, tropical Asia is a home to one fourth of the global

human population, which coupled with economic growth, has resulted in unprecedented land use and other environmental changes in the 20th century (Tao et al., 2013). Across the globe, tropical Asia has experienced the highest deforestation (Millennium Ecosystem Assessment, 2005) and cropland expansion (Tao et al., 2013; Richards and Flint, 1994) following government policies to achieve food sufficiency for growing population. Though, effects of different environmental factors on GHGs emissions are comparatively well-understood in North America (Xu et al., 2012) and China (Ren et al., 2012; Tian et al., 2011b), relatively few attempts have been made to understand magnitude and driving factors of GHGs emissions in tropical Asia. In tropical Asia, India is the biggest country (cover approximately 40% of tropical Asia) with more than 1.2 billion people, where climatic extremes can not only alter the carbon source or sink strength (Nayak et al., 2015) but also may raise the food security concerns (Lobell et al., 2012; DES, 2010). In addition to climate change, air pollution such as tropospheric ozone (O_3) reduces plant growth (Ghude et al., 2014) which can affect carbon cycle in India (Banger et al., 2015).

There are two major constraints in accurately quantifying the terrestrial the GHGs budgets in the tropical Asia. For example, reliable environmental driver datasets is not available for a long time period which could be used in ecosystem models (Banger et al., 2013). The second modeling constraint is the scarcity of lack of modeling framework capable of simulating three GHGs from terrestrial ecosystems. Large scale ecosystem models often ignore phosphorus limitation in the modeling framework. Unlike temperate regions, phosphorus is the dominant limiting factors in the tropical ecosystems (Zhu et

al., 2015), which could produce significant uncertainties in the GHGs estimations (Yang et al., 2014).

Here, I designed a study to improve the existing environmental factors datasets as well as to use the drivers in a process-based model (Dynamic Land Ecosystem Model) to quantify the magnitude and driving factors for GHGs emissions in tropical Asia during 1901–2010. To improve modeling structure, I have incorporated the phosphorus cycle with carbon and nitrogen cycles. This study was conducted to address the following four interlinked questions:

1) To construct the land cover and land use, nitrogen fertilizer, and irrigation datasets at high resolution (5-arc minutes) in India and to integrate newly developed datasets in India with tropical Asia datasets
2) Using newly developed datasets, to quantify how multiple environmental factors have altered SOC and terrestrial NPP in India?
3) To quantify how much CO_2, CH_4 and N_2O were released or uptake by the terrestrial ecosystems over the tropical Asia during 1901–2010?
4) To determine uncertainties in the GHGs emissions estimates associated with phosphorus limitation in tropical Asia

To answer the four questions above, I conducted this study and addressed them one by one (Figure 1.2). In sequence, I prepared the input data for model simulations at 0.25 degree resolution for tropical Asia; then the model parameterization was conducted to determine the values of each parameter for model simulations; the simulations were set up by using the enhanced model and calibrated parameters, in conjunction with the consistent model driving data; the magnitude, spatial and temporal variations in

terrestrial CO_2, CH_4 and N_2O fluxes over the tropical Asia were examined; combining single factor simulations with all combined simulation, I attributed the spatiotemporal variations in terrestrial CO_2, CH_4 and N_2O fluxes to multiple global change factors including climate variability, elevated atmospheric CO_2, NDEP, O_3 pollution, land conversion, and nitrogen fertilizer application.

Therefore, this dissertation is formed under the following framework: chapter 1, introduces the basic scientific questions and significance of this study as examining the terrestrial fluxes of CO_2, CH_4 and N_2O emissions in tropical Asia; chapter 2 describes the modeling framework of the DLEM and provides validations of simulated results with field observations; chapter 3 discusses the development of the high resolution (5-arc minutes) LCLUC, cropping systems, and nitrogen fertilizer datasets for India and tropical Asia; chapter 4 focused on multiple environmental changes effects on the terrestrial net primary productivity in India; chapter 5 provides the magnitude, spatial and temporal pattern of soil organic carbon at 5-arc minutes in India; chapter 6 discusses the magnitude, spatial and temporal pattern of CO_2, CH_4 and N_2O emissions from terrestrial ecosystems at 0.25 degree resolution in tropical Asia; chapter 7 discusses uncertainties associated with input datasets, parameter estimations, and modeling frameworks; and finally chapter 8 provides a summary of the entire work, and concludes the major findings through this study.

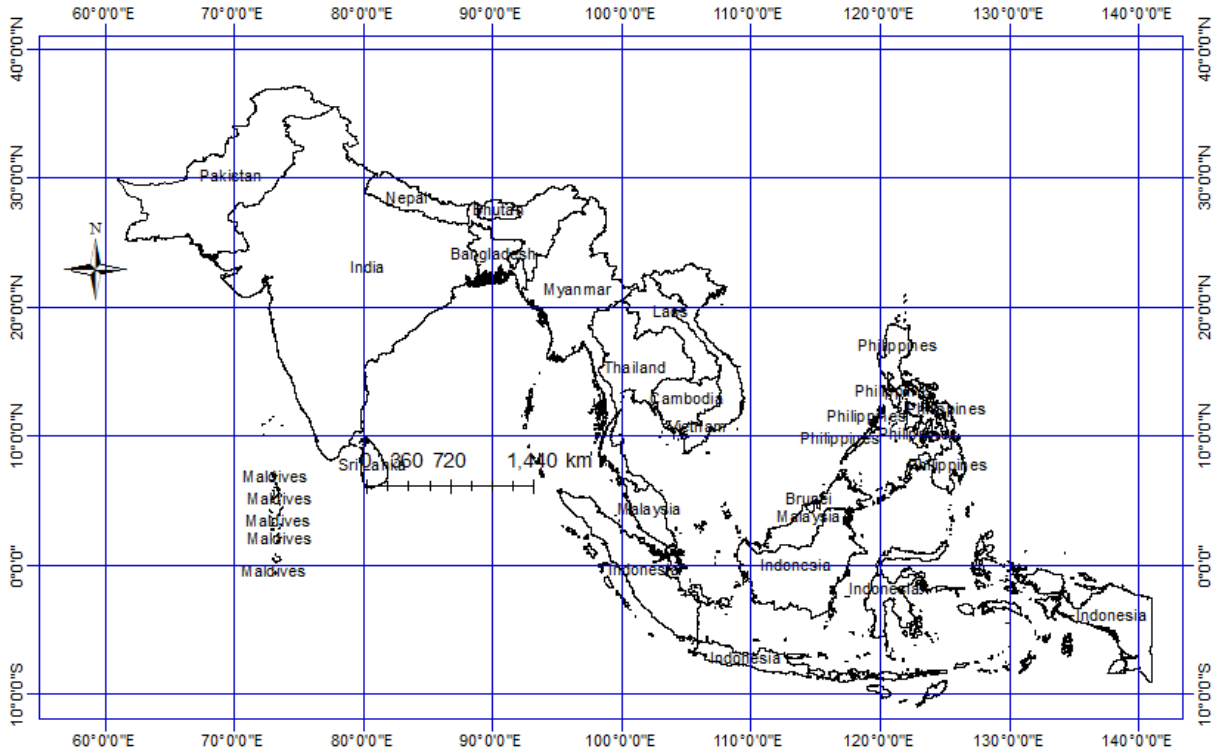

Figure 1.1. Map of South and South East Asia.

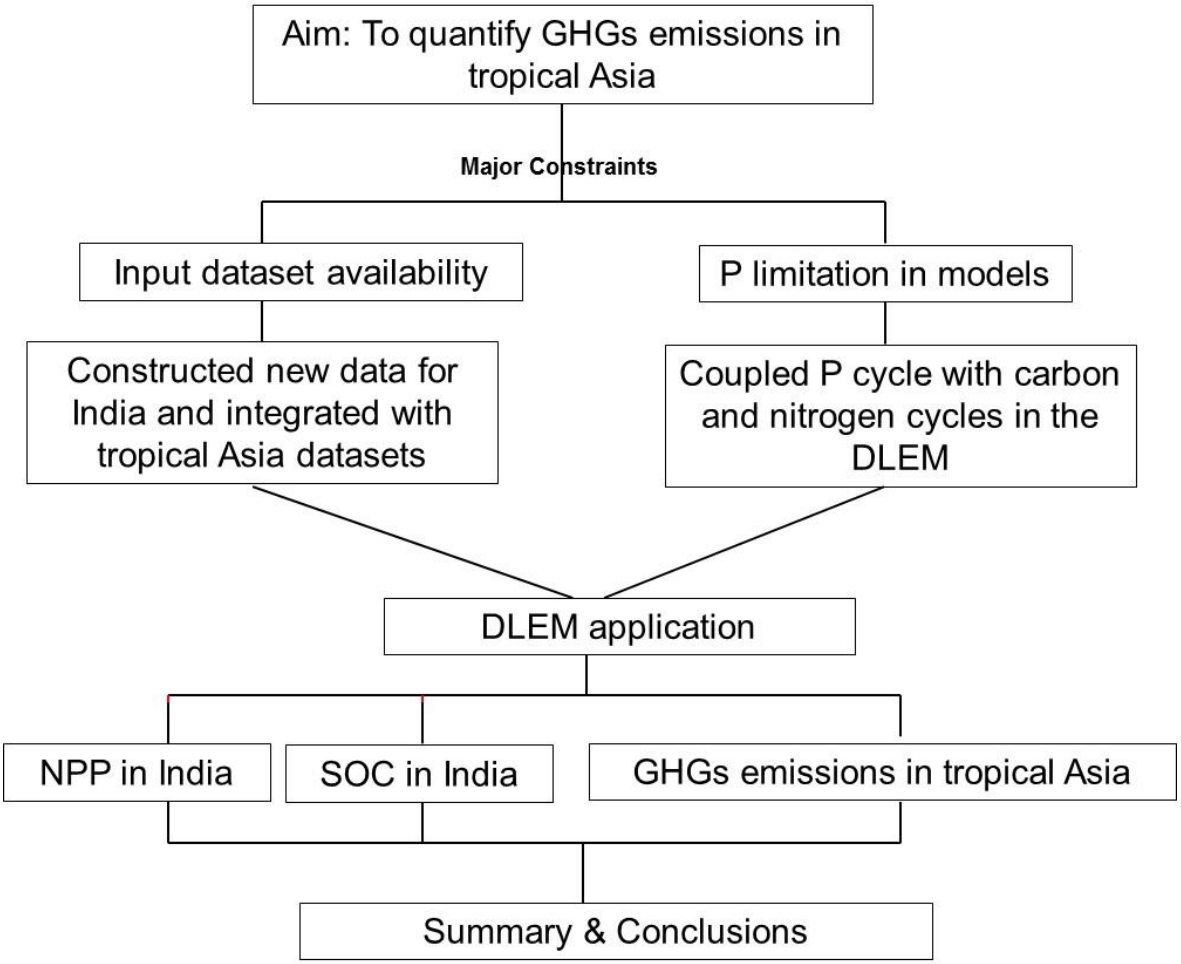

Figure 1.2. Research Plan.

Chapter 2. Description of the Dynamic Land Ecosystem Model, and Model Validations against Field Studies

Abstract

The Dynamic Land Ecosystem Model (DLEM) is a process-based model that simulates daily carbon, water, and nitrogen fluxes as affected by multiple environmental factors including climate, atmospheric compositions (concentrations of CO_2, tropospheric O_3), atmospheric nitrogen deposition (NDEP), and land cover and land use change (LCLUC; land conversions, nitrogen fertilizer, and irrigation management). Here, we provided the framework of the DLEM. To examine model behavior and analyze the potential uncertainties in this study, in this chapter we present the model validation at field scale, comparison of model results with MODIS, and discussed uncertainties in this study. The simulations suggest that the DLEM has ability to capture the field terrestrial net primary productivity (NPP), soil organic carbon (SOC), methane (CH_4), and nitrous oxide (N_2O) emissions. In addition, we have validated the different carbon, nitrogen, and phosphorus (P) stoichiometric ratios in the foliar and litter pools.

2.1 Concept of the Dynamic Land Ecosystem Model

The DLEM is a highly integrated, process-based model that simulates daily carbon, water, and nitrogen as affected by multiple environmental factors including climate, atmospheric compositions (concentrations of CO_2, tropospheric O_3), NDEP, and LCLUC (which includes land conversions, nitrogen fertilizer, and irrigation management). In brief, the DLEM includes five core components including biophysics, plant physiology, soil biogeochemistry, dynamic vegetation, and LCLUC (Figure 2.1). The biophysical component includes the instantaneous exchanges of energy, water,

and momentum between plants and the atmosphere. The plant physiology component in the DLEM simulates major physiological processes such as photosynthesis, respiration, carbohydrate allocation among various organs (root, stem and leaf), nitrogen uptake, transpiration, phenology, etc. The soil biogeochemistry simulates processes such as mineralization, nitrification/denitrification, decomposition, and fermentation.

In the DLEM, carbon balance of vegetation is determined by the photosynthesis, autotrophic respiration, litterfall (related to tissue turnover rate and leaf phenology), and plant mortality rate. Plants assimilate carbon by photosynthesis, and use this carbon to compensate for the carbon loss through maintenance respiration, tissue turnover, and reproduction. The photosynthesis module of the DLEM estimates the net carbon assimilation rate, leaf daytime maintenance respiration rate, and gross primary productivity (GPP, unit: g C/m2/day). The photosynthesis rate is first calculated on the leaf level. The results are then multiplied by leaf area index to scale up to canopy level. Photosynthesis is the first process by which most carbon and chemical energy enter ecosystems so it has critical impacts on ecosystem production. We used a modified Farquar's model (Farquhar et al., 1980) to simulate GPP (g C m^{-2} day^{-1}), which is calculated by scaling leaf assimilation rates (μmol CO_2 m^{-2} s^{-1}) up to the whole canopy. The canopy is divided into sunlit and shaded layers.

$$GPP_a = GPP_o \, f(PAR) \, f(T) \, f(P) \, f(CO_2) \, f(O_3) \, f(N) \, f(VegT)$$

where GPP_a is the actual GPP derived from the potential GPP (GPP_o) under optimized conditions adjusted by environmental factor scalars that directly or indirectly influence carbon assimilation and allocation, including photosynthetic active radiation

f(PAR), climate variability/change including temperature *f*(T) and precipitation *f*(P), atmospheric carbon dioxide *f*(CO_2), tropospheric ozone *f*(O_3), nitrogen availability *f*(N) related to atmospheric nitrogen deposition and nitrogen fertilizer application, and vegetation types *f*(VegT) controlled by LCLUC. R_A in DLEM represents total respirations of growth (construction) (Rg) and maintenance (Rm). We assume that 25% of assimilated carbon is used as Rg while Rm is a metabolic photosynthate- consuming process for maintaining existing biomass and related to nitrogen content and temperature and growth season. More detailed information on the mechanisms and procedures can be obtained from our previous publications (Ren et al., 2012).

In the DLEM, the annual net carbon exchange (NCE) between terrestrial ecosystems and the atmosphere represents the overall carbon budget in the terrestrial ecosystem, which is calculated as:

$$\mathrm{NCE} = \mathrm{NPP} - \mathrm{Rh} - \mathrm{Ec} - \mathrm{Ep}$$

where Rh is carbon loss from soil heterotrophic respiration; Ec is the total carbon loss due to land conversion; Ep is the total carbon loss from products decay. In this way, a positive NCE value means a terrestrial carbon sink, whereas a negative NCE indicates that terrestrial ecosystems are carbon sources to the atmosphere. The land-use change related parameterization for the DLEM follows the empirical parameters established by Houghton (2003), other process-based models (e.g. Terrestrial Ecosystem Model, TEM, Tian et al., 2003) and field observational data. More detailed information on the mechanisms and procedures can be obtained from our previous publications (Ren et al., 2012; Tao et al., 2013; Tian et al., 2011a, b).

In the DLEM, the SOC is composed of woody debris, litter, soil microbial pools, and two slow organic C pools. Based on the C/N ratio, the C inputs received from tissue turnover, manure, crop residues, and branch fragmentation, are allocated to litter C pools. After the allocation to litter pools, the C fluxes occur between soil microbial and slow organic C pools through biological decomposition, physical adsorption, and desorption. The microbial C is divided into three pools namely autochthonous and zymogenous microbial pools which are involved in decomposition of the resistant and easily decomposable C pools. In addition, a third microbial pool is the soil microbial residues. The equations to estimate soil and litter decomposition use first-order decay rate constants (k_{C_Pool}), which are adopted from the models of CENTURY (Parton et al., 1993), CN-SIM (Petersen et al., 2005), and IBIS (Liu et al., 2005). In the DLEM, the decomposition rate of each SOC pool is influenced by soil temperature, soil water content, nutrient availability, and soil texture:

$$k_{C\_Pool} = \frac{K_{max}}{365\, f(T) \times f(W) \times f(N) \times f(clay)} \quad [1a]$$

$$f(T) = 4.89 \exp\left[-3.432 + 0.1T(1 - 0.5T/36.9)\right] \quad [1b]$$

$$f(W) = \begin{cases} \dfrac{1 - e^{-q/q_{sat}}}{1 - e^{-q_{fc}/q_{sat}}} & q \le q_{fc} \\ 1.0044 - \dfrac{0.0044}{e^{-5\frac{q/q_{sat} - q_{fc}/q_{sat}}{1 - q_{fc}/q_{sat}}}} & q > q_{fc} \end{cases} \quad [1c]$$

$$f(\text{clay}) = 1 - 0.75 P_{clay}/100 \quad [1d]$$

$$f(NM) = \begin{cases} 1 - \dfrac{avn - avn_{opt}}{avn_{opt}} & avn > avn_{opt} \\ 1 & avn_{opt}/2 \le avn \le avn_{opt} \\ 1 + \dfrac{0.5 avn_{opt} - avn}{avn_{opt}} & avn \le avn_{opt}/2 \end{cases} \quad [1e]$$

$$f(\mathrm{NI}) = 0.8 + 0.2\,\mathrm{avn}/\mathrm{avn}_{opt} \quad [1f]$$

where k_{C_Pool} is the specific decomposition rate (d^{-1}), K_{max} is the maximum decay rate (d^{-1}); f(T) is the average soil temperature scalar; f(W) is the soil moisture scalar; f(clay) is the soil texture scalar; f(NM) and f(NI) are N scalars in mobilization and immobilization, respectively; T is air temperature (°C); θ is soil water content (mm); θ_{sat} is soil water content at field capacity (mm); θ_{fc} is soil water content at field capacity at wilting point (mm); P_{clay} is the fraction of clay in soil (%); avn is the available soil N (g N m^{-2}); and avn_{opt} is the optimum available soil N (g N m^{-2}).

The CH_4 exchanges between ecosystems and the atmosphere are a combination of CH_4 production, oxidation, and transport from soil pore water to the atmosphere. The DLEM only considers CH_4 production from dissolved organic carbon (DOC), which is indirectly controlled by environmental factors including soil pH, temperature and soil moisture content. CH_4 oxidation during CH_4 transport to the atmosphere, CH_4 oxidation in the soil pore water, and atmospheric CH_4 oxidation on the soil surface, is determined by CH_4 concentrations in the air or soil pore water, as well as soil moisture, pH, and temperature. Most CH_4-related biogeochemical reactions in the DLEM are described by using the Michaelis-Menten equation with two coefficients: maximum reaction rate and half saturation coefficient. Three pathways for CH_4 transport from soil to the atmosphere include ebullition, diffusion, and plant-mediated transport. It is assumed that CH_4-related biogeochemical processes only occur in the top 50 cm of soil profile. The net CH_4 flux between the atmosphere and soil is determined by the following equation:

$$F_{CH4} = F_P + F_D + F_E - F_{air,\ oxidation} - F_{trans,\ oxidation}$$

where F_{CH4} is the flux of CH_4 between soil and the atmosphere (g Cm^{-2} d^{-1}); F_P is plant-mediated transport from soil pore water to the atmosphere (g Cm^{-2} d^{-1}); F_D is the diffusive flux of CH_4 from water surface to the atmosphere (g Cm^{-2} d^{-1}); F_E is the ebullitive CH_4 emission to the atmosphere; $F_{air,\ oxidation}$ is the rate of atmospheric methane oxidation (g Cm^{-2} d^{-1}); $F_{trans,\ oxidation}$ is the oxidized CH_4 during plant-mediated transport (g C m^{-2} d^{-1}). The detailed assumptions and processes are described in our previous publications (Tian et al., 2010).

In the DLEM, the N_2O is produced from the nitrification and denitrification processes. Nitrification is a process of converting ammonium into nitrate, is simulated as a function of soil temperature, moisture, and the ammonium concentration (Xu et al., 2012; Tian et al., 2010). In the denitrification process in DLEM through which the nitrate is converted into nitrogen containing gases, is simulated as a function of soil temperature, moisture, and the nitrate concentration (Lin et al., 2000). The empirical equation reported by Davidson et al. (2000) is used to separate N_2O from other gases (i. e. NO and N_2). The detailed information for the processes related to N_2O emission can be obtained from our publications (Tian et al., 2010, Xu et al., 2012).

2.2 Coupling of the phosphorus with carbon and nitrogen cycles

In the DLEM, P is coupled with carbon and nitrogen in all the plant biomass and soil pools (Figure 2.2). The fluxes of P among different biomass pools are driven by carbon: P ratio. In order to simulate P adsorption and desorption processes in soil, we defined an active soil inorganic P pool and an stable inorganic P pool base (Lewis and McGechan, 2002; Leonard et al., 1987). The detailed description of the P cycle:

$$\frac{dP_{dip}}{dt} = R_w + R_{min} + R_{dep} + R_{ades} + R_{sdes} - R_{imb} - R_{lch} - R_{aads} - R_{sads} - R_{upt}$$

We assume that soil inorganic P is the only readily available P for plant. The soil inorganic P pool is regulated by processes including phosphate weathering (R_w), mineralization of organic phosphorus (R_{min}), desorption of P form active inorganic P pool and stable inorganic P pool (R_{ades} and R_{sdes}), aerial deposition (R_{dep}), immobilization by microbial activities (R_{imb}), leaching with runoff (R_{lch}), adsorption by soil organic matter and soil minerals (R_{aads} and R_{sads}) and uptake by plant root (R_{upt}).

2.2.1 Phosphorus Weathering

In terrestrial ecosystems, phosphate weathering is the primary source of soil P which is controlled by surface area of the phosphate rock, temperature, precipitation, solution composition, and soil pH (Guidry & Mackenzie, 2000). Here, we have obtained the equations for the weathering of P from the Century model (Parton et al., 1988).

$$R_w = Ppar \times wteff \times teff$$

$$wteff = fwater * ftem$$

$$fwater = \begin{cases} 1, & \text{if rwater} > 13 \\ \frac{1}{1+10\times e^{-6\times rwater}} & \text{if rwater} \leq 13 \end{cases}$$

$$rwater = \frac{\Theta - \Theta_{wilt}}{\Theta_{fc} - \Theta_{wilt}}$$

$$ftem = \max\left(\frac{11.75 + (29.7/3.14) \times \tan(3.14 \times 0.031 \times (T - 15.4)}{normalizer}, 0.01\right)$$

$$normalizer = 11.75 + (29.7/3.14) \times tan(3.14 \times 0.031 \times (30 - 15.4)$$

$$teff = 12 \times \frac{tef1 + (tef2/3.14) \times tan(3.14 \times tef3 \times (pfine - 0.7))}{365}$$

$$pfine = clay + silt$$

Where R_w is the weathering rate of parent phosphorus (g P/ m2/day); P_{par} is the parent P in soil column (g P/m^2), which is obtained from soil P synthesis data (Yang and Post, 2011); wteff represent impacts of temperature and soil water content on weathering, and teff is the soil texture factor on weathering, respectively; wteff is the product of the temperature factor and soil water factor; T is soil temperature (ºC); $\boldsymbol{\theta}$ is soil water content of the top 15 cm (%); $\boldsymbol{\theta}$ wilt is soil water content at the wilting point (%). $\boldsymbol{\theta}$fc is the soil field capacity (%); tef1, tef2, tef3, and tef4 are four dimensionless parameters that denote soil texture impacts on weathering; clay is the clay fraction in soil; silt is the silt fraction in soil.

2.2.2 Adsorption and desorption between labile inorganic and active inorganic P pool

The inorganic P can be adsorbed by soil colloids and minerals. Base one the reaction time and reversibility P sorption are usually categorized as fast adsorption and slow adsorption (Zee & Riemsdijk, 1988). Fast adsorption occurs between inorganic P and soil particles, which are usually reversible (McGechan & Lewis, 2002). Adsorbed P can return back to the soil inorganic P pool if the balance of adsorption and desorption is disturbed. In the DLEM, simulation of P fluxes between soil inorganic P pool and active inorganic P pool adopt the method provide by Knisel (1993).

$$R_{ades-aads} = 0.1 \times F_{iw} \times F_{it} \times (P_{dip} - P_{aaip}(\frac{PAI}{1-PAI}))\ ;$$

$$PAI = \begin{cases} 0.0054 \times base + 0.116 \times pH - 0.73; for\ slightly\ weathered\ soils \\ 0.46 - 0.0916 \times \ln(100 \times clay)\ ; for\ highly\ weathered\ soils \end{cases}$$

$$base = 22 \times pH + 10 * clay - 53$$

$$F_{it} = e^{(0.115 \times \mathrm{T} - 2.88)}$$

$$F_{iw} = \frac{\Theta - \Theta_{wilt}}{\Theta_{fc} - \Theta_{wilt}}$$

$$F_{iw} = \begin{cases} \frac{\Theta - \Theta_{wilt}}{\Theta_{fc} - \Theta_{wilt}} & \text{if } \Theta < \Theta_{fc} \\ 0 & \text{if } \Theta > \Theta_{fc} \end{cases}$$

where P_{dip} is the inorganic soil P pool (g P/m^2); P_{aaip} is the active inorganic P pool (g P/m^2); $R_{ades\text{-}aads}$ is the flux between the above two pools (g P/m^2/day), with positive value represents adsorption and negative value denotes desorption. PAI is the soil chemical coefficient; Base is the soil base saturation; pH is soil pH; clay is soil clay fraction; F_{iw} is soil water coefficient; F_{it} is soil temperature coefficient; T is soil temperature (ºC); $\boldsymbol{\Theta}$ is soil water content of the top 15 cm (%); wilt is soil water content at the wilting point (%). $\boldsymbol{\Theta}$fc is the soil field capacity (%).

2.2.3 Adsorption and desorption between active inorganic P pool and stable inorganic P pool.

Slow adsorption refers to the reactions between inorganic P and soil minerals including iron (Fe), aluminium (AL), and calcium (Ca) compounds, which have large binding capacity for P adsorption (Filippelli, 2008). Unlike fast adsorption, this process takes much longer time to reach a balance and could substantially reduce availability of soil inorganic P. In the DLEM, we assume slow adsorption and desorption occur between the active soil inorganic pool and stable soil inorganic pool. The P flux between these two pools is calculated following Knisel (1993) and Chaubey et al., (2006)

$$R_{sdes} = K_{as} \times \left(ras \times P_{aaip} - P_{saip}\right); \qquad ras \times P_{aaip} \geq P_{saip}$$

$$R_{sads} = 0.1 \times K_{as} \times \left(ras \times P_{aaip} - P_{saip}\right); \qquad ras \times P_{aaip} \le P_{saip}$$

$$K_{as} = \begin{cases} e^{-1.77 \times PAI - 7.08} & \text{Non-calcareous soils} \\ 0.00076 & \text{calcareous soils} \end{cases}$$

Where Psaip is the soil stable inorganic P pool (g P/m2); Kas is a flow coefficient; ras is the ratio between stable inorganic P pool and active inorganic P pool which is obtained from Yang and Post (2011).

2.2.4 Phosphorus uptake

Phosphorus uptake in the DLEM is simulated with a similar method for N uptake. The actual amount of plant P uptake is a function of supply, plant uptake potential, and deficiency.

$$P_{up} = \min(P_{pot}, P_{dip}, P_{def})$$

$$P_{pot} = P_{up,max} f(T) f(W, P_{dip})$$

$$f(T) = \frac{(T - T_{max})(T - T_{min})}{(T - T_{max})(T - T_{min}) - (T - T_{opt})^2}$$

$$f\left(W, P_{dip}\right) = \frac{f(w) \times P_{dip}}{f(w) \times P_{dip} + k_{up}}$$

$$\mathrm{f(w)} = 0.9\beta^3 + 0.1$$

$$P_{def} = \sum_{i=1}^{5} \frac{c_i}{CP_{min,i}} - \sum_{i=1}^{5} p_i$$

Where P_{up} is the actual P uptake rate (gP/m^2/day); P_{pot} is the potential P uptake rate (gP/m^2/day; P_{def} is the P needed by plant biomass pools; f(T) is temperature coefficient; T_{max}, T_{min}, and T_{opt} are the maximum, minimum and optimum temperature for

P uptake, respectively; f(w) is soil water coefficient; ci and pi are carbon and P pool sizes, respectively; CP_{min} represents carbon to P ratio in each plant biomass pool.

2.2.5 Phosphorus allocation and limitation on carbon uptake

Distribution of P in each plant biomass pool is determined by the total available P and stoichiometry of different pools. Total P available for allocation include the P in each pool and newly up taken P. Allocation of P to each pool is calculate based on the fraction of maximum P in each pool to the sum of maximum P in all the pools.

$$P_{alloc} = \sum_{i=1}^{5} p_i + P_{up}$$

$$p = P_{alloc} \times \frac{\frac{c_i}{CP_{min,i}}}{\sum_{i=1}^{5} \frac{c_i}{CP_{min,i}}}$$

In the DLEM, carbon uptake is simulated with a method that separates plant canopy into sunlit and shaded leaf groups in order to account for canopy structure impacts on photosynthesis. As a result, P content in leaf canopy is also calculated for each leaf group in order to calculate P limitation impacts on photosynthesis. In the DLEM, photosynthesis is co-limited by leaf nitrogen and P content. Limitation coefficient is calculated with leaf nutrients contents and maximum leaf nutrient levels. When both P and nitrogen limitation impacts is considered, carbon uptake is controlled by the most limiting nutrient.

$$P_{sunc} = \frac{0.45 \times P_{leaf}}{C_{leaf}} / (\frac{LAI_{sun}}{LAI} + \frac{LAI_{shade} e^{-0.5k}}{LAI})$$

$$P_{shadec} = P_{sunc} \times e^{-0.5k}$$

$$P_{maxc} = \frac{0.45}{lcp\_min}$$

$$P_{limit-sun} = \min(\frac{P_{sunc}}{P_{maxc}}, 1)$$

$$P_{limit-shade} = \min(\frac{P_{shadec}}{P_{maxc}}, 1)$$

$$NP_{limit-sun} = \min(N_{limit-sun}, P_{limit-sun})$$

$$NP_{limit-shade} = \min(N_{limit-shade}, P_{limit-shade})$$

Where P_{sunc} and P_{shadec} are P concentrations (g P/g biomass) for sunlit and shaded leaf groups, respectively; LAI_{sun} and LAI_{shade} are leaf area indexes for sunlit and shade leaves, respectively; LAI the total leaf area index of plant canopy; P_{leaf} is leaf P content (g P/m2); C_{leaf} is leaf carbon content (gC/m2); k is canopy extinction coefficient; P_{maxc} is the maximum leaf P concentration; $P_{limit-sun}$ and $P_{limit-shade}$ are P limiting coefficient for sunlit and shaded leaves, respective; $NP_{limit-sun}$ and $NP_{limit-shade}$ are co-limiting coefficients for the two leaf groups, respectively.

2.2.6 Phosphorus mineralization and immobilization

Organic P is returned to soil inorganic pool through soil organic decomposition. Following equations are used to describe P fluxes among litter pools and soil organic pools.

$$\mathrm{P}_{dec} = \mathrm{P}_{pool}\mathrm{k}_{\mathrm{dec}}$$

Phosphorus transfer from organic pools to inorganic forms or to more recalcitrant pools is represented with the above equation. Phosphorus fluxes among different pools are determined by storage and decomposition rate of the specific pool. During soil decomposition, P can either be immobilized or mineralized, depending on carbon decomposition rate, C:P ratios or different soil organic carbon pools and availability of inorganic soil organic matter. For example, mineralization of P occurs when C:P ratio of

the released carbon and P of a given pool is less than the corresponding ratio of that pool. The amount of mineralized P can be calculated with the following equation.

$$\mathrm{P}_{min} = \mathrm{P}_{dec} - \mathrm{C}_{dec}/\mathrm{CP}_{ratio}$$

Where P_{min} is amount of mineralized P from a soil organic pool; P_{dec} is the amount of organic P released during organic decomposition; C_{dec} is the decomposed carbon; CP_{ratio} is the carbon to P ratio of the specific soil organic pool. One the other hand, immobilization happens when the C:P ratio of the decomposed organic carbon and organic P is higher the carbon to P ratio in a specific pool, soil inorganic P can be immobilized to maintain the stoichiometry is soil organic pools.

$$\mathrm{P}_{imob} = \min\left(\frac{\mathrm{C}_{dec}}{\mathrm{CP}_{ratio}} - \mathrm{P}_{dec}, P_{dip}\right)$$

2.2.7 Phosphorus leaching

Phosphorus leaching could substantially reduce soil P content over long time period and could potentially lead to water quality problems (Walker & Syers 1976; Del Campillo *et al.* 1999). In the DLEM, we simulated leaching of different P species with the following equations:

$$R_{lchdip} = \min(R_{lchdip\_pot}, P_{dip})$$

$$R_{lchdip\_pot} = P_{dip} \times fflow \times \frac{P_{dipc}}{P_{dipc} + lchb_{dip}}$$

$$fflow = \frac{q_{srun} + q_{drain}}{\theta + q_{srun} + q_{drain}}$$

$$P_{dipc} = \frac{P_{dip}}{W_{soil}}$$

Where R_{lchdip} is the leaching rate of inorganic P (g P/m^2/day); R_{lchdip_pot} is the potential rate of inorganic P leaching (g P/m^2/day); fflow is the runoff coefficient for

leaching; q_{srun} is the surface runoff (mm); q_{drain} is the drainage runoff (mm); $\boldsymbol{\theta}$ is soil water content (mm). P_{dipc} is the concentration of inorganic P (g P/g soil); W_{soil} is soil weight of the top 50 cm (g/m^2). Similarly, leaching of organic P is simulated as:

$$R_{lchdop} = P_{dop} \times \min(ffow \times \frac{P_{dopc}}{P_{dopc} + lchb_{dop}}, 1)$$

$$P_{dopc} = \frac{P_{dop}}{W_{soil}}$$

$$P_{dop} = P_{dec} \times f_{dop-dec}$$

where R_{lchdop} is the leaching rate of dissolved organic P (g P/m^2/day). P_{dopc} is the concentration of dissolved organic P (g P/g soil); P_{dop} is the total amount of soil dissolved organic P (g P/m^2). P_{dec} is the total amount of decomposed organic P (g P/m^2/day); $f_{dop-dec}$ is the faction of decomposed organic P that is dissolvable.

Besides leaching of DOP and DIP, we also simulate leaching of particulate organic P. Particulate organic P is transported from land to rivers together with soil organic matter and sediment through soil erosion. Soil erosion rate is calculated with the Modified Universal Soil Loss Equation (MUSLE) erosion equation (Williams & Berndt 1977; Chaubey et al., 2006).

$$R_{lchpop} = T_{opc} \times R_{erosion}$$

$$T_{opc} = \frac{T_{op}}{W_{soil}}$$

Where R_{lchpop} is the leaching rate of particulate organic P (g P/m^2/day). T_{opc} is the concentration of organic P in soil column (g P/g soil); T_{op} total organic P in soil; $R_{erosion}$ is the soil erosion rate (g soil/day).

2.3 Validations of the DLEM simulated results with field observations

To conduct model validation and uncertainty analysis, this study used the available databases, including field measurements, survey records, remote sensing observations, and published results in scientific journals.

2.3.1 Net Primary Productivity

The DLEM simulation results were validated against the independent site-level observations in croplands, forests, and grasslands. In addition, a validation process at the country scale was performed using results from previous meta-analysis (Bhattacharyya et al., 2000). For the validations at site level, we have collected the NPP estimates from previous field scale published research papers in different biome types (Figure 2.3A). In the croplands, crop yield was reported in the field scale studies which were converted into NPP using harvest index values for individual crops. The harvest index values for different crops were obtained from previously published literature in India (Das et al., 2014; Tripathi, 2010; Zaidi and Singh, 2005). The DLEM simulated NPP was comparable with the site-level observation in croplands, forests, and grasslands ($y= 0.9317x + 41.809$; $R^2= 0.94$). In addition to the site level observations, we have compared terrestrial NPP at biome level estimated by different methods. In addition to the field observations, we compared the NPP simulated by the DLEM with observations from MODIS database (Figure 2.3B) during 2000–2010.

2.3.2 Soil Organic Carbon

In this study, the DLEM results have been validated with the independent site level observations on net primary productivity and SOC contents in the croplands, forests, and grasslands. Here, we are providing validation of DLEM simulated SOC with

field studies compiled from meta-analysis previously published research papers in croplands and forests at different locations (Figure 2.4). The observation data we collected ranged from <2000 g C m^{-2} to >20000 g C m^{-2} in croplands and forests. In general, model simulated SOC was closer (r^2 = 0.67; y = 0.9439x+788.2) to the site level observation, which suggest that the DLEM was able to capture the spatial variability of SOC stocks in forest and agricultural sites.

2.3.3 Nitrous oxide

The simulation results have also been evaluated with independent field observational data, inventory data, and regional estimations on N_2O emissions in India (Sharma et al., 2011). In general, DLEM has been able to simulate the N_2O emissions (R^2 = 0.96) observed in the field scale studies in India (Figure 2.5).

2.3.4 Methane

In this study, we are presenting the validation of CH4 flux only for which we used field data from rice fields and wetlands (Figure 2.6). In the field observations, CH_4 emissions ranged from < 1 g C m^{-2} $year^{-1}$ to > 140 C m^{-2} $year^{-1}$ in India. In brief, the DLEM simulated CH_4 emissions were closer (r2= 0.85) to the field scale observations in rice fields and wetlands (Figure 2.7).

2.3.5 Litter carbon to phosphorus ratio

Previously, it has been demonstrated that nutrients concentrations of C, N, and P were highly constrained in forest foliar biomass and litterfall production worldwide in different geographical regions (McGroddy et al., 2004). Our analysis differs from earlier examinations of terrestrial plant C: N: P relationships (Deevey, 1970; Elser et al., 2000) in that we focus on the scale of entire forests (as opposed to individual plants or

species) and variations in C: N: P relationships at this scale across forest ecosystems worldwide. The stoichiometry of the C: N: P in the plant biomass and litter pools can be modified by the P availability, soil conditions, as well as plant functions types (Chapin 1980, Chapin et al. 1993).

We obtained the carbon to P ratio in the litter pools from previously databases as well as from individual research publications in different geographical locations within tropics (Vitousek et al., 1984). Using datasets from 62 sites, Vitousek et al., (1984) reported the patterns of carbon to P ratio in the litterfall in the tropical ecosystems, which was utilized in our study for calibrating the newly incorporated P module in the DLEM. In the observational database, the carbon to P ratio ranged from <500 to > 2500 indicating not all the tropical trees efficiently cycle P in the systems. This could be true as the carbon to P ratio in the litter pools are controlled by the P availability, and as will be discussed below, phosphorus-deficient soils are much more commonly found in the tropics than the temperate zone. The DLEM simulations were able to capture the variability in the carbon to P ratio in the litter pools in different geographical regions of tropics (Figure 2.7).

2.3.6 Foliar nitrogen to phosphorus ratio

It has been demonstrated that foliar concentrations of nitrogen and P represents the soil fertility (Vitousek and Farrington, 1997; Vitousek, 2004). Thus, foliar N and P concentrations are often viewed as an index of nutrient status that may provide insight into processes such as net primary productivity (NPP), and SOC decomposition. More recently, a growing focus on ecological stoichiometry (Sterner and Elser, 2002) has led to a broader use of N: P ratios in leaves to infer potential nutrient limitation of terrestrial

NPP. Aerts and Chapin (2000) suggest that N limitation likely occurs at N: P ratios <14, with P limitation probable at values >16. These and other authors (Sterner and Elser, 2002; Reich and Oleskyn, 2004) are careful to point out that life-form and even species level variation in nutrient requirements are likely to create different breakpoints between N and P limitation, but nonetheless, it is instructive to view our data in light of the hypothesized transition at N: P values of 14–16.

In this study, we obtained foliar nitrogen to P ratio from Townsend et al., (2007) as well as from the previously published literature elsewhere. Townsend et al., (2007) compiled the foliar nitrogen and P concentrations from 150 mature canopy tree species in Costa Rica and Brazil, and combine those data with a comprehensive new literature synthesis to explore the major sources of variation in foliar N:P values within the tropics. Our newly developed DLEM is able to capture the overall variability in the N: P ratio (Figure 2.8). However, the DLEM slightly underestimated the N: P ratio in the tropical ecosystems. In the Townsend et al., (2007) meta-analysis, foliar N: P ratio showed seasonal variations that foliar N: P values differed by 25% between wet and dry seasons.

2.4. Summary and future recommendations

In this study, model results validations and comparisons all indicate that the DLEM model has the ability to capture variations in carbon fluxes and pools. The simulated NPP, SOC, CH_4, N_2O, foliar N: P ratio, and litter C: P ratio were comparable to field observations in the croplands, forests, and grasslands. Discrepancies may exist in the results of various studies are primarily due to input data and the gaps in different methods (e.g. modeling mechanisms). In the South-East Asia, peatland distribution,

which are important for carbon cycling, is missing in the current land cover and land use datasets and therefore efforts should be made to quantify the peatland areas in the future. Currently available land-cover and land use datasets ignored distribution of peatlands in the grid format. In the modeling mechanism, significant uncertainties existed in the magnitude of carbon uptake limited by the P limitation in this study. We have validated the carbon to P ratio and nitrogen to P ratio in the foliar, significant uncertainties may exist in the magnitude of carbon uptake limited by the P limitation. To the best of our knowledge, P fertilizer experiments in the tropical forests are lacking in the tropical Asia. Therefore, this is a preliminary attempt that incorporated P cycling in the DLEM, and future efforts should focus on designing P fertilizer experiments in the forest areas.

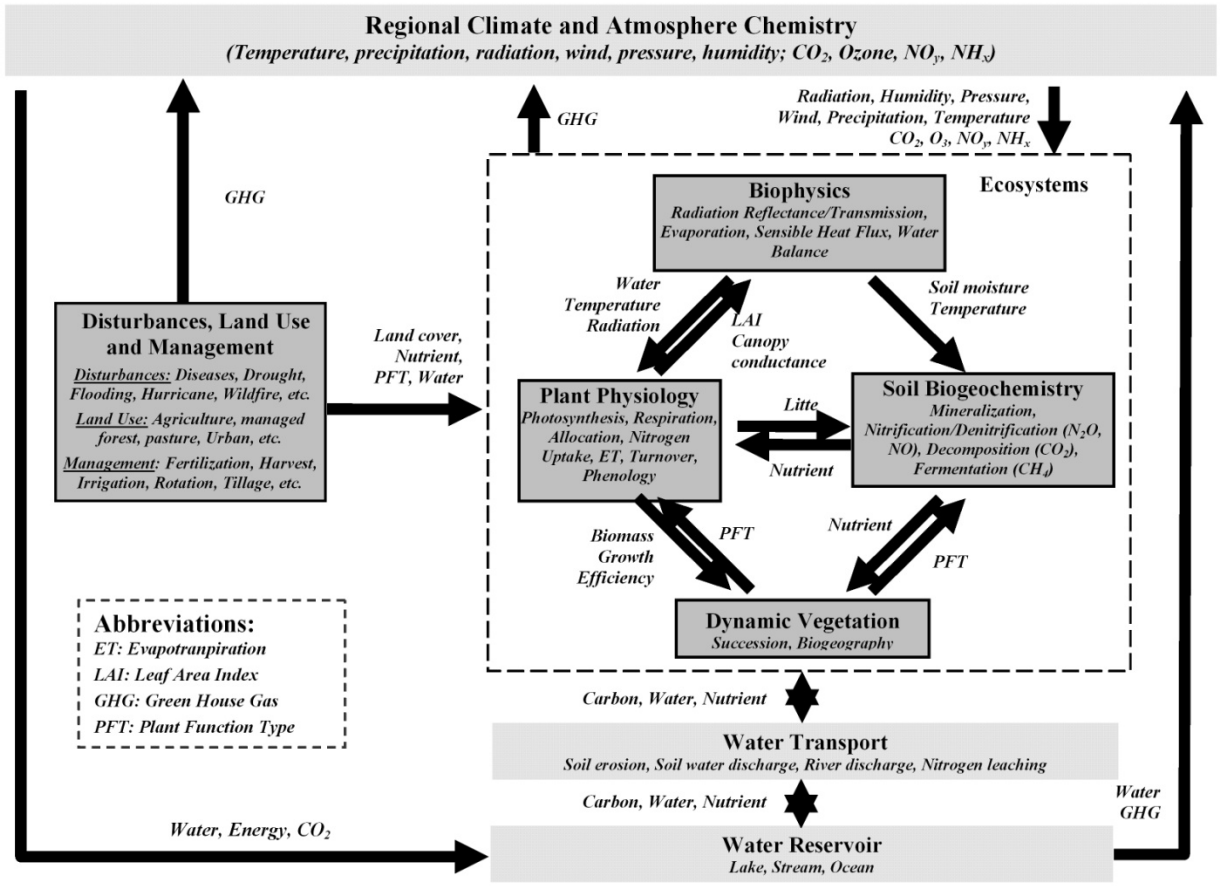

Figure 2.1 Conceptual model of the Dynamic Land Ecosystem Model (DLEM)

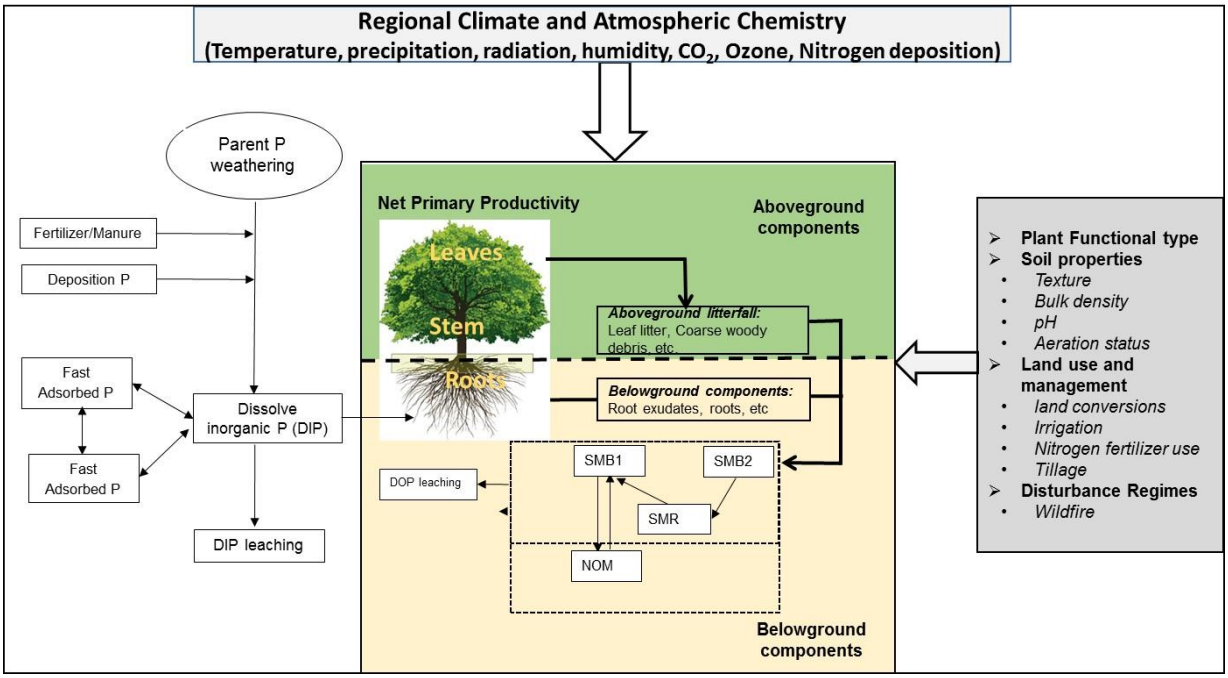

Figure 2.2 Phosphorus processes in the Dynamic Land Ecosystem Model (DLEM).

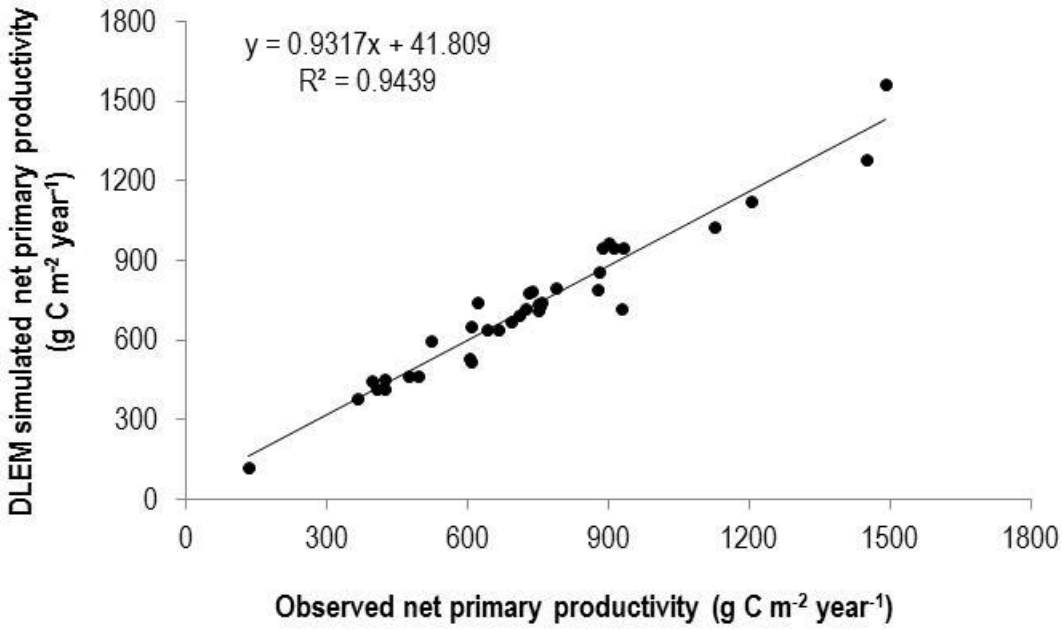

Figure 2.3A Validation of DLEM (Dynamic Land Ecosystem Model) simulated net primary productivity with field scale studies. Observational dataset was obtained from Croplands (AICRP, 2012); Forests (Devi & Yadava, 2009; Pandey et al., 2005; Joshi & Pant, 2012; Garkoti et al., 1995; Singh et al., 2011; Kumar et al., 2011; Baishya and Barik, 2011); Grasslands (Behera et al., 1994; Billore et al., 1977; Misra, 1973; 1978; Singh and Yadav, 1974; Varshey et al., 1972; Ambasht et al., 1972; Misra et al., 1978; Shankar et al., 1993; Pradhan, 1994; Aggarwal & Goyal, 1987; Pandey et al., 2005).

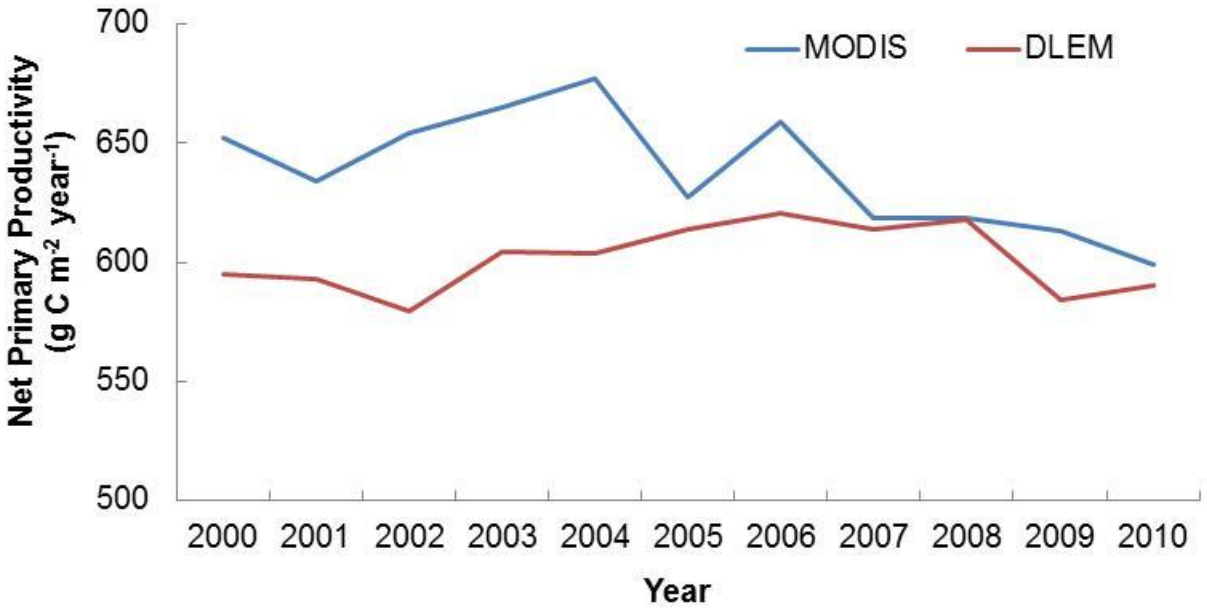

Figure 2.3B. Validation of the DLEM (Dynamic Land Ecosystem Model) simulated terrestrial net primary productivity (g C m^{-2} $year^{-1}$) with observations from MODIS database.

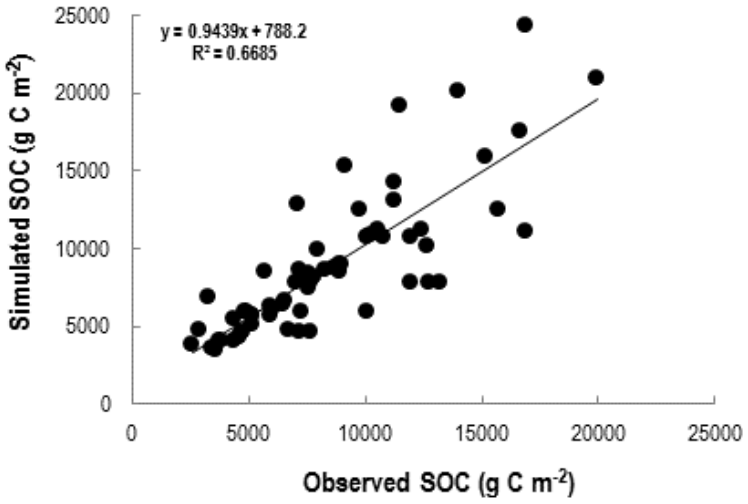

Figure 2.4 Field site locations for validating DLEM (Dynamic Land Ecosystem Model) simulated soil organic carbon stocks with field observations. Observational dataset was obtained from 1. Croplands (Bhattacharyya et al., 2006; Banger et al., 2009; Kundu et al., 2007; Ghosh et al., 2013; Manna et al., 2005; Yadav et al., 2000; Mandal et al., 2007; Majumder et al., 2008; Prasad and Sinha, 2000; Rudrappa et al., 2006; Sharma et al., 1995; Yaduvanshi and Swarup, 2005; Nayak et al., 2009; Vineela et al., 2008; Hati et al., 2007) and 2. Forests (Singh and Datta, 1983; Yadav and Sharma 1968; Srivastava et al., 1991; Verma et al., 1990; Singh et al., 1991; 1995; Prasad et al., 1985; Totey et al., 1986; Nair et al., 1989; Samra et al., 1985; Balagopalan and Jose, 1986; Raina et al., 1999; Ganeshamurthy et al., 1989; Tamgadge et al., 2000).

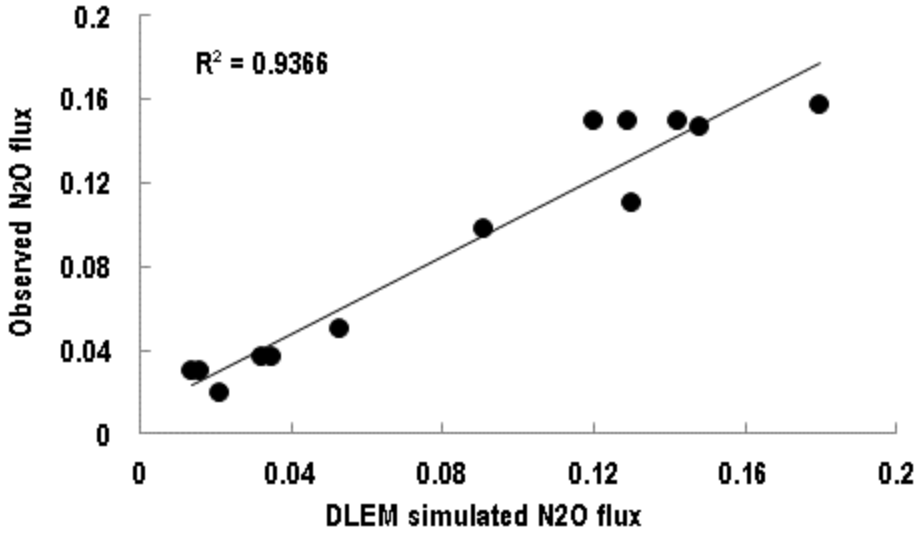

Figure 2.5. Validation of DLEM (Dynamic Land Ecosystem Model) simulated nitrous oxide flux with field scale studies.

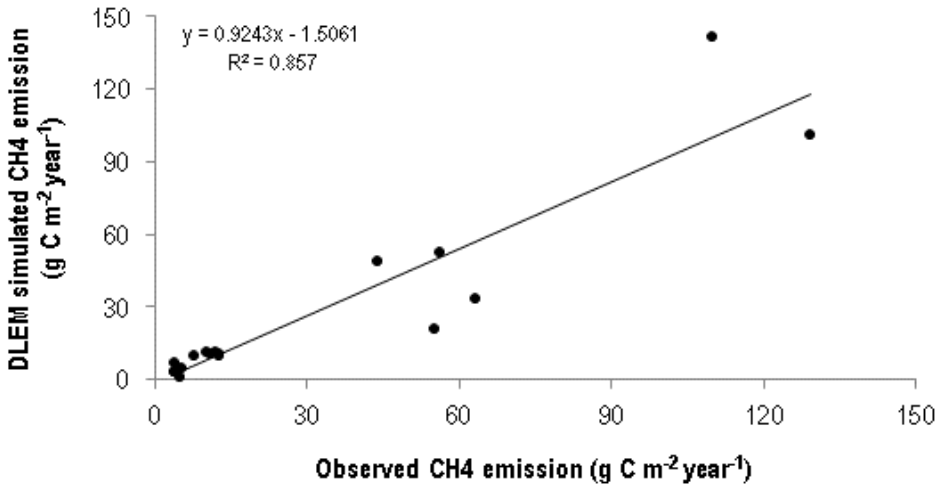

Figure 2.6 Comparisons of DLEM (Dynamic Land Ecosystem Model) simulated and observed methane emissions. The dataset was obtained from previously published literature (Adhya 2000; Banik 1996; Barman et al., 2000; Bharati et al., 2000; Bhattacharyya 2013; Ghosh et al., 2003; Mandal et al., 2008; Pathak et al., 2003; [£]Purvaja and Ramesh, 2001; Rath et al., 2002; Singh et al, 1999); [£]indicates the reference for wetlands

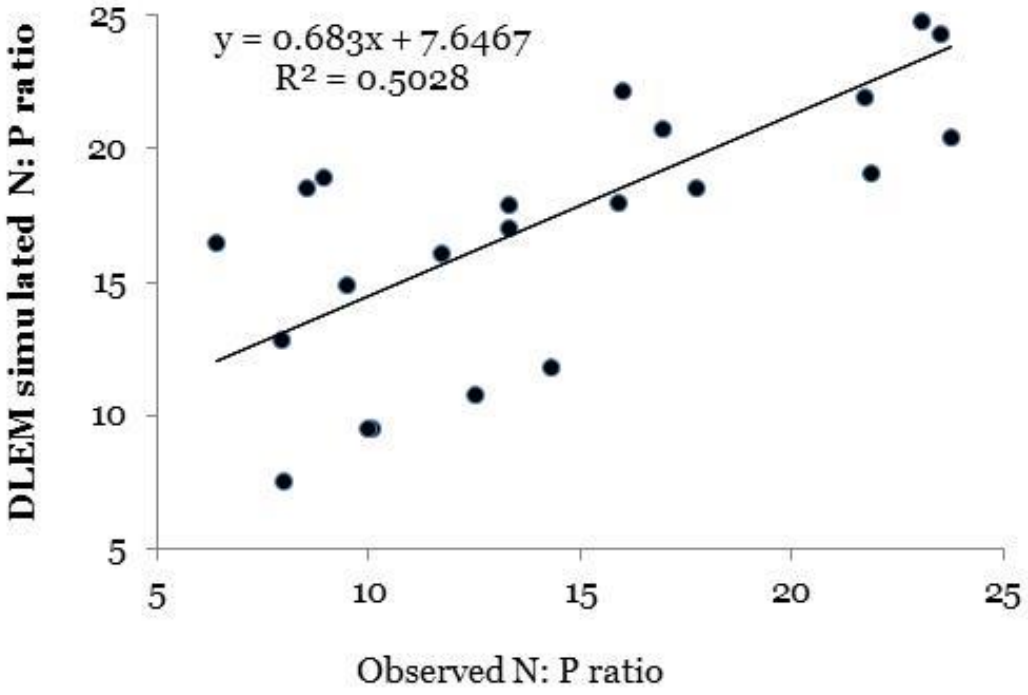

Figure 2.7 Comparison of nitrogen to phosphorus ratio simulated by the DLEM with the observed values from previously published literature.

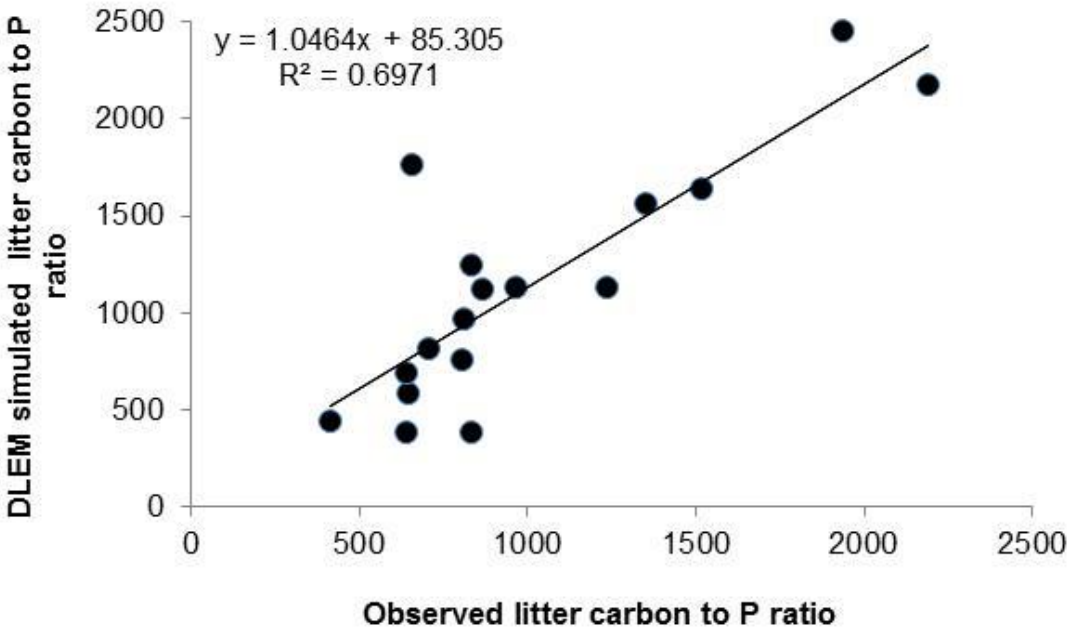

Figure 2.8 Comparison of the DLEM simulated carbon to phosphorus ratio with the observed values in different geographical locations of the tropics.

Chapter 3. History of Land Use in India during 1880-2010: Large-Scale Land Transformations Reconstructed From Satellite Data and Historical Archives

Abstract

In India, human population has increased six folds from 200 million to 1200 million that coupled with economic growth has resulted in significant land use and land cover (LULC) changes during 1880–2010. However, large discrepancies in the existing LULC datasets have hindered our efforts to better understand interactions among human activities, climate systems, and ecosystem in India. In this study, we incorporated high-resolution remote sensing datasets from Resourcesat-1 and historical archives at district (N=590) and state (N=30) level to generate LULC datasets at 5-arc minute resolution during 1880–2010 in India. Results have shown that a significant loss of forests (from 89 million ha to 63 million ha) has occurred during the study period. Interestingly, the deforestation rate was relatively greater under the British rule (1880–1950's) and early decades after independence, then decreased after the 1980s due to government policies to protect the forests. In contrast to forests, cropland area has increased from 92 million ha to 140.1 million ha during 1880–2010. Greater cropland expansion has occurred during 1940–1980's that coincided with the period of farm mechanization, electrification, and introduction of high yielding crop varieties as a result of government policies to achieve self-sufficiency in food production. The rate of urbanization was slower during 1880–1940 but significantly increased after 1950s probably due to rapid increase in population and economic growth in India.

This chapter has been published in *Global and Planetary Change*; the citation is: Tian, H.Q., K. Banger, B. Tao, and V.K. Dadhwal. 2014. History of land use in India during 1880–2010: Large-scale land transformations reconstructed from satellite data and historical archives. Global Planet. Change 10.1016/j.gloplacha.2014.07.005.

Our study provides the most reliable estimations of historical LULC at regional scale in India. This is the first attempt to incorporate newly developed high-resolution remote sensing datasets and inventory archives to reconstruct the time series of LULC records for such a long period in India. The spatial and temporal information on LULC derived from this study could be used by ecosystem, hydrological, and climate modeling as well as by policy makers for assessing the impacts of LULC on regional climate, water resources, and biogeochemical cycles in terrestrial ecosystems.

3.1 Introduction

Human activities have altered the Earth's environment by changing the land use and land cover (LULC) in the past several centuries (Hurtt *et al.,* 2006; Liu et al., 2005; Liu and Tian, 2010). LULC changes are major driving forces for biogeochemical cycles, climate change, and food production from regional to global scales (Houghton and Hackler, 2003; Feddema *et al.,* 2005; Jain and Yang, 2005; Tian *et al.,* 2012a; Tao et al, 2013). Since 1850, LULC change alone has contributed to the approximately 35% of anthropogenic carbon dioxide (CO_2) emissions across the globe (Houghton *et al.,* 2012). However, these environmental changes occur at multiple spatial and temporal scales that may highly differ among regions. In the 20th century, India has experienced 6-folds increase in population (200 million to 1200 million) coupled with economic growth (especially after 1950's) that has resulted in LULC transformations including deforestation, cropland expansion, and urbanization (Richard and Flint, 1994; DES, 2010). For example, Richards and Flint, (1994) have reported that total forest area decreased from 100 million ha to 81 million ha while cropland area increased from 100 million ha to 120 ha during 1880–1950. The temporal pattern of deforestation during

1880–2000 has major control over temporal pattern of carbon emissions due to land use change (Chhabra and Dadhwal, 2004a). Therefore, accurate LULC estimation is key for understanding interactions among human activities, climate systems, and ecosystem as well as for the formulation of policies at national level (Houghton and Hackler, 2003; Tian *et al.,* 2003).

In India, detailed LULC dataset collected from village level survey and aggregated at district level (N=590) is available only for the recent years (1950–2010) from Department of Economics and Statistics (DES), Government of India (DES, 2010). In addition, Richards and Flint (1994) have compiled the historical LULC archives including cropland, forests, grasslands\shrublands, and built-up areas at state level (N= 30) in India during 1880–1980. However, there are certain limitations of the inventory LULC datasets. For example, LULC datasets in the tabular forms are inadequate for the use in climate, hydrological and biogeochemical models that require LULC in the gridded format (Feddema *et al.,* 2005; Liu *et al.,* 2008; Tian *et al.,* 2010). On the other hand, the remote sensing makes it possible to monitor contemporary LULC pattern at high spatial resolution but only covers relatively shorter time period. In India, several coarse resolution LULC dataset products such as moderate resolution imaging spectroradiometer (MODIS; Loveland and Belward,1997; Hansen *et al.,* 2000), Globcover developed from Envisat's Medium Resolution Imaging Spectrometer (MERIS; Arino *et al.,* 2008), and GLC2000 based on SPOT4 satellite (Bartholome and Belward, 2005) are available for the recent years. In addition, a regional LULC dataset based on the Advanced Wide Field Sensor of Resourcesat-1 has been developed at a spatial resolution of 56-m by National Remote Sensing Agency, India during 2004–2010

(NRSA, 2007). Linking remote sensing data (short time series but high spatial resolution) and inventory data (long time series but coarse spatial resolution in tabular format) is also a big challenge (Verburg *et al.,* 2011).

Recently, Banger et al., (2013) reported that contemporary total cropland and forest area estimated at state level from inventory DES was better represented by LULC datasets developed from Resourcesat-1 than global scale remote sensing datasets in India. It is difficult to generate the historical LULC datasets using coarse resolution global remote sensing datasets that have large discrepancies with the inventory datasets in India. Therefore, it is imperative to integrate contemporary remote sensing datasets from Resourcesat-1 with the historical tabular archives to generate more reliable and useful LULC datasets, which cover longer time periods in India. Previously, several global scale LULC datasets have been developed by combining remote sensing and inventory land use records at state level in India (Ramankutty and Foley, 1999; Klein Goldewijk *et al.,* 2011). In this study, we made the first attempt to integrate the high-resolution satellite (Resourcesat-1 at 56-m resolution) and existing inventory datasets at district and state levels to generate the LULC datasets at 5-arc minute resolution for the period of 1880–2010 in India. We focused on five major LULC including cropland, forest, grasslands\shrublands and shrubland complexes, wastelands, and built up or settlement areas. We believe that our newly developed LULC dataset would provide more detailed and accurate information on the spatial and temporal pattern of LULC changes in India. Previous studies have shown that land conversions among these LULC types as well as associated management practices may have significant effects on the terrestrial biogeochemical cycles at regional and

global scales (Banger *et al.,* 2012; Tao *et al.,* 2013). Therefore, our LULC datasets would be greatly helpful to enhance our understanding on the impacts of LULC on regional climate, water resources, and terrestrial biogeochemical cycles.

This chapter is organized into three different sections: a description of the input data sources, methodologies for constructing the gridded LULC datasets at 5-arc minute resolution, and an analysis of the magnitude as well as major drivers for land conversions during 1880–2010. In addition, we also discussed the uncertainties in our newly developed LULC datasets and made recommendations to cautiously use these LULC datasets for scientific research and formulation of policies.

3.2 Data and methods

India is located between 8–38^{o} N latitudes and 66–100 ^{o} E longitudes, covering a geographical area of approximately 328 million ha. There are four distinct seasons in India including: winter (December–February), summer (March–June), south-west monsoon season (June–September), and post-monsoon season (October–November) (Prasad et al., 2007). Four months period of south-west monsoon season accounts for approximately 80% annual rainfall in the country. However, there is large spatial variability in the south-west monsoon rainfall that gives rise to different kinds of vegetation across India. Natural vegetation ranges from tropical evergreen in the south to the alpine meadows in the north, the deserts in the west to the evergreen forests in the north-east of India (Joshi *et al.,* 2006).

3.2.1 Land use and land cover databases

In this study, we focused on the five dominant LULC types including cropland, forest, grasslands\shrublands, wastelands, and built-up or settlement areas. Cropland

category is defined as the land cultivated for crops including single season, double or triple crops, shifting cultivation, horticultural plantations, and orchards. Food and Agricultural Organization of the United Nations (FAO) has also included temporary fallow lands into Agricultural Area category (FAO, 2013). However, we did not include fallow lands in cropland category since fallow lands have significantly different influence on the biogeochemical and hydrological cycles (Tian *et al.,* 2003). Forest category includes the area evergreen and deciduous trees with > 10% canopy cover as well as degraded forest types that has <10% of the canopy cover. This definition is similar to the forest cover definition used by national remote sensing center, India (NRSA, 2007). The built-up or settlement area is defined as the land occupied by buildings, roads and railways. In the historical archives, it is difficult to differentiate the grasslands, grazing areas, and shrublands. Therefore, we classified the term grasslands\shrublands as the areas occupied by grasslands\shrublands and permanent pastures, meadows, and shrublands. Wastelands include the area that cannot be brought under cultivation such as area covered by mountains, deserts, and ice caps, etc.

In this study, we used inventory LULC datasets available at district (N=590) and state level (N=30) from different sources along with the LULC datasets developed from remote sensing datasets available from Advanced Wide-Field Sensor (AWiFS) of Resourcesat-1 to construct LULC at 5-arc minute resolution during 1880–2010 (DES, 2010; Richard and Flint, 1994; Table 3.1). The LULC generated in this study are represented in fractional forms which consists percentages of five LULC types (cropland, forest, grasslands\shrublands, wastelands, and built-up) in each grid cell.

3.2.2 Contemporary land cover and land use datasets from Resourcesat-1

We used a contemporary LULC datasets (for the year 2005 and 2009) generated from imagery of the satellite Resourcesat-1 (NRSA, 2007). Resourcesat-1 was launched in 2003 with a near-polar sun synchronous orbit at a mean altitude of 817 km. Two main imaging sensors of the satellite include Linear Imaging Self-Scanner (LISS-III) and AWiFS. The AWiFS sensor operates in four spectral bands with three in the visible and near-infrared bands and one in the short-wavelength infrared region. The swatch size of AWiFS is 740 km with temporal resolution of 5-days and spatial resolution of 56-m at nadir. Based on the imagery of AWiFS sensor, National Remote Sensing Agency, India (NRSA) has generated yearly 19-LULC classes at 56-m grid resolution in India during 2005–2009 (NRSA, 2007). In brief, NRSA, (2007) has used 680 multi-temporal quadrant data that covered different crop growing seasons were used to generate the LULC datasets. Stratified random points generated through ERDAS imagine software was used to assess the accuracy of the LULC classes generated by the Resourcesat-1. A minimum of 20 sample points were considered for each class to estimate the accuracy of the classified output. Ground truth data, legacy maps, and multi-temporal FCC have formed the basis for assessment and generation of Kappa co-efficient (NRSA, 2007). In this study, we used the following LULC classes from the Resourcesat-1 datasets: urban (built-up), cropland (kharif crop, rabi crop, shifting cultivation, plantation/orchards, and zaid crop only), forest (evergreen forest, deciduous forest, scrub, and degraded forest), grasslands\shrublands (grasslands and shrubland), and wastelands (snow covered, gullied, rann, and other wastelands).

However, we did not use the water-bodies, littoral swamps, and current fallow LULC categories available in the Resourcesat-1 datasets.

3.2.3 District level datasets during 1950–2010

In India, district level (N = 590) yearly LULC are available from the Directorate of Economics and Statistics (DES), India during 1998–2010 (DES, 2010, http://eands.dacnet.nic.in/ accessed in September, 2012). Of the total geographical area of 328 m ha, LULC datasets are available for only 305 m ha. The land use survey is conducted annually and is based on 9-classes including (i) forests, (ii) area under non-agricultural uses, (iii) barren and uncultivable land, (iv) pastures and other grazing land, (v) land under miscellaneous tree crops, (vi) culturable waste land, (vii) follow land other than current fallows, (viii) current fallows, and (ix) net area sown area. The LULC data is collected at village level and is later aggregated to higher hierarchical units such as districts and states in India.

District level LULC datasets were not available for the years earlier than 1998 (DES, 2010). Therefore, we collected the district level LULC datasets from Indiastat datasets during 1950–2000 (http://www.indiastat.com/aboutus.aspx, accessed September 2012). Indiastat is a private organization that collects, collates, and compiles the socio-economic information about India. LULC classes archived by the Indiastat were similar to the 9-folds LULC classification system developed by DES. Their district level LULC datasets were collected at a decadal time scales during 1950–2000.

3.2.3 State level datasets during 1880–1950

Richards and Flint (1994) have compiled the historical LULC archives at state level for five time periods including 1880, 1920, 1950, and 1980 in India. They collected

the LULC datasets from official agricultural and economic statistics; historical and demographic texts, reports, and articles; and from any other available datasets for the region. In brief, LULC categories in their datasets included temporary and permanent crops, settled and built up areas, forests, grasslands and shrubland, wetlands, and surface waters (Richards and Flint, 1994). For this study, we collected the state level LULC datasets for three time periods including 1880, 1920, and 1950. In order to make the LULC classification from Richards and Flint, (1994) similar to other LULC datasets, temporary and permanent crops were aggregated and classified as cropland, grasses and shrubland were aggregated as grasslands\shrublands category, while built-up and forests were used as such from Richards and Flint, (1994).

3.2.4 Algorithm for the reconstruction of LULC during 1880–2010

Several studies have combined the contemporary remote sensing datasets with historical LULC archives to construct the distributions of cropland and forest cover over several centuries (Ramankutty and Foley, 1999; Ramankutty et al., 2008; Klein Goldewijk, 2001; Leff *et al.,* 2004; Fuchs et al., 2013). For India, global scale studies have used the LULC records at state level (N=30) to reconstruct the historic LULC datasets which may produce significant discrepancies (Banger et al., 2013; Leff *et al.,* 2004; Ramankutty and Foley, 1999). In this study, we used finer scale district level (N=590) datasets during 1950–2010 and state level (N=30) LULC records during 1880–1950 combined with remote sensing datasets from Resourcesat-1 to reconstruct LULC at 5-arc minute resolution during 1880–2010 in India. During the study period, several bifurcations as well as exchange of boundaries have occurred in different states and districts in India. Therefore, our first task was to construct the uniform boundaries

throughout the study period for district and state units in India. In this study, the inventory LULC datasets from two or more states that are bifurcated or exchanged boundaries in recent years were aggregated to make state boundary similar to ones used Richards and Flint (1994). For example, we aggregated LULC datasets and Uttar Pradesh and Uttarakhand; Madhya Pradesh and Chhattisgarh; Bihar and Jharkhand, where bifurcations occurred during the study period. A similar exercise of aggregating the LULC records was performed for several districts in order to make uniform district boundaries in India. In 2010, approximately 590 districts existed and we aggregated LULC datasets from two or more districts that exchanged boundaries that made a total of 290 district units throughout the study period

In this study, LULC records from inventory datasets were calibrated with Resourcesat-1 datasets to construct LULC at 5 arc minute resolution during 1880–2010. Flow chart of the procedure followed for generating historical LULC using remote sensing and inventory datasets is provided in the Figure 3.1. We integrated the 56-m datasets from Resourcesat-1 into 5-arc minute resolution datasets and determined the fractional area under built-up, cropland, forest, grassland/shrublands, and wastelands. The LCLU reconstruction begins with the contemporary Resourcesat-1 and DES datasets that went back upto 1880 based on the inventory datasets. In brief, the objective of our calibrations was to estimate total as well as spatial distribution of historical built-up, cropland, forest, grassland/shrublands, and wastelands areas in each district or state by comparing the baseline of Resourcesat-1 datasets. Assuming a time series of i and j, i and j have an originally estimated or recorded area of A and B, respectively. If the calibrated area in time i (such as Resourcesat-1 2005) is known as

A′, the calibrated area in time j (B′) can be estimated as (B/A) × A′. The ratio of A′ and A, or the ratio of B′ and B, is called the calibration coefficient. In order to generate the fractional grid datasets, we applied the principle that the district or state area (UA) of each LULC category should stay consistent within the original constructed unit area (RUA).

During the calibration process, built-up areas are generated first followed by croplands, forests, grasslands\shrublands, and wastelands in turn. In the DES datasets, urban or settlement areas were not separately reported, while another category “non-agricultural area” was available that included the land occupied by buildings, roads and railways or under water, e.g. rivers and canals, and other land put to uses other than cropland (DES, 2013). We generated the historical built-up area from non-agricultural area category available in the DES datasets. Firstly, we assumed that area under water-bodies has not changed during 1950–2010 and therefore calculated area under water-bodies using Resourcesat-1 and subtracted it from non-agricultural area to generate the inventory settlement area in the DES datasets. Then, we used the ratio of contemporary built-up area in Resourcesat-1 to contemporary settlement area in the inventory datasets and used this factor to generate historical built-up areas in each district or state in India. There are several procedures to allocate the built-up areas in pixels within a district or state (Fuchs et al., 2013; Lu et al., 2008). In this study, the location of the changes in the built-up areas in pixels within a district or state was determined by the population density based on the assumption that urban sprawl tends to occur in the region with higher population density (Fuchs et al., 2013).The 5-arc minute population

layers were generated by combining global 1 km population maps (CIESIN, 2011) and state level population data in India.

In the calibration process, the allocation of the cropland within a state or district was determined by the crop suitability index, a similar approach used by Fuchs et al., (2013). The crop specific suitability index was available at 5-arc minute by FAO (2013). The crop suitability index of FAO is based on the multiple factors affecting crop production such as long term average climate data (during 1960–1990), soils, land cover, and elevation (http://www.fao.org/nr/gaez/faqs/en/#sthash.sS02NC2r.dpuf). The allocation of cropland within a state or district was a two-step process. Firstly, we generated the distribution of different crop types using DES datasets at state level. After developing the crop distribution maps, we extracted the cropland suitability maps for the relevant crop types generated at 5-arc minute resolution by FAO (2013). During the calibration process, if total cropland area has to be decreased in a state or district, the pixels with lowest cropland suitability probability were reduced at a greater rate than pixels with higher suitability index within a district or state. On the contrary, if the cropland area has to be increased during the calibration process, the pixels with higher cropland suitability index were increased at a higher rate than pixels with lower cropland suitability index.

In contrast to built-up and cropland, uniform suitability or probability of changes is assigned to all locations within a state or district for the forests and grasslands\shrublands. In this study, we assumed that each grid cell is initially covered by undisturbed potential vegetation and other land cover types (i.e. water body, bare land, glacier, river, lake, ocean, etc); the surface areas of lakes, streams, oceans,

glaciers, and bare ground in each grid do not change over the study period. When a land conversion occurs, such as cropland expansion from forest, a new cohort is formed and cropland within the grid cell is then subtracted from the undisturbed potential vegetation proportionally. We acknowledge that our assumptions may bring uncertainties, but this is the best way to quantify land conversions given detailed land use/cover information are not available at grid cell level. In this way, changes in the changes in natural vegetation types (deforestation, conversion of grasslands\shrublands to cropland, built-up etc) partially determined the allocation of natural vegetation in pixels within a district or state level. Other land uses which are not classified into any of the category primarily include fallow lands.

3.3 Results

3.3.1 Overall changes in land cover and land use during 1880-2010

India has experienced significant loss of grasslands\shrublands and forests followed by the expansion of cropland as well as built-up areas during 1880–2010 (Table 3.2; Figure 3.2a and 3.2b). A total of 26 million ha forest areas (from 89 million ha in 1880 to 63 million ha in 2010) and 20 million ha of grasslands\shrublands (from 45 million ha to 25 million ha) has decreased in India. In contrast, total cropland area has increased by 48 million ha (from 92 million ha in 1880 to 140 million ha in 2010). The built-up area was one order of magnitude lower than forest, cropland, and grasslands\shrublands but has increased by 5-folds from 0.46 million ha to 2.04 million ha during 1880–2010.

3.3.2 Land Conversions during 1880–2010

In this study, we determined the conversions between different LULC types during 1880–2010 (Figure 3.3). The results have shown that majority of the cropland expansion has been resulted from conversion of forest (16.9 million ha), grasslands\shrublands (14.8 million ha) as well as other LULC that include fallow lands. Interestingly, 77% (16.9 million ha) of the deforestation has occurred due to cropland expansion while only 23% of the forests were converted into grasslands\shrublands and built-up or settlement areas during 1880–2010. Our results have shown that majority of the urbanization has primarily occurred in the cropland areas (0.7 million ha) while only 0.12 million ha of the forest areas were cleared for urban development during 1880–2010 (Figure 3.3).

3.3.3 Spatial and Temporal Variations of LULC changes during 1880–2010

The landscape of India is diverse with substantial heterogeneity in the climate, soil, as well as has different socio-economic factors that may alter the LULC changes (Joshi et al., 2006; Mishra, 2002). Therefore, there were significant variations in spatial and temporal distribution of LULC changes in India during 1880–2010 (Figure 3.2a and 3.2b). For example, deforestation has occurred in the central east and west coastal areas while cropland expansion has occurred widely across the entire country during 1880–2010. However, cropland expansion in the central east and southern parts was primarily from the forest clearing while in the Indo-Gangetic plains it was from grasslands\shrublands and other land uses that primarily include fallow lands. Urbanization has occurred in small patches all over India; however urbanization was more conspicuous in the Indo-Gangetic plains during 1880–2010.

Results of our study have shown that three time periods (1880–1950, 1950–1980, and 1980–2010) have distinctive LULC conversions in India (Figure 3.3 and Figure 3.4). For example, deforestation has occurred by approximately two million ha per decade during 1880–1980 while forest area remained similar (62–64 million ha) in the late half of 20th century. The time period from 1980–2010 was unique that had significant reforestation through the forest regeneration programs in India (Bhat et al., 2001). Therefore, net changes in the total cropland and forest area were negligible during 1980–2010. In contrast, total cropland area showed a significant increasing trend during 1880–2010 (Figure 3.4). However, majority of cropland expansion has occurred over a period of two decades (8 million ha increase per decade) from 1950 to 1970. Interestingly, total grassland area remained constant during1880–1980 that showed decreasing trends after the 1980's (Figure 3.4).

Total built-up or settlement areas increased from 0.43 million ha to 2.02 million ha during 1880–2010 and the rate of urbanization was relatively slower (0.03 million ha per decade) during 1880–1950 and then built-up areas increased by 0.26 million ha per decade from 1950 to 2010.

3.4 Discussion

In this study, we have tried to understand the major drivers that caused LULC changes in India during 1880–2010. For this purpose, we divided the time period from 1880–2010 into different sub-groups when the land conversions were significantly greater than other years. In addition, we compared the newly developed LULC datasets with existing datasets for several time periods.

3.4.1 Major land conversions in India during 1880–2010

Results of our study have shown that majority of the deforestation has occurred during British government as well as early years after independence that include the time period of 1880–1980 (Figure 3.3 and Figure 3.4). The British government policies that were focused on increasing revenue from timber export as well as infrastructure development may have resulted in the large deforestation in India. For example, in the National Forest Policy of India (1894) of the British government, significant emphasis was given to generate maximum revenue through timber cultivation as well as permanent agricultural crops rather than forest sustainability in India (Negi, 1986; Gadgil and Guha, 1995). The rate of the deforestation decreased and afforestation has occurred in several patches in India during 1980–2010 (Figure 3.3). After independence (1947) afforestation and protection of the forests has started in the late half of 20th century following the government policies to protect forests in India (Bhat *et al.,* 2001; Forest Conservation Act, 1980; The National Forest Policy of India, 1952). For example, The National Forest Policy of India (1952) stipulated to maintain one-third of its total land area under forest for securing ecological stability (FSI, 1999). After the passage of the National Forest Policy of India (1952), another act Forest Conservation Act (1980) banned forest clearing in India. Under the provisions of this act, approval by the Central Government is necessary for the states to divert forest for cropland and other infrastructural facilities. Under the same act, individual states were directed to raise the compensatory forest equivalent to the forest area being diverted into other land uses. Similarly, The National Forest Policy of 1988 also set the target of 33% forest cover in plains and 66% in forest cover in hilly and mountainous areas in order to prevent

erosion and ecosystem degradation (Joshi *et al.,* 2011). Therefore, the government's forest protection policies may have decreased the deforestation rate in the late half of the 20th century in India.

Our results have shown that rate of cropland expansion was significantly greater (8 million ha increase per decade) during 1950–1970 than other time periods (Figure 3.3). This might be the result of the special programs such as Grow More Food Campaign (1940s) that was undertaken to improve food and cash crops supply in India. In addition, mechanization, electrification, and the use of high yielding crop varieties and chemical fertilizers made cropland a profitable business resulting in rapid expansion of cropland during 1950–1970. This time period is also coincides with the green revolution (in 1960's) when food production became sufficient to feed the population of India.

The rate of urbanization was relatively slower in 1880–1950 (0.03 million ha per decade) the increased after 1950's in India. Another interesting observation was a population growth after 1950 due to food security due to food security as well as improvements in the health facilities. Greater increase in human coupled with economic growth may have resulted in rapid growth of built-up areas during 1950–1980 and 1980–2010 in India (Figure 3.4).

3.4.2 Comparison of Cropland, Forest, and Built-up areas with other datasets

In order to investigate discrepancies among LULC datasets, we compared total forest, cropland, grassland, wasteland, and urban areas from different regional and global LULC data sources. For this effort, we used consistent boundary area for India which is slightly lower than the land boundary used by the NRSA (2007).

3.4.3 Cropland area

Previously, large discrepancies in the total cropland areas in India have been reported by various remote sensing LULC datasets (Table 3.2; Hansen et al., 2000; Klein Goldewijk, 2001; Bartholomé and Belward, 2005). Contemporary cropland area estimated by our newly developed datasets was 135–140.1 million ha in 2005–2010 which is lower than estimates from Food and Agricultural Organization (FAO) of United Nations, MODIS-IGBP, MODIS-UMD, and GlobCover (Table 3.2). Among all the global datasets, total agricultural area is highest in FAO datasets (179 million ha in 2005) which also include fallow lands and pastures in the cropland land category (FAO, 2013).

In this study, we have compared the temporal trends in the total cropland area with The International Satellite Land-Surface Climatology Project (ISLSCP II) which are available at 0.5 degree grid resolution (Klein Goldenwijk, 2007). Our study has shown agriculture area has increased from 92 million ha in to 140 million ha during 1880–2010 which is similar to ISLSCP II; however the magnitude of increase was different (Table 3.2). Another long-term study by Dadhwal and Chhabra (2002) also reported an increase in cropland area and production in the Indo-Gangetic Plain region during the period 1901–1990. The increased agricultural production resulted to six-eight folds increase in primary production indicating an intensification of carbon cycling in this agriculturally dominant 'food basket' region of the country. Therefore, cropland datasets developed by our study reflects the long term trends recorded by the national surveys and high-resolution datasets in addition to providing the extent and spatial distribution of such LULC changes.

3.4.4 Forest Cover

In this study, we have compared our historical forest cover estimates with 0.5 degree grid resolution datasets available from ISLSCP II (Klein Goldenwijk, 2007). In 1950 and 1970, forest cover in ISLSCP II ranged from 33–36 million ha which is significantly lower than inventory based forest cover estimates from Richard and Flint, (1994) and DES, (2010). In this way, inclusion of inventory datasets in this study represents an improvement in the forest cover estimations in India.

Except few global scale datasets, only few coarse historical forest cover estimations exit for India. Therefore, we are restricting our discussion to contemporary estimates of forest cover from different remote sensing datasets (Table 2.2). Various remote sensing and inventory LULC datasets showed significant discrepancies in the contemporary forest area estimations in India (Table 3.2). Our datasets showed that forest area was 63 million ha in which is comparable to the 66–69 million ha forest area estimated by the Forest Survey of India in 2010(FSI, 2012). In contrast to our estimation, the global remote sensing datasets including MODIS-IGBP, MODIS-UMD, and Globcover have estimated significantly lower forest area (24–40 million ha) in 2005. Greater discrepancy in the forest area estimation may be attributed to the differences in the definition of forest cover in various remote sensing methods (Banger *et al.,* 2013). For example, MODIS-UMD and MODIS-IGBP which consider area with > 60% canopy cover as forest area showed approximately 30 million ha lower forest area than our dataset in which forest area is covered by > 10% canopy cover. We used the forest definition similar to the NRSA, (2007) where forests include evergreen, deciduous (> 10% canopy cover) and degraded forest (<10% canopy cover) in India. When MODIS

derived Vegetation Continuous Field (VCF) is segmented with tree fraction similar to definitions adopted by Forest Survey of India and NRSA, the MODIS estimated forest cover as well as its spatial correspondence with FSI and NRSA estimates is much higher (Jegnnatahn et al., 2009).

3.4.5 Built-up areas

To the best of our knowledge, none of the national level LULC datasets showed the changes in the built-up areas over such a long time period in India. However, urbanization has received more attention due to harmful effects on water and air quality, natural resources, and social sustainability (Lu et al., 2010). Contemporary built-up areas estimated by our LULC datasets were similar to HYDE 3.1 datasets in 2005. Among the global remote sensing datasets, only MODIS-IGBP datasets showed built-up areas of approximately 8 million ha in 2005 (Banger *et al.,* 2013). In MODIS-IGBP, built-up areas were land areas covered by buildings and other man-made structures were overlaid from the populated places layer from the EDC Global Land Cover Characterization project (GLCC, http://edcdaac.usgs.gov/glcc/glcc.html). In another study on the comparison of urban areas by six methods, Potere and Schneider (2007) have reported urban area has a wide range from 0.81 to 20.4 million ha in India. Overall, our results have shown that Built-up areas followed the trends similar to the population growth which showed a significant increase after 1950s (Figure 3.5). We believe that further efforts are needed to adequately map the built-up areas in India. In this study, we have made the first attempt to reconstruct the historical built-up areas by combining Resourcesat-1 and national inventory datasets during 1880–2010.

3.4.6 Concerns for environment and food security

Our results have shown that those human activities have caused significant alterations in the LULC including deforestation, cropland expansion, and built-up growth during 1880–2010. In the recent three decades (1980–2010), total forest and cropland areas have not significantly changed; however built-up areas are increasing to accommodate more and more people (Figure 3.3). It is projected that that population will keep on increasing for coming two decades in India. One of the biggest concerns is how to increase the food production to feed increasing population? First way of increasing food production by cropland expansion by conversion of forests and other natural vegetation that occurred during 1950–1980's. Currently, forest cover is lower than 33% plains and 66% in hilly and mountainous areas, a minimum standard set by National Forest Policy of 1988 in order to prevent erosion and ecosystem degradation (Joshi *et al.,* 2011). Further, deforestation may result in ecosystem degradation from soil erosion and carbon flux to the atmosphere. Another way of increasing food production is following intensive agricultural management practices (more fertilizers, improved irrigation facilities, increasing cropping intensity etc) on existing croplands. Previously, Mishra (2002) reported that population growth has significant effects on each indicator of agricultural intensification. The agricultural intensification may substantially alter regional climate, water resources, and biogeochemical cycles in India (Ren *et al.,* 2012; Tian *et al.,* 2012b).

3.5 Uncertainties and future needs for LULC data development

In this study, we focused on the development of spatial and temporal LULC patterns at 5-arc minute resolution by integrating remote sensing datasets from

Resourcesat-1 and existing inventory archives during 1880–2010. Due to limited availability of the historical archives, our datasets results may not have caught significant fluctuations in LULC changes over short time periods. One of the major uncertainties associated with our newly developed LULC datasets is the estimation of the forest area. Currently, forest area includes any area with more than 10% of the canopy cover. However, canopy cover density has not been provided in the inventory surveys. The built-up area is also based on the assumption as built-up category is not available in the DES datasets (DES, 2010). We derived built-up area from non-agricultural category that includes land occupied by buildings, roads and railways or under water, e.g. rivers and canals, and other land put to uses other than 19 folds classes. From this non-agricultural LULC category, we excluded the area under water-bodies calculated from Resourcesat-1 datasets assuming that area under water-bodies remained constant during 1950–2010. However, this assumption may be fallacious as many manmade reservoirs have been developed during 1880–2010 (Panigraphy *et al.,* 2012). In this case, constant water spread assumption could lead to some under-estimation of the historical built-up area in India.

In order to improve current understanding of the LULC patterns and their driving forces, further studies are still needed. Firstly, although the new datasets have the most reliable estimations of historical land use, they are still based on the assumption that the current LULC patterns mimic their historical distributions, which may be problematic, as suggested by Houghton and Hackler, (2003). Secondly, more data sources especially historical land survey data on forest plantations as well as built-up area are needed to generate more reliable LULC datasets in India. However, it may be very difficult to

obtain more information on the historical LULC in India. Therefore, it is essential that long-term historical datasets be reconstructed using validated, spatially explicit land use models. These spatially explicit land use models can be used to reconstruct historical LULC and project future LULC with high spatial resolutions by coupling land survey data, socioeconomic factors, and biophysical and biogeochemical processes (Kaplan et al., 2009; Klein Goldewijk and Verburg, 2013; Verburg *et al.,* 1999). This model is based on a non-linear relationship between population density and land use, which translates into a decrease in per-capita land use over time.

Thirdly, more specific efforts should be made to study the impact of extreme events including droughts and floods as well as political and policy shifts on land use dynamics. These investigations could be made on a national scale or by focusing on small-scale case studies. Quantifying the changes in characteristics of LULC is essential for assessing its impacts on regional climate, biogeochemical cycles, and hydrological processes.

Our results have shown significant alterations in the LULC; however such changes were driven by complex climatic and socio-economic factors during the study period. The major LULC changes include the loss of forests, expansion of cropland, and urbanization during 1880–2010. Greater deforestation occurred during 1880–1950 due to British rule policies to increase income from the timber products and cropland. However, deforestation decreased after 1980s due to formulation of government policies to protect forests. Cropland expansion rate was greater in three decades time period from 1950 to 1980 primarily due to expansion of irrigation facilities, farm mechanization, electrification, use of high yielding crop varieties that resulted from

Government policies of achieving self-sufficiency in food production. Our results have shown that urbanization which was negligible during 1880–1950 became one of the most important land conversions after 1950s due to population and economic growth in India. The spatial and temporal information on LULC changes produced in this study can be used by ecosystem, hydrological, and climate models for assessing the impacts of LULC on regional climate, water resources, and biogeochemical cycles in terrestrial ecosystems. To further reduce the uncertainties of LULC data and make reliable projections for the future, we need to advance our understanding of its driving forces and incorporate information from coupling remotely sensed data, vegetation dynamics, and socio-economic factors.

3.6 Acknowledgments

This study has been supported by NASA Land Cover and Land Use Change Program (NNX08AL73G_S01; NNX14AD94G) and US National Science Foundation Grants (AGS-1243220, CNS-1059376).

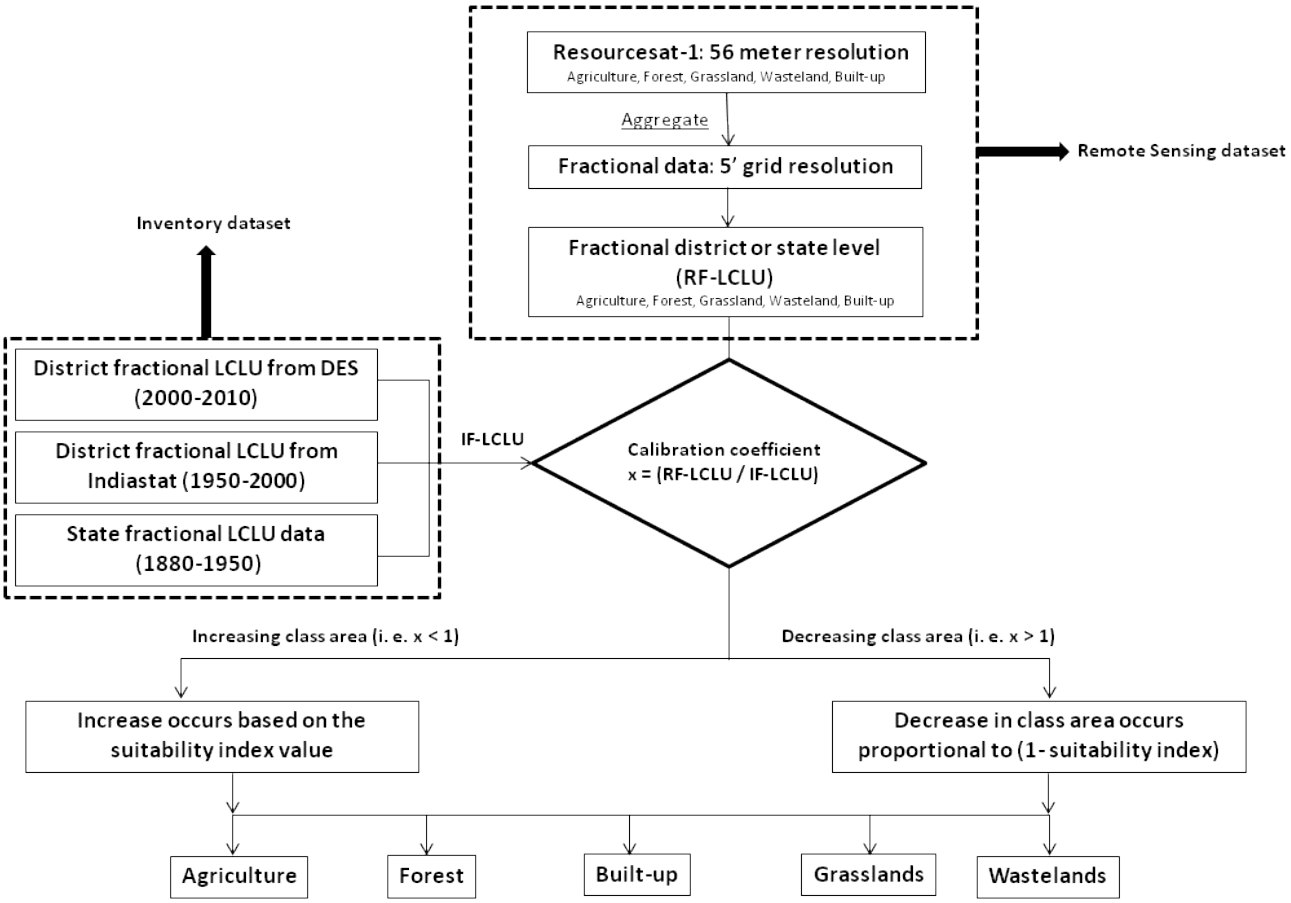

RF-LCLU: Remote sensing fractional land cover and land use; IF-LCLU: Inventory fractional land cover and land use; DES: Department of Economics and Statistics, India

Figure 3.1. Procedure for generating the historic Land Cover and Land Use dataset using remote sensing and inventory datasets during 1880–2010.

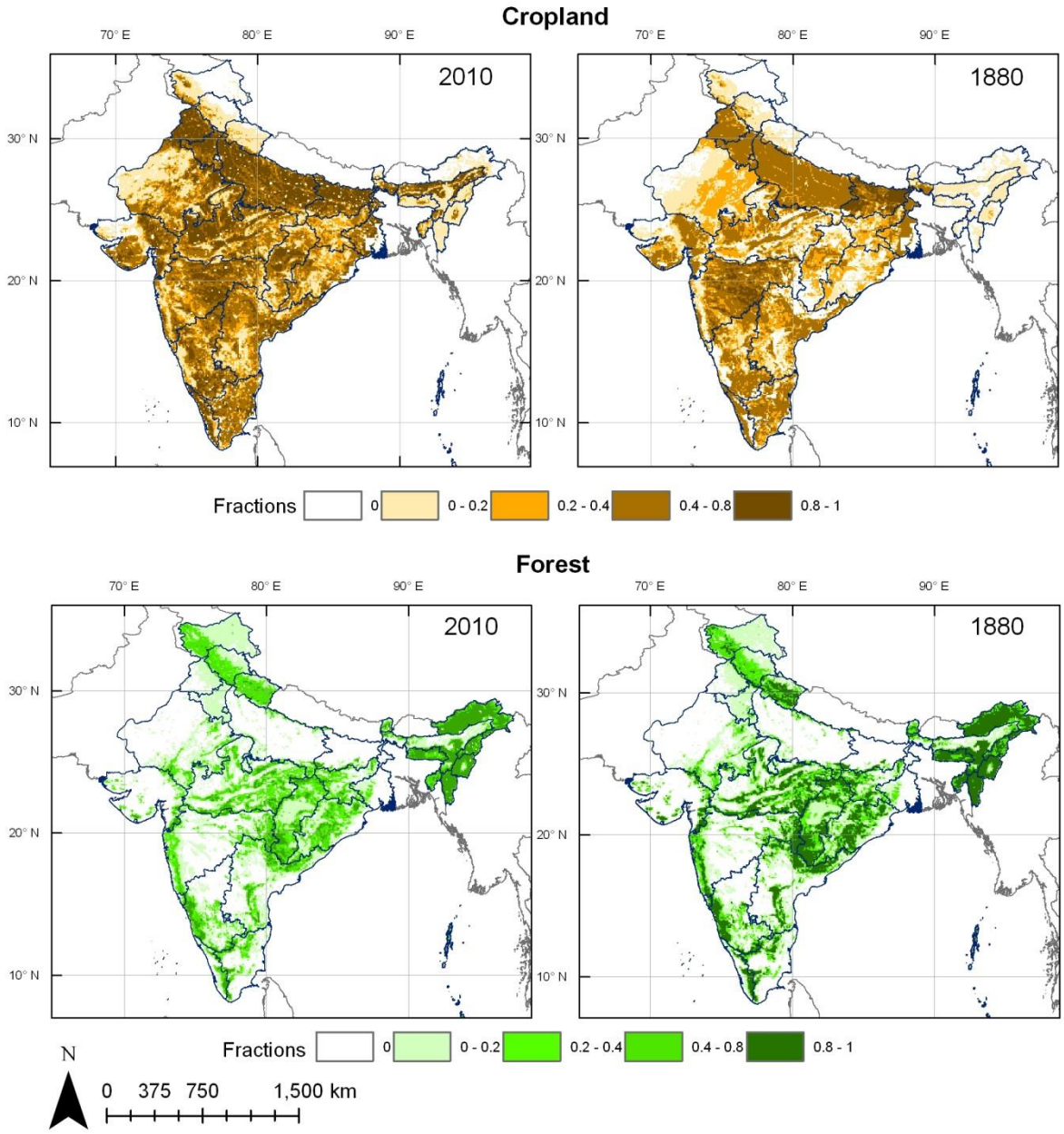

Figure 3.2a. Spatial Pattern of Croplands and Forests in India during 1880–2010.

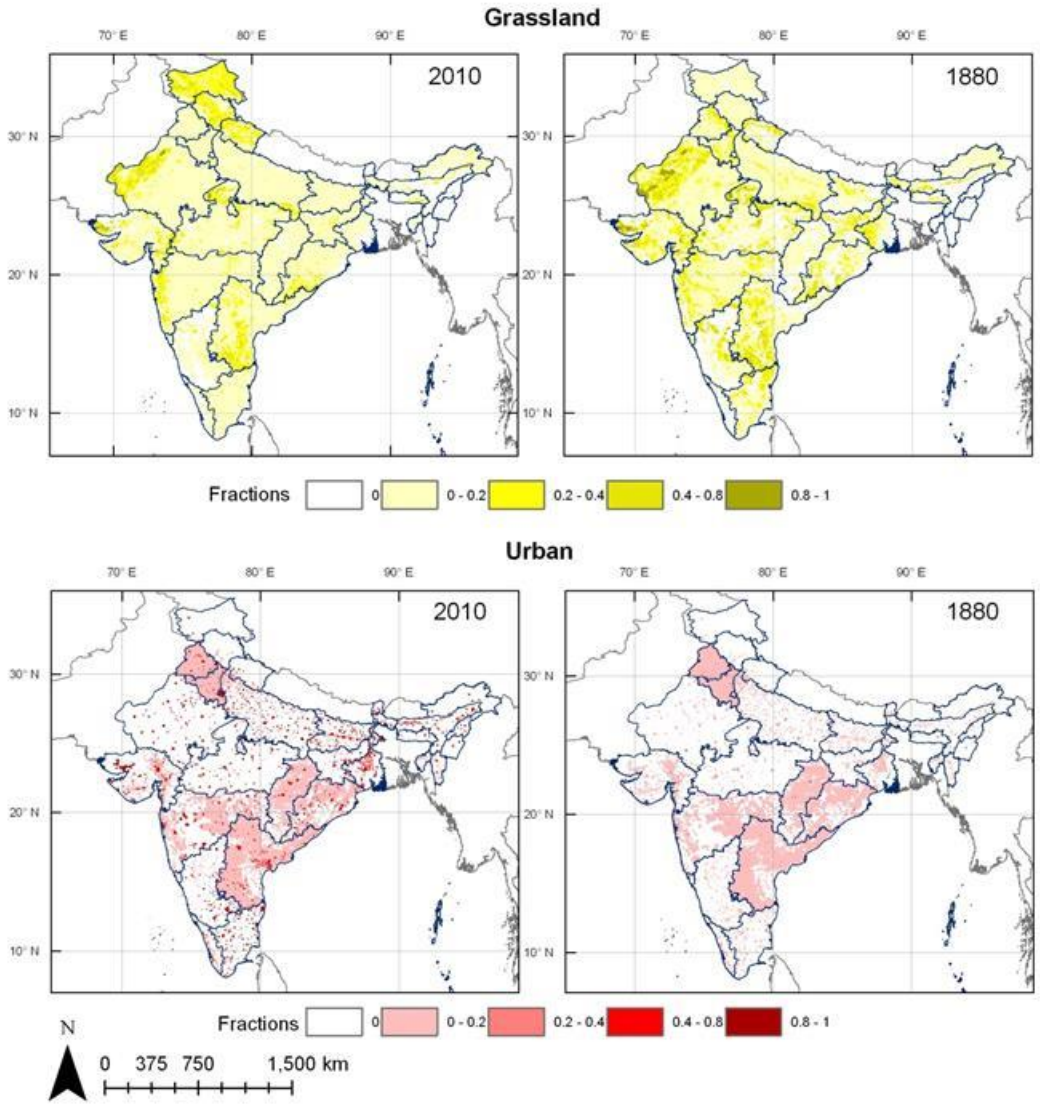

Figure 3.2b. Spatial Pattern of Grasslands and Urban areas in India during 1880–2010.

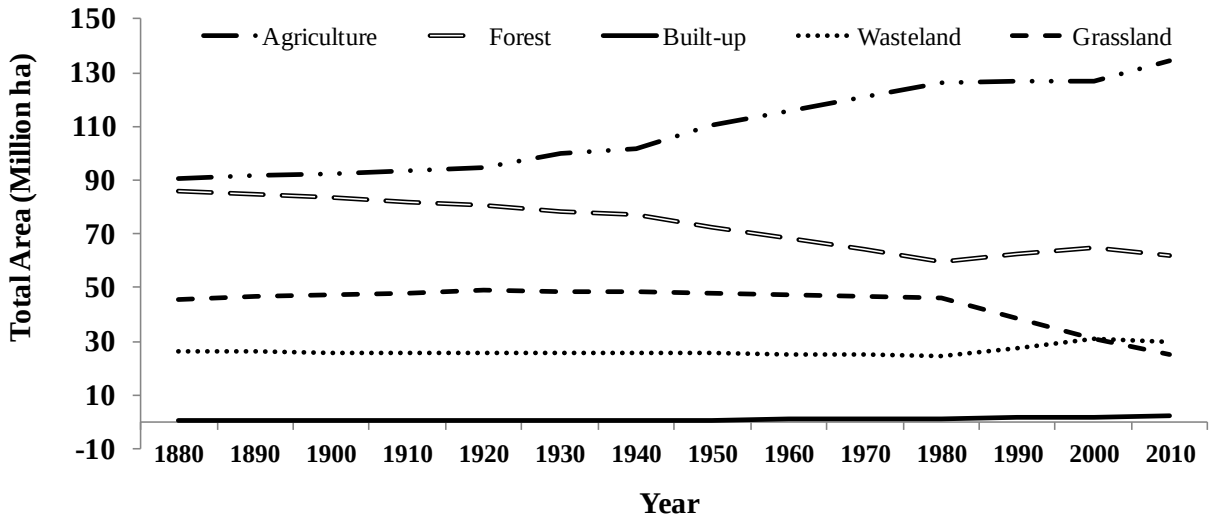

Figure 3.3. Temporal Pattern of Land Cover and Land Use Change during 1880–2010.

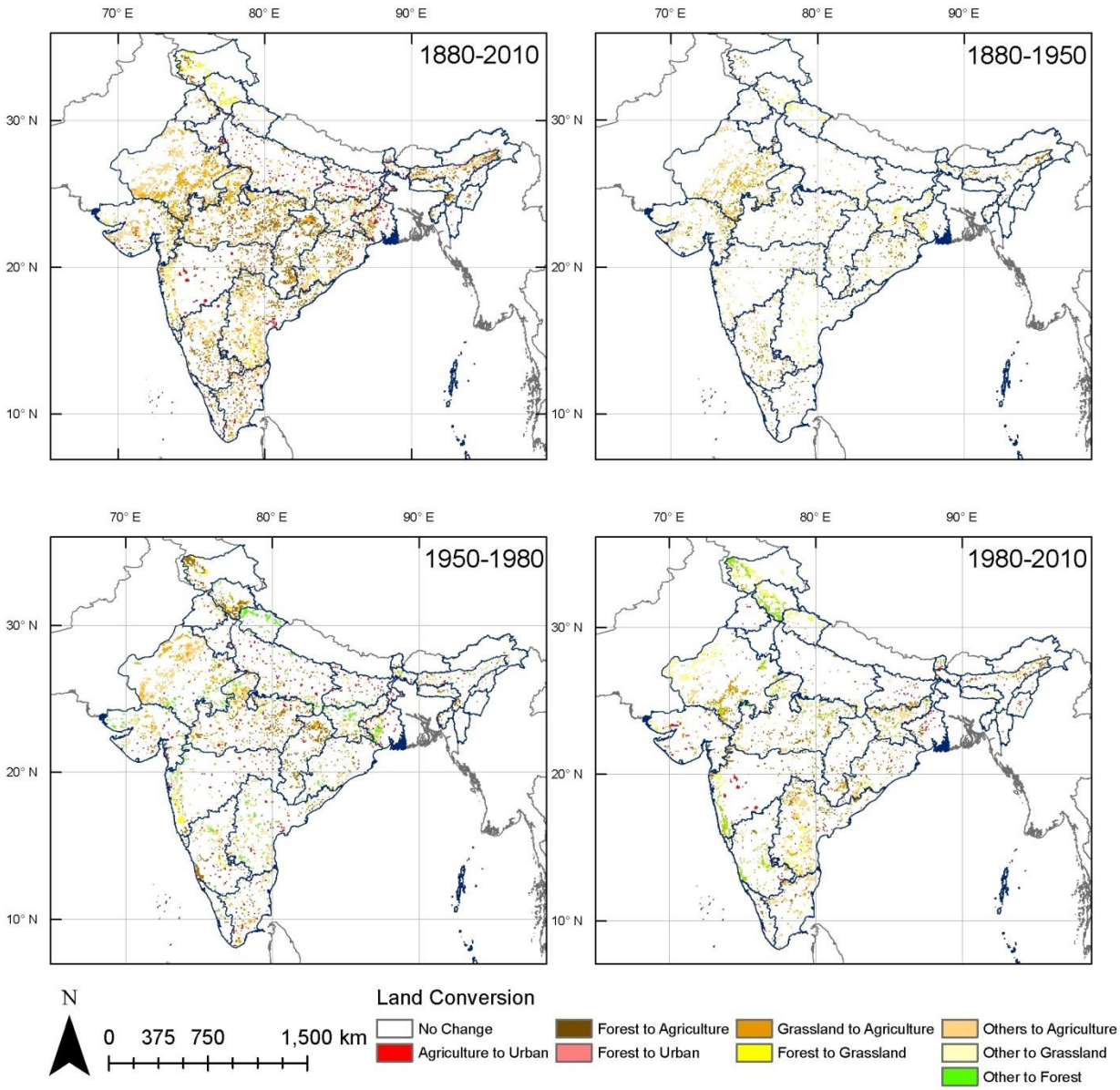

Figure 3.4. Land Conversions in India during 1880–2010.

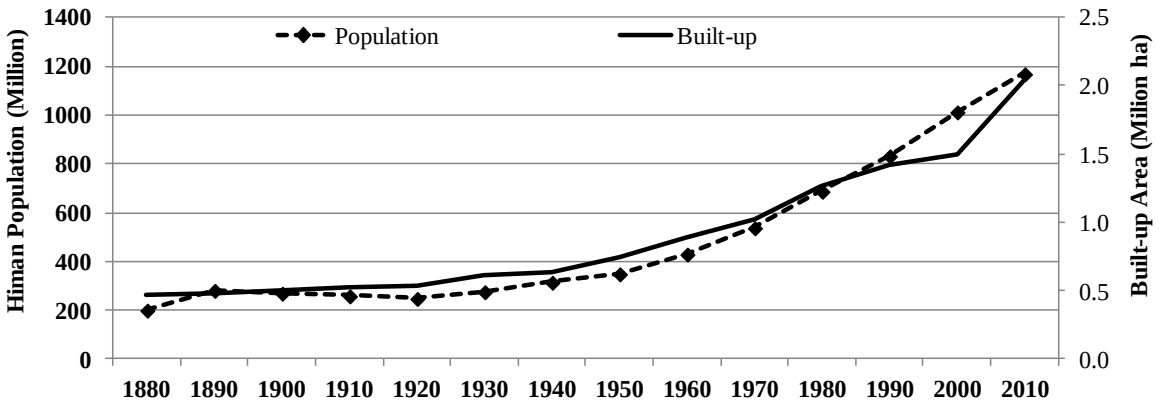

Figure 3.5. Changes in the Human Population and Built-up Area in India during 1880–2010.

Dataset	Methodology	Spatial Resolution	Time Period	LCLU[£] Types
Department of Economics and Statistics	Inventory	District level	2000–2010	9- folds LCLU classes
Indiastats	Inventory	District level	1950–2000	9- folds LCLU classes
Flint and Richard, 1994	Inventory	State level	1880–1920	Agriculture, forests, wastelands, grasslands, Built-up
Resourcesat-1	Remote Sensing	meter	2005–2009	19-folds LCLU classes

[£]LCLU: Land Cover and Land Use

Table 3.1. Land Cover and Land Use Datasets used to construct high resolution datasets in India.

Dataset	Year	Cropland	Forest	Built-up	References
This study	1880	92.6	89.7	0.46	
	1950	110.1	71.1	0.74	
	1970	120.4	64.7	1.02	
	2005	135.0	65.1	1.7	
	2010	140.1	63.4	2.04	
DES, India	2005	143.26	70.9	-	DES, India
ISLSCP II	1950	132.6	36.4	-	Klein Goldewijk, (2007)
ISLSCP II	1970	153.2	33.8	-	Klein Goldewijk, (2007)
ISLSCP II	1990	158.5	35.1	-	Klein Goldewijk, (2007)
HYDE 3.1	1880	-	-	0.27	Klein Goldewijk, (2011)
HYDE 3.1	1950	-	-	0.36	Klein Goldewijk, (2011)
HYDE 3.1	1970	-	-	0.58	Klein Goldewijk, (2011)
HYDE 3.1	2005	-	-	1.48	Klein Goldewijk, (2011)
MODIS-UMD	2001	163.7	29.1	3.9	Hansen et al., (2000)
MODIS-IGBP	2001	159	28.9	8.04	Loveland et al., (2000)
GlobCover	2005	150.0	24.12	2.64	Bicheron et al., (2008)
GLC 2000	2000	135.2	60.3	1.4	Bartholome and Belward, (2005)
FAO datasets	2000	179.85¶	67.71	-	FAOSTAT, (2012)

FAO datasets also include fallow lands in croplands; therefore, total area may be more than croplands.

Table 3.2. Comparison of Land Cover and Land Use estimated (in million ha) by different data sources in India.

Chapter 4. Terrestrial net primary productivity in India during 1901–2010: Contributions from multiple environmental changes

Abstract

India is very important but relatively unexplored region for carbon studies, where significant environmental changes have occurred in the 20th century that can alter terrestrial net primary productivity (NPP). Here, we used a process-based, Dynamic Land Ecosystem Model (DLEM) driven by land cover and land use change (LCLUC), climate, elevated CO_2 concentration, atmospheric nitrogen deposition (NDEP), and tropospheric ozone (O_3) to estimate terrestrial NPP in India. In this study, we used the newly developed high resolution (5-arc minute) LCLUC datasets with other driving forces downscaled from global datasets during 1901–2010. Over the country, terrestrial NPP showed significant inter-annual variations ranging 1.2 Pg C year^{-1} to 1.7 Pg C year^{-1} during the 1901–2010. Overall, multiple environmental changes have increased terrestrial NPP by 0.23 Pg C year^{-1}. Elevated CO_2 concentration has increased the NPP by 0.29 Pg C; however climate change has offset a portion of terrestrial NPP (0.11 Pg C) during the study period. On an average, terrestrial NPP reduced by 0.12 Pg C year^{-1} in drought years, when precipitation was at least 100 mm year^{-1} lower than long term average, suggesting that the carbon cycle in terrestrial India is strongly linked to climate. LCLUC, which includes the effects of both land conversions and cropland management, increased terrestrial NPP by 0.043 Pg C year^{-1} over the country.

This chapter has been accepted in *Climatic Change*; the citation is: Banger, K., Tian, HQ, Bo Tao, Ren, W, Pan, S, Shree, SRS, & Yang, J, (2015). “Contribution of multiple environmental factors on terrestrial net primary productivity in India during 1901–2010”.

Tropospheric O_3 pollution reduced terrestrial NPP over the country by 0.06 Pg C year^{-1} and the decrease was comparatively higher in croplands that other biomes after 1980s. Our results have shown that climate change and tropospheric O_3 pollution may significantly offset the increase in terrestrial NPP due to elevated CO_2 concentration, LCLUC, and NDEP over India.

4.1 Introduction

Net primary productivity (NPP) is defined as the rate at which terrestrial plants capture atmospheric carbon dioxide (CO_2) in plant biomass per unit time and space (Chapin et al., 2006). At global scale, NPP plays an important role in regulating the atmospheric CO_2 concentration (Keeling et al., 1996) while also acts as a useful tool for estimating crop yield, forest production (Krausmann et al., 2013), as well as understanding the impacts of climate change on carbon cycle in the terrestrial-biosphere (Nemani et al., 2003). Therefore, terrestrial NPP has been measured at various spatial scales in major ecosystems across the globe (Scurlock et al., 1999; Cramer et al., 2001; Pan et al., 2014a).

The terrestrial NPP in India, home to 1.2 billion people, has been estimated from 0.4 Pg C to 4.6 Pg C year^{-1}by different inventory, modeling, and remote sensing methods (Hooda et al., 1996; Hingane, 1991; Chhabra and Dadhwal, 2004; Panigraphy et al., 2004; Nayak et al., 2013). In the last 110 years, the forest area has decreased from 90 million ha to 63 million ha and the croplands have increased from 92 million ha to 140 million ha (Tian et al., 2014), which could change the spatial and temporal pattern of terrestrial NPP in India. Various studies have shown that nitrogen fertilizer usage and irrigation over the country have increased crop productivity (DES, 2010).

In addition to cropland management, urbanization and industrial growth after 1950s have resulted in degradation of air quality with higher atmospheric nitrogen deposition (NDEP) and tropospheric ozone (O_3) pollution (Dentener et al., 2006; Ghude et al., 2014). Tropospheric O_3 influences stomatal conductance and photosynthesis processes, thereby impacting plant growth (Tjoelker et al., 1995; Booker et al., 2009). Using surface level measurements from Pune, India, Beig et al. (2008) have recently calculated the accumulated O_3 concentration over a threshold of 40 ppb (AOT40) and shown that O_3 concentration have surpassed the threshold levels that can inhibit vegetation and forest carbon uptake. In contrast, NDEP is a nitrogen source and therefore can stimulate plant growth.

Several studies have determined the long term trends in the terrestrial NPP in response to multiple environmental factors in India. For example, Nayak et al., (2013) reported that terrestrial NPP over the country increased linearly from 1.36 Pg C $year^{-1}$ to 1.47 Pg C $year^{-1}$ during 1981–2005, where the increase in cropland NPP was 5-folds greater (0.0036 Pg C $year^{-1}$) than forest (0.0007 Pg C $year^{-1}$). Using Advanced Very High Resolution Radiometer (AVHRR) satellite data with the Global Production Efficiency Model (GLO-PEM), Singh et al., (2011) reported that NPP has increased by 30% (from 3.56 Pg C $year^{-1}$to 4.57 Pg C $year^{-1}$) during 1983–1999, due to higher increase croplands while NPP in the forested regions remain unchanged. In another study, Bala et al., (2013) reported NPP that has increased from 0.83 Pg C $year^{-1}$ to 1.42 Pg C $year^{-1}$ and was driven mainly by elevated CO_2 concentration in different ecosystems. These studies have indicated an increase in terrestrial NPP; however did not quantify the effect of individual factor on changes in the terrestrial NPP for a long

time period. A better understanding of different factors affecting terrestrial NPP will improve the future terrestrial C flux and will be helpful tools to design regional scale mitigation strategies for reducing C emissions. Specifically in India, majority of the area is under croplands (Tian et al., 2014) and therefore alteration in the terrestrial NPP would be associated with food security.

In this study, we used a process based Dynamic Land Ecosystem Model (DLEM) to quantify the contribution of different environmental factors to determine the spatial and temporal pattern of terrestrial NPP in India during 1901–2010. Specific objectives of this research were to estimate the magnitude and trends in the terrestrial NPP over the country and to quantify the relative contributions of atmospheric CO_2 concentration, climate changes/variability, LCLUC, atmospheric nitrogen deposition (NDEP), and tropospheric O_3 on terrestrial NPP during 1901–2010.

4.2 Methods

4.2.1 Study area

India is located between 8–38^o N latitudes and 66–100^o E longitudes, covering a geographical area of approximately 328 million ha. The monsoon has significant influence on climate that accounts for approximately 80% annual rainfall in the country. In the recent decades, the economic growth and industrialization coupled with population rise has resulted in the LCLUC, NDEP, and tropospheric O_3 pollution which may alter terrestrial NPP over the country.

4.2.2 Dynamic Land Ecosystem Model (DLEM)

4.2.3 Input datasets

The DLEM needs five types of data sets including: (1) daily climate condition including average, maximum, and minimum temperature, precipitation, shortwave solar radiation, and relative humidity; (2) LCLUC datasets; (3) topography and soil properties (including elevation, slope and aspect; pH, bulk density, and soil texture represented as the percentage content of sand, silt, and clay); (4) atmospheric chemistry (e. g. tropospheric O_3, atmospheric CO_2 concentration and atmospheric nitrogen deposition) and (5) cropland management practices (nitrogen fertilizer usage, irrigation).

To generate annual LCLUC datasets at 5-arc minute grid resolution (approximately 8 km by 8 km), we incorporated high-resolution remote sensing datasets from Resourcesat-1 with historical archives at district and state levels in India (Tian et al., 2014). We focused on ten major crops that are representative of both dry farmland and rice fields or C_3 and C_4 plants, including: rice, wheat, cotton, millets, groundnut, sorghum, soybean, rapeseed, corn, and sugarcane. We used single cropping systems, and double cropping systems (rice-wheat; millet-wheat; soybean-wheat; rice-rapeseed; maize-wheat; cotton-wheat; rice-rice). The main crop categories in each grid were identified based on the global crop geographic distribution map available at 5-arc minute resolution (Leff et al., 2004), and were then modified according to the state level census data derived from Department of Economics and Statistics (DES, 2010). The nitrogen fertilizer datasets in the grid format were developed by using the fertilizer inventories available at the Department of Economics and Statistics, Government of India (DES, 2010).The annual irrigation maps were developed by integrating remote sensing

datasets with inventory datasets at district and state levels from the Ministry of Water Resources (http://wrmin.nic.in/) during 1901–2010. The information on the topography (elevation, slope, and aspect) was generated at 5-arc minute resolution (Banger et al., 2015).

The climate data were obtained from Climate Research Unit, National Centers for Environmental Prediction (CRUNCEP) at 0.5 × 0.5 degree resolution and were statistically downscaled from to 5-arc minute resolution using linear interpolations. Annual precipitation showed significant inter-annual variations; however no significant trend was observed. On the other hand, annual temperature has shown an increasing trend during the study period. The atmospheric CO_2 concentration data in the grid format was derived from the Carbon Dioxide Information Analysis Center (CDIAC, http://cdiac.ornl.gov/), which has shown that atmospheric CO_2 concentration increased from 295 ppm in 1901 to 392 ppm in 2010. The information on AOT40 dataset and NDEP was obtained from global datasets (Felzer et al., 2005; Dentener et al., 2006). The datasets were developed in different time steps. For example, climate and the AOT40 index data were organized at a daily time step, while the atmospheric CO_2 concentration, NDEP, and LCLUC data sets were developed at an annual time step.

4.2.4 Experimental Design

The implementation of the DLEM simulation includes the following steps: 1) equilibrium run, 2) spin-up run and 3) transient run. The primary purpose of the equilibrium run is to achieve the equilibrium state when net carbon exchange for 50 consecutive years is <0.5 g C m^{-2}, the net water pool change is <1.0 mm and the net nitrogen change is < 0.5 g N m^{-2} is made. At this step the model is driven by average

climate conditions from 1901 to 1930 and land use and land cover data in 1900. After that three thirty-year spin-up runs, driven by random data sequence of de-trended climate during 1901–1930, are conducted to reduce the biases in the simulations. In the transient run, the environmental factors from 1901 to 2010 were used to drive the model to produce transient simulation.

To determine the magnitude and relative contribution of different environmental factors, a total of seven simulation experiments were designed (Table 4.1). One overall simulation experiment (Multifactor) was set up to simulate the combined effect of seven environmental factors on terrestrial NPP over the country during 1901–2010. In addition, six experiments were set up to determine the relative contribution of individual environmental factor (climate, atmospheric CO_2 concentration, tropospheric O_3 pollution, NDEP, LCLUC, and nitrogen fertilizer on terrestrial NPP during 1901–2010. In the multifactor experiments all the environmental factors were transient during 1901–2010. In the other experiments, one factor was kept constant (to the level of 1901) while others were transient. One exception was No-Climate experiment in which climate was the 30-year mean of 1901–1930 (Table 4.1).

4.3 Results

4.3.1 Magnitude of Net Primary Productivity

The DLEM simulations have shown that terrestrial NPP over the country showed significant inter-annual variations ranging from 1.2 Pg C $year^{-1}$ to 1.7 Pg C $year^{-1}$ during 1901–2010 (Figure 4.1). Large spatial variations in the terrestrial NPP existed ranging from negative values to 1380 g C m^{-2} with a mean value of 460–530 g C m^{-2} during 1901–2010 (Figure 4.2). In general, there was a positive gradient of the terrestrial NPP

from drier north-western to northern-eastern regions (Prasad et al., 2007). Among the different land use types, NPP was highest in different types of forests (179–969 g C m^{-2}) followed by grasslands (324–927 g C m^{-2}) than croplands (342–431 g C m^{-2}) and shrublands (< 407 g C m^{-2}) (Table 4.2).

Among the different biomes, forests contributed to the highest amount of terrestrial NPP (0.63–0.67 Pg C $year^{-1}$; 41–47%) followed by croplands (0.33–0.59 Pg C $year^{-1}$; 25–38%) during the study period. However, relatively lower amount of terrestrial NPP was contributed by grasslands (11–16%) and shrublands (8.3–9.1%) during the study period.

4.3.2 Temporal Pattern of Net Primary Productivity

For studying the temporal pattern, we compared the decadal mean of terrestrial NPP over the country from the 1900s (mean of 1901–1910) to the 2000s (mean of 2001–2010). Our analysis has shown that total NPP at the national level has increased by 0.23 Pg C $year^{-1}$ (from 1.24 Pg C $year^{-1}$ to 1.49 Pg C $year^{-1}$) over the 20^{th} century and then leveled off or even had a slight decrease to 1.48 Pg C in the 2000s (Figure 4.1A). The increasing trend for terrestrial NPP was not linear during the study period. For example, rate of increase of terrestrial NPP was approximately 5-folds greater during 1951–2010 (0.0037 Pg C $year^{-1}$) than1901–1950 (0.002 Pg C $year^{-1}$). Among the biomes, the NPP has increased from 342 g C $year^{-1}$ to 431 g C $year^{-1}$ in croplands, 179–823 to 249–969 g C $year^{-1}$ in forests, and 282 g C $year^{-1}$ to 406 g C $year^{-1}$ in shrublands, and 324–927 g C $year^{-1}$to 406–837 g C $year^{-1}$ in grasslands during the study period (Figure 4.1A).

4.3.3 Relative contribution of environmental factors

The DLEM simulation results have shown that relative contribution of the different environmental factors on terrestrial NPP has varied significantly in India (Figure 4.1A). Among the factors studied, elevated CO_2 concentration was the most important factor that increased total NPP over the country by 0.29 Pg C (approximately 96 g C m^{-2}) during the study period. The response of atmospheric CO_2 concentration was lower in the first half of 20th century that increased in the later years due to higher increase in atmospheric CO_2 concentration as well interaction with other factors (e. g., nitrogen fertilizer usage and NDEP). Climate produced inter-annual variations since the precipitation anomaly was positively correlated (r = +0.34; *P< 0.001*) with terrestrial NPP during 1901–2010. Based on variation in 30-year averaged precipitation (1901–1930), we divided years into four categories (> 100 mm deficient, 1–100 mm deficient, 1–100 mm excess, and > 100 mm excess precipitation). In general, the terrestrial NPP was lower in the drought years during the study period. On an average, decrease in the terrestrial NPP was > 0.112 Pg C $year^{-1}$ when precipitation was >100 mm $year^{-1}$ lower than the long term average values. Overall, the climate factor has decreased the terrestrial NPP by 0.11 Pg C $year^{-1}$ during study period.

In this study, the LCLUC was the combined effect of two factors including land conversions and cropland management. In the central-east regions, a slight decrease in the terrestrial NPP was observed due to deforestation occurring during 1901–1950 (Figure 4.2). LCLUC increased terrestrial NPP by mean value of 0.043 Pg C $year^{-1}$ during 1901–2010 (Figure 3.1B). Majority of the increase in terrestrial NPP due to LCLUC has occurred in the croplands as a result of nitrogen fertilizers usage and

improvements in the irrigation facilities. Overall, NDEP has stimulated terrestrial NPP by 0.044 Pg C $year^{-1}$ and the response of NDEP on terrestrial NPP was relatively higher in the natural vegetation types indicating the nitrogen limitation of the natural vegetation in India. In the recent three decades, tropospheric O_3 pollution has become a significant factor that decreased terrestrial NPP by 0.061 Pg C $year^{-1}$.

4.4 Discussion

In this study, the DLEM simulated terrestrial NPP over the country ranged from 1.2 Pg C $year^{-1}$ to 1.7 Pg C $year^{-1}$ with strong inter-annual variations during 1901–2010 (Figure 3.1A). Overall, the terrestrial NPP estimated in this study is in the range of inventory based estimates of 1.24–1.6 Pg C $year^{-1}$(Dhadwal and Nayak, 1993; Hingane, 1991). In 2003, Nayak et al., (2010) estimated the terrestrial NPP in India using the CASA model (1.57 Pg C $year^{-1}$), C-Fix (1.45 Pg C $year^{-1}$), and MODIS NPP algorithms (1.30 Pg C $year^{-1}$), which are similar to the DLEM estimate (1.5 Pg C $year^{-1}$). However, the DLEM-based NPP estimate is lower than estimated using NOAA-AVHRR satellite data and the GLO-PEM model for 1981–2000 (Singh et al., 2011). It is possible that GLO-PEM ignores the nitrogen limitation and therefore overestimating the terrestrial NPP. Recently, Dan et al., (2007) shown that global and regional scale (China, USA, and Australia) terrestrial NPP estimated by the GLO-PEM was atleast 50% greater than the MODIS, IGBP, and CASA estimates. However, our estimations were similar but slightly higher than the MODIS based NPP estimates during 2001–2010. Usually, the MODIS products tend to be underestimate NPP in high productivity sites such as irrigated croplands because of relatively low values for vegetation light use efficiency in the MODIS GPP algorithm (Turner et al., 2006).

In this study, croplands contributed 25–38% of the terrestrial NPP over the country. However, the proportion of croplands to terrestrial NPP is lower than estimated by the CASA (56%) and C-fix (53%) models possibly due to higher due to higher cropland area (53%) in their LCLUC datasets (Nayak et al., 2010; Banger et al., 2013). The differences in the NPP in different biomes could be due to model mechanisms for treating LCLUC datasets. For example, some models can process only one plant functional type (PFT) in one grid cell while others adopt cohort structure containing more than one PFT per grid. Even for models with cohort-PFTs, their maximum PFT numbers in one grid cell may vary significantly.

4.4.1 Elevated atmospheric CO_2 concentration

Several field scale studies have shown that elevated CO_2 concentration (600 ppm) stimulated the plant biomass in grasslands (from 2.0 g $plant^{-1}$ to 2.87 g $plant^{-1}$), forests (Nataraja et al., 1998), and croplands (Vanaja et al., 2011). Using multivariate analysis, Bala et al., (2013) reported that elevated CO_2 concentration was the most important factor in increasing total NPP in India during 1982–2006. Results from Bala et al., (2013) were based on the correlation which has not quantified the magnitude of increase in total NPP due to elevated CO_2 concentrations. In another study, Bala et al., (2011) used the terrestrial carbon model to simulate the effects of increased CO_2 levels (735 ppm) on terrestrial carbon uptake in India by the end of 21st century. Interestingly, they found that elevated CO_2 concentrations would contribute to approximately 84% increase in total NPP over the country by the year 2100 relative to 1975. Our DLEM simulations have shown that elevated atmospheric CO_2 concentration was the most important factor in increasing total NPP in 20th century in India.

4.4.2 Climate Change and variability

Our results agree with previous studies that reported strong inter-annual variations in total NPP resulted from climate variation tropical ecosystems (Bala et al., 2013; Singh et al., 2011; Tian et al., 1998; Tian et al., 2000; Tian et al., 2003). It has been demonstrated that in the EI-Nino years, which are anomalously warm and dry globally, Amazon evergreen rainforest act as C sources which are otherwise C sinks (Tian et al., 1998).

In India, Panigraphy et al., (2005) reported that terrestrial NPP was significantly lower in the drought year of 2002–2003 (1.88 Pg C $year^{-1}$) than normal year of 2004–2005 (2.51 Pg C $year^{-1}$) indicating the climate could introduce strong inter-annual variations in the NPP over the country. A drought year with > 100 mm $year^{-1}$ deficient annual precipitation decreased NPP by 0.12 Pg C $year^{-1}$ over the country. Our analysis has suggested that spatial pattern of precipitation played a significant role in dictating terrestrial NPP over the country. Interestingly, precipitation anomaly was positively correlated ($r = +0.34$; $P< 0.001$) with terrestrial NPP suggesting that droughts can strongly decrease the terrestrial NPP over the country. Using DLEM simulations, Pan et al., (2014b) reported that precipitation explained approximately 63% of the variation in terrestrial NPP, while the rest was attributed to changes in temperature and other environmental factors at a global scale. However, we are unable to separately quantify the effect of temperature and precipitation on terrestrial NPP in this study. The concerns about temperature extremes on croplands has been raised by scientific community; Lobell et al., (2012) reported that extreme temperature at grain filling stages in wheat could cause serious decreases in grain number and weight. However, the effect of

extreme climatic events at panicle stage is lacking in the DLEM. Overall, our results have demonstrated that climate variability can provide significant feedback to regional carbon cycle as well as food security in India.

4.4.3 Land cover and land use change

Similar to other studies, we found that land converted from low productive natural vegetation (C_3 grasslands and shrubs) to irrigated cropland could stimulate aboveground biomass production (Ren et al., 2012; Davidson & Ackerman, 1993). In southern Idaho, US, Entry et al. (2002) reported that irrigated croplands under conservation tillage significantly increased plant biomass production over the native sagebrush ecosystem. This was evident from the fact that majority of the increase in total NPP due to LCLUC has occurred in the croplands for which nitrogen fertilizer application was the dominant factor after the 1950s. It has been reported in several field scale studies that nitrogen fertilizer application increased NPP in southern (Banger et al., 2009; Banger et al., 2010), northern (Ghosh et al., 2009), and north eastern parts of India (Mandal et al., 2007). Interestingly, the response of nitrogen fertilizer application started in the 1960s and increased linearly up to the 1980s then leveled off and decreased in 2000s. This has indicated that croplands in India might have attained nitrogen saturation or the plant growth might have been limited by other environmental factors studied. This could be partially supported from the fact that NDEP has not significantly affected the terrestrial NPP in cropland dominated Indo-Gangetic plains.

4.4.4 Tropospheric Ozone pollution

Tropospheric ozone (O_3) is currently considered to be the most important air pollutant affecting plant productivity in most parts of the world (Ollinget et al., 1997;

Reich, 1987; Mittal et al., 2007; Ren et al., 2011), not only because of its phytotoxicity (Krupa et al., 2001) but also because its concentration has risen at a rate of 0.5–2% per year during the past three decades (Vingarzan, 2004). A global photochemical model identified parts of Asia including the northern part of India as having the highest rate of increasing O_3 concentrations by 2030 using a business-as-usual scenario (Dentener et al., 2005). Recently, assessment of ground level data from different areas of Asia clearly showed that O_3 concentrations have already reached to the levels which can significantly reduce agricultural productivity across Asia (Mittal et al., 2007).

We estimated that elevated O_3 concentration has decreased the overall NPP in all the biomes by 4.2% (0.06 Pg C $year^{-1}$) during 1901–2010. The biome level analysis has shown decline in NPP due to tropospheric O_3 was higher in the croplands (7.4%) in 2000s. By using the district wise crop distribution maps and response of O_3 to crop yield for the year 2005, Ghude et al., (2014) reported that O_3 has reduced crop yield by 9.2% over the country. Our DLEM simulations have estimated a loss of 8.3% loss in NPP in the year 2005 which is comparable with Ghude et al., (2014). In a meta-analysis based on database from 53 studies carried out between 1980 and 2007, Feng et al., (2008) reported that elevated O_3 (an average of 72 ppb) has decreased the grain yield by 29% and above ground biomass by 18% in modern wheat varieties (Feng et al., 2008). In studies where elevated O_3 range was 31–59 ppb (average 43 ppb) has resulted in a decrease of 18% grain yield relative to the control treatment in wheat crop. For example, Ambasht and Agrawal (2003) reported that exposure of enhanced ozone (0.7 µmol mol^{-1}) has decreased the spring wheat yield by 10% (from 472 g m^{-2} in control to 431 g m^{-2} in elevated O_3 treatment) in India. This is the first quantification that shown

that elevated O_3 concentration can decline the terrestrial NPP not only in croplands but also in natural vegetation types over the country. However, our results warn scientific community and policy makers that elevated O_3 concentration has significantly affected NPP in croplands and therefore is a threat to food security in India.

4.5 Uncertainties

In this study, we believe that several uncertainties could have arisen from model structure, parameter estimations, and input datasets. Though, we have intensively calibrated the DLEM simulation results against field scale observations, however still several uncertainties exist in the calibration process. In croplands, we used crop yield as well as harvest index values from literature which may introduce some uncertainties in the calibration process. The studies on the belowground carbon pools were lacking in the field studies used in the validation and therefore our model validation is based on the aboveground biomass only. Currently, we have assumed only two irrigation scenarios in the croplands. In the first scenario, irrigation is always applied once the water content is below the field capacity while in the second scenario irrigation is never applied in the croplands. However, irrigation application depends on the water availability and is not always applied immediately after water content comes below field capacity. The nitrogen fertilizer dataset in the grid format was generated using the nitrogen fertilizer application at state level which is improvement over the FAO datasets available at national level only. In the future, nitrogen fertilizer dataset can further be improved using district level fertilizer statistics. In the tropical ecosystems, phosphorus limitation can affect NPP which was lacking in the current version of the DLEM. In this way, the DLEM might have ignored few divergences in the NPP due to phosphorus

limitation especially in the highly weathered soils which are distributed in the southern parts of India.

4.6 Conclusions

Using the DLEM simulations, we have shown that the terrestrial NPP ranged from 1.2 Pg C $year^{-1}$ to 1.7 Pg C $year^{-1}$ over India during 1901–2010. The terrestrial NPP has increased linearly from the 1900s to the 1980s and then reached plateau resulting in overall increase of 0.23 Pg C $year^{-1}$ during the 110 year time period. Elevated CO_2 concentration stimulated terrestrial NPP by 0.29 Pg C $year^{-1}$ which was partially offset by climate that not only produced inter-annual variations but also decreased terrestrial NPP by 0.11 Pg C $year^{-1}$ during the study period. LCLUC stimulated the terrestrial NPP over the country. However, the response of nitrogen fertilizer to terrestrial NPP was comparatively higher during 1960–1980s than later years indicating that crop growth was limited by other environmental factors. In the recent three decades, tropospheric O_3 pollution reduced the terrestrial NPP by 4.2% (0.06 Pg C $year^{-1}$) and the effect is slightly higher croplands (7.4%) than other biomes in the 2000s thereby suggesting that tropospheric O_3 pollution is a threat to Indian food security. In this study, we used several observations on the cropland management on crop yield (and NPP) changes but site level observations on the influence of several environmental changes (elevated CO_2 concentration, NDEP, and tropospheric O_3 pollution) were limited. We believe that future efforts on the field scale studies would be useful asset for calibration and validation of process-based modeling approaches.

4.7 Acknowledgments

This study has been supported by NASA Land Cover and Land Use Change Program (NNX08AL73G_S01; NNX14AD94G) and US National Science Foundation Grants (AGS-1243220, CNS-1059376).

A. Magnitude of NPP in different simulation scenarios

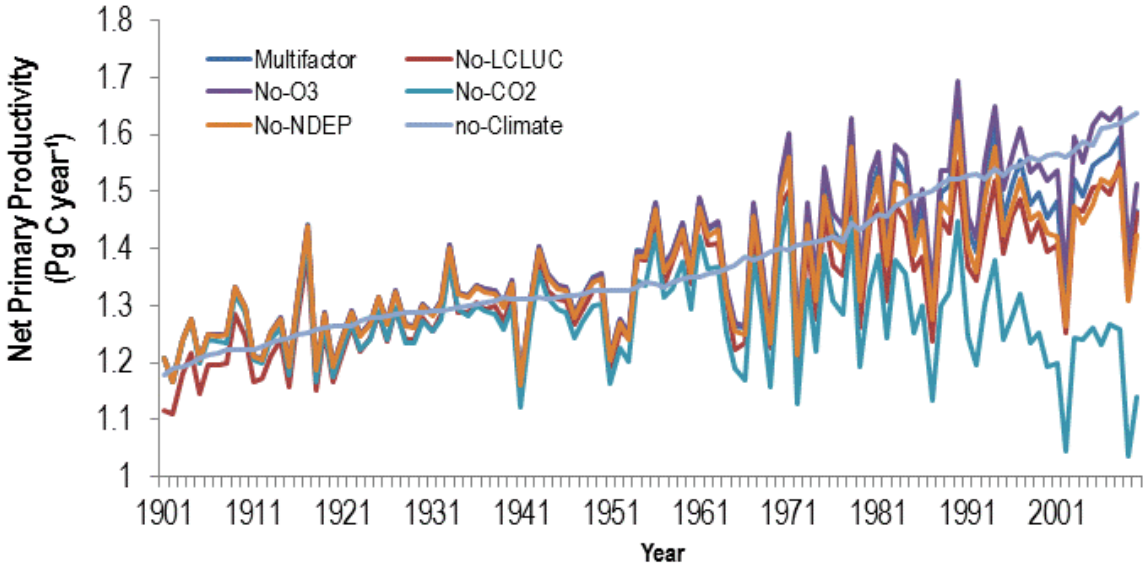

B. Contribution of different factors to changes in NPP

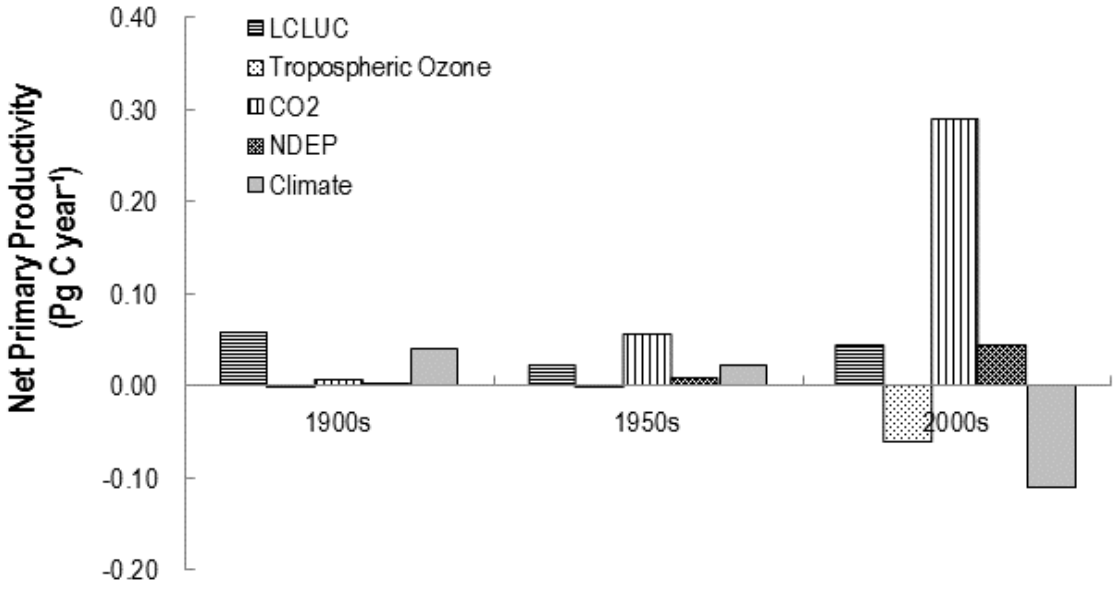

Figure 4.1. Contribution of the land cover and land use change (LCLUC), tropospheric ozone (O_3) concentration, elevated carbon dioxide (CO_2) concentration, atmospheric nitrogen deposition (NDEP), and climate on net primary productivity (Pg C $year^{-1}$) during 1901–2010.

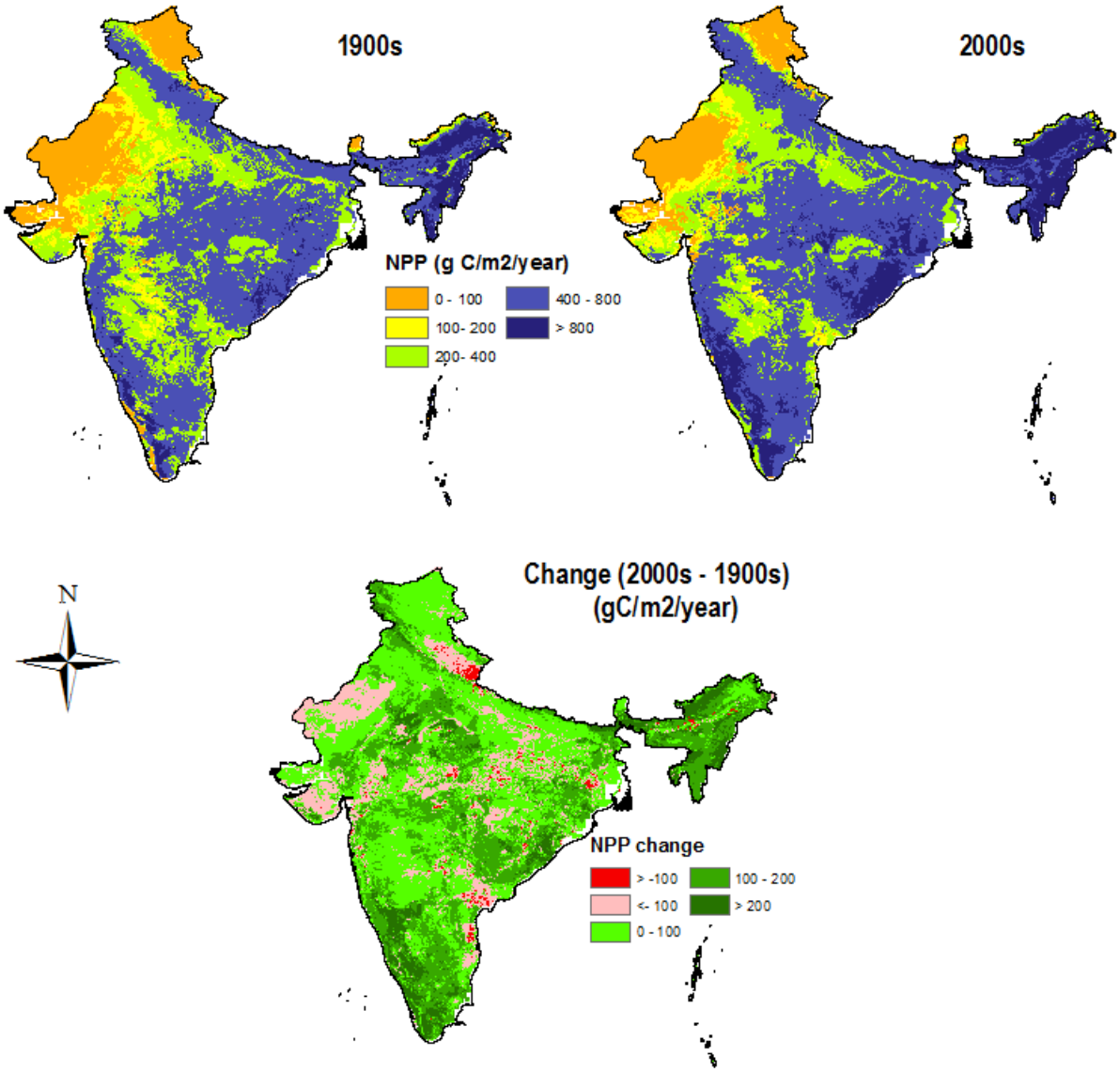

Figure 4.2. Contemporary spatial pattern and long term trends in the net primary productivity (g C m^{-2}) in India during 1901–2010.

	Simulation	Climate	CO_2	O_3	NDEP	LCLUC	Nfer	Irrigation
1	Multifactor	1901–2010	1901–2010	1901–2010	1901–2010	1901–2010	1901–2010	1901–2010
2	No-Climate	30-year average£	1901–2010	1901–2010	1901–2010	1901–2010	1901–2010	1901–2010
3	No-CO_2	1901–2010	1901	1901–2010	1901–2010	1901–2010	1901–2010	1901–2010
4	No-O_3	1901–2010	1901–2010	1901	1901–2010	1901–2010	1901–2010	1901–2010
5	No-NDEP	1901–2010	1901–2010	1901–2010	1901	1901–2010	1901–2010	1901–2010
6	No-LCLUC	1901–2010	1901–2010	1901–2010	1901–2010	1901	1901	1901
7	No-Nfer	1901–2010	1901–2010	1901–2010	1901–2010	1901–2010	1901	1901–2010

£ indicate the 30 year mean value from 1901-1930. Multifactor includes historical changes in climate, carbon dioxide (CO_2), tropospheric ozone (O_3), atmospheric nitrogen deposition (NDEP), Land cover and land use change (LCLUC), nitrogen fertilizer (Nfer); No-Climate, No-CO_2, No-O_3, No-NDEP, No- land conversions, No-Nfer are the Multifactor simulation experiments without changes in climate (precipitation, temperature, short wave radiation), CO_2, O_3, NDEP, land conversions, and Nfer, respectively.

Table 4.1. Experiment design for quantifying the magnitude as well as attribution of different environmental factors on net primary productivity in India.

Biome	Net Primary productivity (g C m^{-2} $year^{-1}$)		
	1900s	1950s	2000s
Croplands	342.0±23.0	354.1±34.2	431.3±42.4
Temperate Broadleaf Deciduous Forest	499±36.5	541.0±45.5	619.2±76.8
Temperate Broadleaf Evergreen Forest	740.4±22.2	816.9±34.8	937±39.1
Temperate Needle leaf Deciduous Forest	511±25.9	554±50.2	654±59.9
Temperate Needle leaf Evergreen Forest	179±45.4	193±43.3	249±66.4
Tropical Broadleaf Deciduous Forest	679±56.7	742±113.6	811±83.9
Tropical Broadleaf Evergreen Forest	823±36.5	889±48.8	969±67.1
Shrubs	282±14.1	309±16.2	406±30.1
C3-Grass	324±26.7	339±39.3	360±27.1
C4-Grass	927±56.7	924±99.3	837±67.1

Table 4.2. DLEM simulated net primary productivity (g C m^{-2} $year^{-1}$) in different biomes.

Chapter 5. Magnitude, Spatiotemporal Patterns, and Controls for Soil Organic Carbon Stocks in India during 1901–2010

Abstract

To the best of our knowledge, no attempts have been made to understand how environmental changes that occurred in the 20th century have altered soil organic carbon (SOC) dynamics in India. In this study, we applied a process-based Dynamic Land Ecosystem Model (DLEM), to estimate the magnitude as well as to quantify the effects of climate change and variability, land cover and land-use change (LCLUC), carbon dioxide (CO_2) concentration, atmospheric N deposition (NDEP), and tropospheric ozone (O_3) on SOC stocks in India during 1901–2010. The DLEM simulations have shown that SOC stock ranged from 20.5 to 23.4 Pg C (1 Pg = 10^{15} g), majority of which is stored in the forest covers located in the north-east, north, and few scattered regions in the southern India. During the study period, soils have sequestered SOC by 2.9 Pg C over the country. Elevated CO_2 concentration has increased total SOC stocks over the country by 1.28 Pg C, which was partially offset by climate change (0.78 Pg C) and tropospheric O_3 pollution (0.20 Pg C) during 1901–2010. Interestingly, LCLUC increased SOC stock by 1.7 Pg C thereby suggesting that SOC loss from deforestation was offset by the conversion of low productive fallow lands and other lands to croplands that received irrigation along with N fertilizers. Atmospheric N deposition (NDEP) has increased biomass production and increasing SOC by 0.5 PgC

This chapter has been accepted in *Soil Science Society of America Journal*; the citation is: Banger, K., Tian, HQ, Tao, Bo, Lu, C, Ren, W, & Yang, J, (2014). “Magnitude and drivers for soil organic carbon stocks in India during 1901–2010” (accepted in Soil Science Society of America Journal, in press).

over the country. This study has demonstrated that the benefits from elevated CO_2 concentration, cropland management practices, and NDEP in sequestering SOC stocks were offset by climate change and tropospheric O_3 pollution which should be curbed using policy framework in India.

5.1 Introduction

Soil organic carbon is the largest (1400–1500 Pg C) and one of the most important terrestrial carbon pool (Johnston et al., 2004) that can alter ecosystem functions by affecting soil physical (Six et al., 2002) and biogeochemical properties (Banger et al., 2010). Soil organic C stock represents the net balance between C inputs from litter falls and the C losses such as CO_2 release because of microbial decomposition, fires, natural methane (CH_4) emissions, as well C export from hydrological leaching and soil erosion (Regnier et al., 2013; Scharlemann et al., 2014). Therefore, accurate estimation of the magnitude and trends in the SOC stocks at regional scales may help us better understand the interactions among climate, ecosystems, and humans, as well as to better assess C exchanges between the terrestrial biosphere and the atmosphere (Tian et al., 2003).

In general, global environmental factors can alter the C input and output balance in terrestrial ecosystems resulting in changes in the SOC stocks (Jenny and Raychaudhuri, 1960; Davidson and Janssens, 2006). For example, rising temperature can decrease the SOC stocks by stimulating decomposition while the response may be modified by soil properties and hydrological conditions (Davidson and Janssens, 2006). Elevated CO_2 concentration increases above and below ground plant biomass (Norby et al., 2004; Jastrow et al., 2000; de Graaff et al., 2006) thereby enhancing the SOC

stocks (Jastrow et al., 2005). The effects of land conversions on SOC stocks are complex which depend on land conversion types, climate, and cultivation stage (Don et al., 2011; Wei et al., 2014). In a region of 88, 000 km^2 in south India, Lo Seen et al., (2010) reported that despite the deforestation, SOC stock was maintained due to C sequestered by the irrigated croplands elsewhere in the landscape during 1977–1999. Several studies have demonstrated that N fertilizers usage increased SOC stocks (Banger et al., 2010; Mandal et al., 2008; Tian et al., 2012).

In India, large changes in the environmental factors have occurred in the 20th century that can affect SOC stocks. For example, total forest cover has decreased from 90 to 63 million ha while total cropland area has increased from 92 to 140 million ha during 1901–2010 (Tian et al., 2014). In addition, N fertilizer usage that started in the 1950s and increased to >7 g N m^{-2} in the 2000s, which can have significant effects on the SOC stocks in croplands (Banger et al., 2010; Mandal et al., 2007). The urban expansion was significant especially after the 1950s that coupled with industrial growth has resulted in air pollution (Tian et al., 2014). Using surface level measurements from Pune, India, Beig et al. (2008) have recently reported that tropospheric O_3 concentration have surpassed the threshold level in most parts of the year that can decrease SOC stocks by reducing plant growth. In this way, regional changes (LCLUC, air pollution etc.) coupled with several global scale changes (climate, elevated atmospheric CO_2 concentration, and NDEP) that may have significant effects on the SOC stocks in India.

Several studies have estimated SOC stocks using SOC densities and land use area in India. By multiplying the area under different land use type with SOC density obtained from Ajtay et al. (1979) and Schlesinger (1983), Dadhwal and Nayak, (2003)

estimated SOC stock in the range of 23.4 to 27.1 Pg C. Gupta and Rao (1994) analyzed SOC density in 48 soil series and estimated the SOC stock of 24.3 Pg C (soil depth of 44 to 186 cm), which was approximately three folds lower (63 Pg C) than estimated by Bhattacharyya et al. (2000). In another study using SOC densities in different soil orders and agro-ecological regions, Velayutham et al. (2000) have estimated SOC pool as 47.5 Pg C in India. Interestingly, these studies extrapolated national SOC from field scale SOC densities and showed significant discrepancies which may be due to lack of accurate representation of actual environmental conditions (Powers et al., 2011). These studies indicate that a significant uncertainty exists in the magnitude of SOC stocks in terrestrial ecosystems of India.

In the previous studies, one of the major drawbacks was lack of quantitative estimation of effects of different environmental factors that have occurred in 20th century on SOC stocks in India. In this study, we used the process-based DLEM (Tian et al., 2011) to estimate magnitude of SOC stock as well as the impacts of its controlling factors during 1901–2010. Specific objectives of this research were to (i) estimate the magnitude of SOC, (ii) assess the spatial and temporal patterns of SOC stocks during 1901–2010, and (iii) quantify the effects of different driving forces (Climate, atmospheric CO_2 concentration, tropospheric O_3 pollution, NDEP, LCLUC) on the changes in SOC stock in India during 1901–2010.

5.2 Materials and methods

5.2.1 Study area

Same as described in chapter 2.

5.2.2 Dynamic Land Ecosystem Model

Same as described in chapter 2.

5.2.3 Input data

Same as described in chapter 2.

5.2.3 Experimental Design

The implementation of DLEM simulations includes the following steps: (i) equilibrium run, (ii) spinning-up run and (iii) transient run. In the equilibrium run, an assumption is made that natural ecosystem should reach an equilibrium state at stable climate conditions with net C exchange for 50 consecutive years is <0.5 g C m^{-2}, the net water pool change is <1.0 mm, and the net N change is <0.5 g N m^{-2}. At this step the model is driven by average climate condition from 1901 to 1930 and LULC in 1900. After that 33-yr spin-up runs, driven by random data sequence of de-trended climate during 1901–1930, are conducted to reduce the biases in the simulations. In the transient run, the environmental factors from 1901 to 2010 were used to drive the model to produce transient simulation of ecosystem dynamics.

In this study, a total of seven simulation experiments were designed to determine the relative contribution of climate, atmospheric CO_2 concentration, tropospheric O_3 pollution, NDEP, and LCLUC on SOC stocks during 1901–2010. One overall simulation experiment (Multifactor) was set up to simulate the SOC stocks by considering the temporal and spatial dynamics of seven environmental factors on SOC stocks during 1901–2010 (Table 1). In addition, six experiments were set up to determine the relative contribution of individual environmental factor on SOC stocks during 1901–2010. In the Multifactor experiments all the environmental factors were dynamic during 1901–2010.

In the other experiments, one factor was kept constant (to the level of 1901) while others were dynamic. One exception was No-Climate experiment in which climate was the 30-yr mean of 1901–1930 (Table 5.1).

5.3 Results

5.3.1 Magnitude of Soil Organic Carbon Stocks

The DLEM simulations have shown that total SOC pools over the country ranged from 20.5 to 23.4 Pg C during 1901–2010 (Figure 5. 4). Of the total SOC stocks, forests stored largest portion (9.9–11.4 Pg C; 47–57% of total SOC) followed by croplands (3.9–7.8 Pg C; 19–33%). Other biomes including grasslands and shrublands stored approximately 20% of the total SOC at national level during 1901–2010. Among different land use types, mean SOC density was highest in forests (13231–25905 g C m^{-2}) followed by croplands (5937 g C m^{-2}), shrublands (2667–5095 g C m^{-2}), and grasslands (4359–6158 g C m^{-2}; Table 5.3).

5.3.2 Spatial and Temporal Pattern of Soil Organic Carbon

Regional analysis has shown that the SOC density varied four orders of magnitude ranging from <10 g C m^{-2} in the western to >24000 g C m^{-2} in the eastern regions with a mean value of 7786 to 8230 g C m^{-2} over the country (Figure 5.3). There was negative gradient in SOC density from forest dominated and high precipitation areas in the north-east to relatively drier north-western parts.

During the study period, SOC stock has increased by 2.9 Pg C from 20.5 Pg C in 1901 to 23.4 Pg C in 2010 (Figure 5.4). Our analysis has demonstrated that a trend in the total SOC stock over the country was not linear during the study period. Overall, the SOC accrual rate per year was three folds lower in the first half (14.4 Tg C yr^{-1}) than

later half of 20th century (44.7 Tg C yr^{-1}). Comparatively, higher increase in the SOC density has occurred in the Indo-Gangetic plains and few scattered areas in the north-eastern and southern parts where croplands are dominant (Figure 5.3). However, SOC density decreased in the north-western dry regions as well in the central India during the study period.

5.3.3 Contribution of Environmental Factors to Changes in the Soil Organic Carbon

The multifactor simulation experiment has shown that total SOC stock has increased during 1901–2010, however, the relative contribution of the different environmental factors varied during the study period (Figure 5.5). This study has shown that elevated atmospheric CO_2 concentration accounted for 42% of the increased SOC stocks (1.28 Pg C) over the period of 110 yr. The LCLUC contributed to 35% of the increase in SOC stocks (1.7 Pg C) which is primarily due to the improvements in the cropland management which stimulated the plant growth during the study period in India. Of the LCLUC, N fertilizer usage alone increased the SOC stocks by 0.68 Pg C. Atmospheric N deposition contributed to 14.9% of the increase in the total SOC stocks, majority of which has occurred in the forest and grasslands but not in croplands.

The DLEM simulations have shown that benefits from elevated CO_2 concentration and NDEP in increasing SOC stocks were partially offset by climate change that decreased SOC stocks by 0.78 Pg C during the study period. In addition to climate change, tropospheric O_3 pollution had smaller but negative effects that decreased total SOC stocks by ~6.8% (0.20 Pg C) over the country. Regional analysis

has shown that the decrease in SOC stocks due to tropospheric O_3 pollution has occurred in the croplands in the Indo-Gangetic plains as well as central India.

In the 110-yr time period, the relative contribution of different environmental factors on SOC stock showed temporal variations (Figure 4. 5). In the 1900s and 1950s, the changes in the SOC stocks were primarily driven by LCLUC and climate change while CO_2 concentration had smaller effect on SOC stocks. However, elevated atmospheric CO_2 concentration became dominant in the 2000s followed by LCLUC, climate, NDEP, and tropospheric O_3 pollution.

5.4 Discussion

In this study, the DLEM simulated SOC in soils of India ranged 20.5 to 23.4 Pg C which accounts for approximately 2% of the global SOC (Table 5.2). Our results were similar to estimates from Dadhwal and Nayak, (1993), who reported total SOC stocks in the range of 23.4 to 27.1 Pg C in India (Table 4.2). For estimating the SOC stocks, Dadhwal and Nayak, (1993) multiplied average global SOC densities obtained from Ajtay et al. (1979) and Schlesinger (1983) with total area under different land use and land cover types. In an another study, Gupta and Rao, (1994) estimated total SOC stock as 24.3 Pg C by using SOC density in 48 soil series representative sites for all 12 soil classes in 22 agro-ecological regions. In contrast, Bhattacharyya et al. (2000) reported higher range for SOC stock (20.9 Pg C at 0 to 30 cm to 63 Pg C at the 0- to 150-cm depth) thereby indicating that soil depth considered may significantly alter SOC stock estimates. However, Bhattacharyya et al. (2000) estimates were based on physiographic regions and did not SOC density in different land use and land cover types.

The biome level analysis has indicated that our estimate of SOC stocks in forest soils were higher (9.9–11.4 Pg C) than previous ones based on average global SOC densities in forests (5.4–6.7 Pg C) by Dadhwal et al. (1998) and Chhabra et al. (2003) who considered the soil depth up to 100 cm. In a recent study, Velmurugan et al. (2014) have estimated that SOC stocks in the forest soils was 7.6 Pg C up to a depth of 100 cm. Lower soil depth may be the reason for the underestimation of SOC stocks in forest soils by Velmurugan et al. (2014) in India.

5.4.1 Temporal Pattern of Soil Organic Carbon Stored in Different Biomes

The DLEM simulations indicate that multiple environmental changes have increased total SOC stock over the country by 2.9 Pg C from 20.5 Pg C in the 1900s to 23.4 Pg C in the 2000s (Figure 5.4). The biome level analysis has shown that SOC stock in the forest soils has decreased from 11.4 to 9.9 Pg C primarily due to deforestation that has occurred during 1901–2010. Previously, Richard and Flint, (1994) computed that the historic loss of SOC stocks due to deforestation was 4 Pg C during 1880–1980. However, Richard and Flint, (1994) have used constant SOC density while significant increase in the SOC density has occurred in India due to elevated CO_2 concentration and NDEP, which stimulates plant growth.

In our study, contribution of croplands to total SOC stock has increased from 19% in the 1900s to 39% in 2010. This is the combined result of croplands expansion as well as higher biomass production in croplands that increased SOC density from 4282 to 7765 g C m^{-2} during the study period. In India, where majority of the population depend on the farming, monitoring long-term changes in the SOC stocks and identifying

the factors driving such changes are essential to maintain and improve crop productivity.

5.4.2 Atmospheric Carbon Dioxide Concentration

In this study, we quantified the effects of different environmental factors on total SOC stocks during 1901–2010 (Figure 5.5). The DLEM simulation results showed that elevated atmospheric CO_2 concentration has increased SOC stocks over the country by 1.28 Pg C during 1901–2010. Elevated CO_2 stimulates photosynthesis and thereby increase above and belowground biomass resulting in increases in the SOC stocks (Morgan et al., 2004; Jastrow et al., 2005; de Graaff et al., 2006). In India, elevated atmospheric CO_2 concentration increased net primary production during 1982–2006 that can increase the plant residues entering into the soils (Bala et al., 2013). A few studies showed that elevated atmospheric CO_2 concentration experiments increase SOC stocks in native grasslands of Kansas (Jastrow et al., 2000; Williams et al., 2000, 2004). In a meta-analysis, Jastrow et al. (2005) reported that SOC stock has increased by 5.6% in over 2 to 9 yr due to higher root production in response to the elevated CO_2 concentration. The DLEM simulations have shown that rising CO_2 concentration increased the terrestrial net primary productivity by 0.29 Pg C yr^{-1} over the country during the study period (data not shown). Therefore, increase in the SOC stock due to elevated CO_2 concentration can be attributed to the increased terrestrial biomass production during the study period.

5.4.3 Climate Change and Variability

The DLEM simulation results showed that climate change and variability has reduced the SOC stock over the country by 0.78 Pg C during 1901–2010. Interestingly,

majority of the climate-induced decline in the SOC stocks has occurred after the 1950s due to relatively higher increase in temperature as well as occurrence of rapid extreme drought years that affected net primary productivity (Chapter 4). In general, net primary productivity in the monsoon Asia depends on the climate change that can alter C balance (Tian et al., 2003). It has been shown that higher temperature especially the extreme climatic events (high temperature and lower precipitation) decreases net primary productivity resulting in lower C inputs into the soils. In this study, highest decrease in the SOC stocks due to climate change has occurred in the 2000s due to occurrence of two extreme drought years (2002 and 2009) that significantly decreased net primary productivity over the country (data not shown). Further, higher temperature increases soil respiration (Bond-Lamberty and Thompson, 2010) and thereby decreasing SOC stocks. Therefore, the DLEM simulations have shown a positive feedback between climate change and SOC decline, which may have long-term implications for SOC stocks in India

5.4.4 Land Cover and Land-Use Change

Land cover and land-use change has increased SOC stock over the country by 1.7 Pg C during 1901–2010 (Figure 5.5). In India, major land conversion included the cropland expansion from low productive fallow lands, grasslands, and forests which is one of the major drivers for changes in the SOC stocks in monsoon Asia (Tian et al., 2014; Tao et al., 2013). In general, conversion of productive forests into croplands decreases SOC stocks as a result of disturbance as well as lower inputs of non-soluble C materials in croplands than forests (Davidson and Ackerman, 1993; Post and Kwon, 2000). However, the DLEM simulated results have shown that net SOC stock has

increased due to LCLUC during the study period. This means that SOC lost due to deforestation was offset by the cropland expansion and cropland management in the low productive grasslands and fallow lands which had lower SOC density than croplands. Similarly, Lo Seen et al. (2010) reported that SOC from deforestation was offset by the development of irrigated croplands in southern India. In this study, we are unable to quantify changes in SOC stocks due to different types of land conversions. In southern Idaho, USA, Entry et al., (2002) reported that irrigated croplands under conservation tillage significantly increased SOC over the native sagebrush ecosystem. Natural vegetation in the low annual precipitation that supports relatively low plant production may experience SOC increases after conversion to irrigated agriculture systems due to higher biomass production.

In croplands, N fertilizer usage in croplands has increased SOC stocks by 0.68 Pg C during 1901–2010. This finding is supported from several field scale studies, which reported that N fertilizer improve the crop yield and biomass resulting in SOC sequestration in southern (Banger et al., 2009), northern (Kukal et al., 2009; Ghosh et al., 2009), and northeastern parts of India (Mandal et al., 2007). In our study, SOC density in the croplands has increased from 4282 to 7765 g C m^{-2} primarily due to the cropland management practices followed during 1901–2010 (Table 5.3). In the rice fields, which were dominant in the Indo-Gangetic plains, N fertilizer usage could significantly alter the balance of methane and nitrous oxide emissions (Banger et al., 2012). Therefore, increase in the SOC stocks due to N fertilizer usage does not necessarily mean cooling feedbacks to the climate in Indian soils.

5.4.5 Other Environmental Factors

In this study, we have quantified the effects of NDEP and tropospheric O_3 pollution on SOC stocks in India during 1901–2010 (Figure 5 5). Overall, the combined contributions of these changes to changes in SOC were <15% during 1901–2010. Our results can be supported from previous studies that have shown positive effects of NDEP and the negative effects of tropospheric O_3 concentration on SOC stocks in China (Ren et al., 2011; 2012).

Elevated O_3 concentration tends to decrease plant biomass production by producing active oxygen species after diffusing into plant cells (Feng et al., 2008). Decline in the rate of carboxylation is also attributed to the negative effect of O_3 on Rubisco in rice seedlings (Agrawal et al., 2002). For example, Ambasht and Agrawal (2003) reported that tropospheric O_3 concentration reduced wheat yield from 472 to 431 g C m^{-2}. In a meta-analysis on 53 studies between 1980 and 2007 has shown that elevated levels of O_3 (an average of 72 ppb) have decreased grain yield by 29% and above ground biomass by 18% in modern wheat varieties (Feng et al., 2008). In a recent review, Ghude et al. (2014) reported that tropospheric O_3 can decrease crop yield over the entire country by 9.2% which may probably provide negative feedback to the SOC stocks in India. Therefore, tropospheric O_3 concentration has reduced SOC stocks by altering the biomass production during the study period. Till date, no other study is available that quantified contribution of these environmental factors on SOC stocks for such a long-time period in India.

5.5 Uncertainty and Needs for Future Research

We believe that several uncertainties could have arisen from model structure, parameter values, and input datasets used for the SOC estimation in our study. For example, phosphorus limitation that affects net primary production as well as C entering into the soils via biomass is lacking in the current version of the DLEM. In this way, DLEM might have ignored few divergences in the SOC density due to phosphorus limitation especially in the highly weathered soils in the southern parts of India. The parameter values estimated during the calibration process from errors in the measurements could be the source of uncertainty. In this study, we have calibrated DLEM against site level observations in the croplands and forests in different geographical regions (Figure 5.2b). We used several observations on the cropland management on SOC changes but site level observations on the influence of several environmental changes (elevated CO_2 concentration, NDEP, and tropospheric O_3 pollution) were lacking. Therefore, site level studies focusing on the influence of these global change factors on SOC stocks could further help modeling efforts for SOC estimation in India. Several discrepancies existed in the currently available land use and land cover datasets (Banger et al., 2013), we have used newly developed LULC datasets based on high resolution remote sensing datasets and finer resolution historical archives (Tian et al., 2014). However, uncertainties still existed in the forest cover density and cropping systems which were not reported in the inventory reports (DES, 2010). Although, we refined the FAO datasets on N fertilizer maps which used one value in India to state level fertilizer information compiled by DES (2010). However, specific information on manures (amount and type of manure) uses is still lacking.

5.5 Conclusions

The DLEM simulations have shown that SOC stock has increased by 2.9 Pg C from 20.5 to 23.4 Pg C during 1901–2010. Of the environmental factors studied, elevated atmospheric CO_2 concentration that stimulates plant biomass production has increased SOC stocks over the country by 1.28 Pg C during 1901–2010. Land cover and land-use change has increased SOC stocks by 1.7 Pg C primarily in the croplands where N fertilizer and irrigation management have increased crop growth resulting in SOC sequestration. Atmospheric N deposition has played smaller but significant role that increased SOC stock by 0.45 Pg C during study period. Climate was the single most important factor that decreased SOC stocks by 0.78 Pg C due to increase in heterotrophic respiration as well as due to frequent occurrence of drought years that reduced biomass production over the country. Tropospheric O_3 pollution that decreased plant biomass production has decreased SOC stocks by 0.2 Pg C though majority of the decline has occurred during 1980–2010. Therefore, climate change and tropospheric O_3 can significantly reduce SOC stocks over the country if not curbed by forming policies.

5.6 Acknowledgements

This study has been supported by NASA Land Cover and Land Use Change Program (NNX08AL73G_S01; NNX14AD94G) and US National Science Foundation Decadal and Regional Climate Prediction using Earth System Models Grants (AGS-1243220).

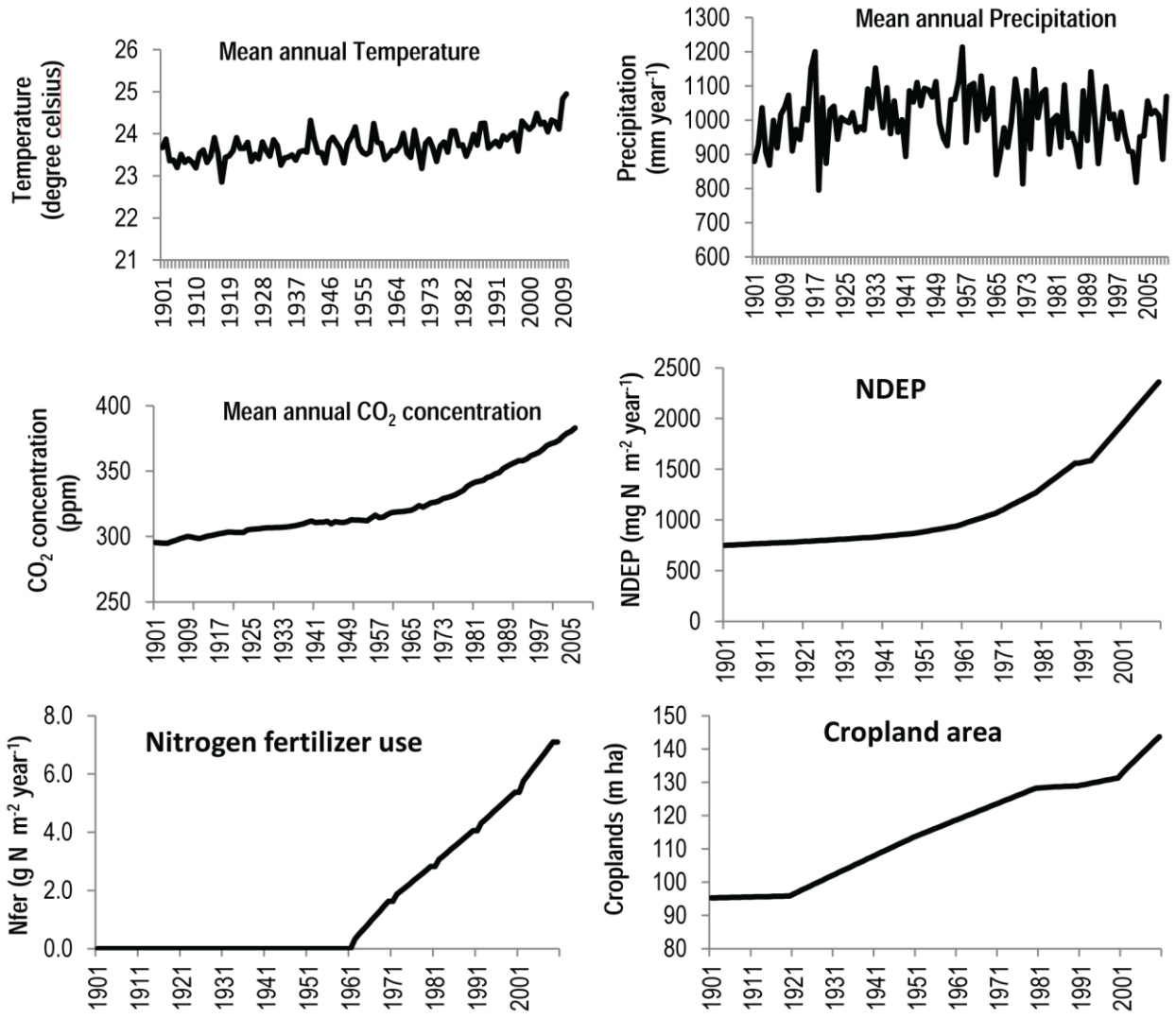

Figure 5.1. Temporal trends in the environmental factors in India during 1901–2010.

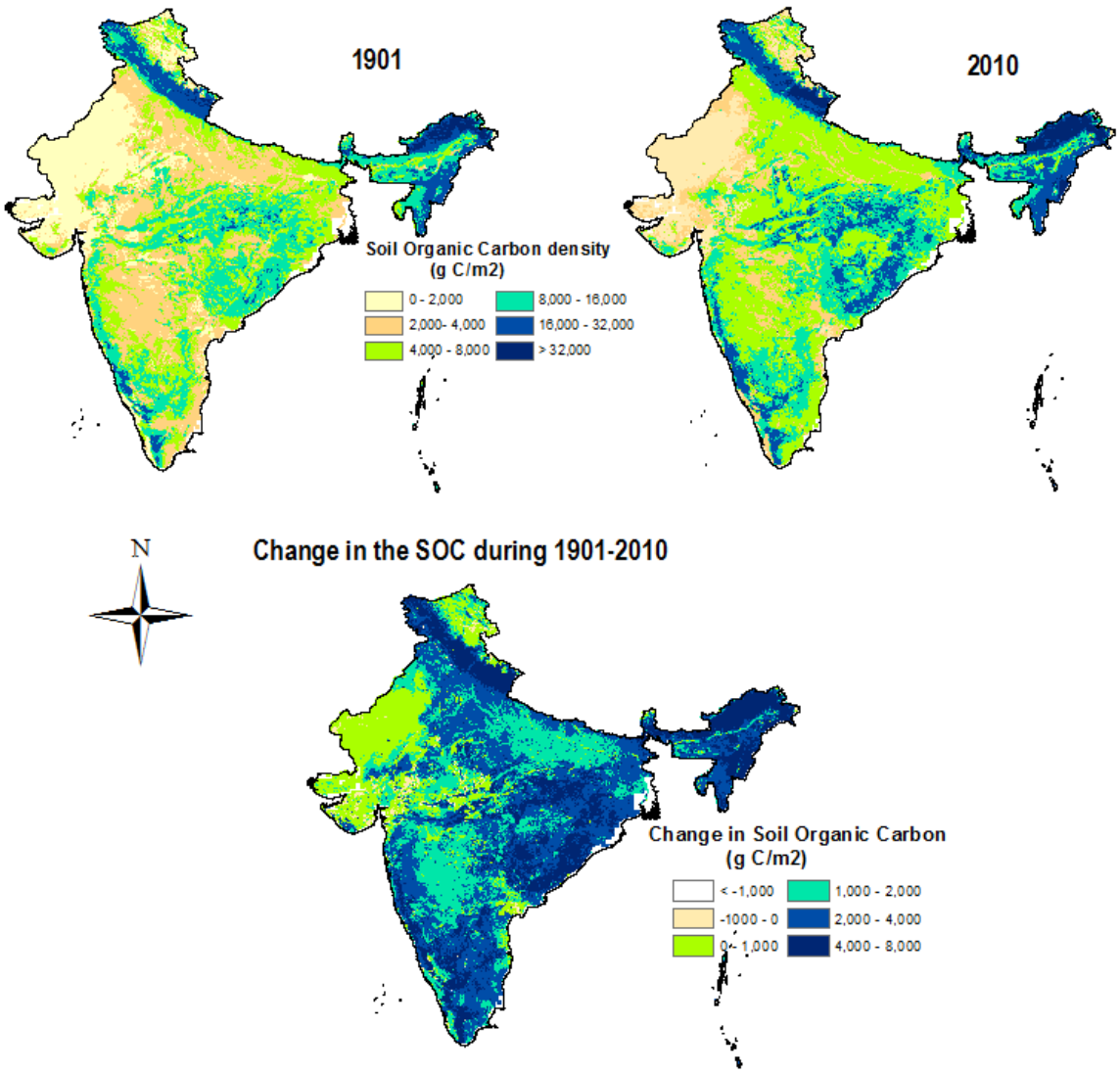

Figure 5.3 Spatial pattern and changes of soil organic carbon density (g C m^{-2}) during 1901–2010 in India.

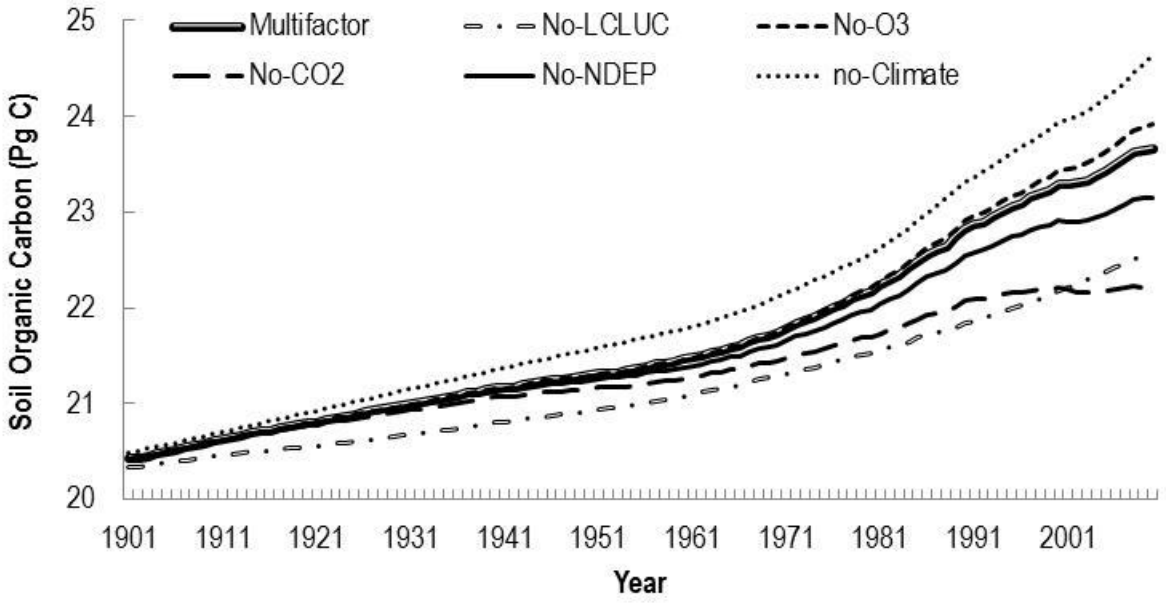

Figure 5.4 Temporal patterns of soil organic carbon (Pg C) in different simulation scenario's during 1901–2010.

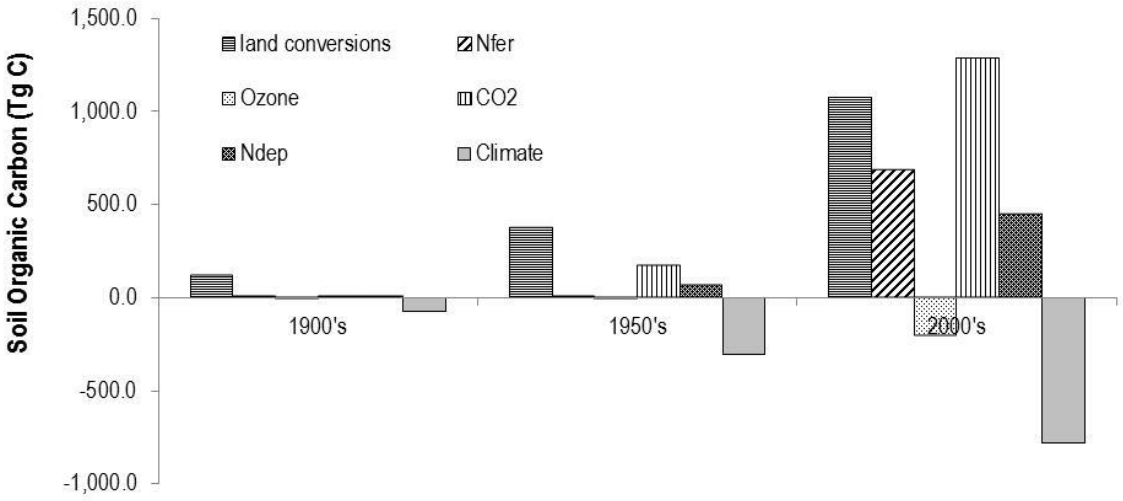

Figure 5.5 Relative contribution of the land conversion, nitrogen fertilizer (Nfer), tropospheric ozone (O_3) concentration, elevated carbon dioxide (CO_2) concentration, and atmospheric nitrogen deposition (NDEP) to soil organic carbon (SOC) stocks in India. Land cover and land-use change effects the sum of land conversions and land management.

	Simulation	Climate	CO_2	O_3	NDEP	LCLU	Nfer	Irrigation
1	Multifactor	1901–2010	1901–2010	1901–2010	1901–2010	1901–2010	1901–2010	1901–2010
2	No-Climate	30-yr average‡	1901–2010	1901–2010	1901–2010	1901–2010	1901–2010	1901–2010
3	No-CO_2	1901–2010	1901	1901–2010	1901–2010	1901–2010	1901–2010	1901–2010
4	No-O_3	1901–2010	1901–2010	1901	1901–2010	1901–2010	1901–2010	1901–2010
5	No-NDEP	1901–2010	1901–2010	1901–2010	1901	1901–2010	1901–2010	1901–2010
6	No-LCLUC	1901–2010	1901–2010	1901–2010	1901–2010	1901	1901	1901
7	No-Nfer	1901–2010	1901–2010	1901–2010	1901–2010	1901–2010	1901	1901–2010

†Multifactor includes historical changes in climate, carbon dioxide (CO_2), tropospheric ozone (O_3), atmospheric nitrogen deposition (NDEP), Land cover and land use (LCLU), nitrogen fertilizer (Nfer); No-Climate, No-CO_2, No-O_3, No-NDEP, No- land conversions, No-Nfer are the Multifactor simulation experiments without changes in climate (precipitation, temperature, short wave radiation), CO_2, O_3, NDEP, land conversions, and Nfer, respectively.

‡ indicate the 30 yr mean value from 1901–1930.

Table 5.1 Experiment design for quantifying the magnitude as well as attribution of different environmental factors on soil organic carbon in India.

Soil organic carbon	Soil depth	Method	Reference
Pg C	cm		
23.4–27.1	–	inventory	Dadhwal and Nayak 1993
24.4–26.5		inventory	Dadhwal and Nayak 1993
24.3	44–186	inventory	Gupta and Rao 1994
47.5	100	inventory	Velayuthum et al., 2000
20	0–30	inventory	Bhattacharyya et al., 2000
63	0–150	inventory	Bhattacharyya et al., 2000
20.5–23.4	–	DLEM	This study
5.4 (only forests)	–	inventory	Ravinderanath et al., 1997
5.9–6.2 (forests)	–	inventory	Dadhwal et al., 1998
7.6	0–100	inventory	Velmurugan et al., 2014
11.0–11.8 (forests)	–	DLEM	This study

Table 5.2 Comparison of different soil organic carbon estimations in India.

Land cover and land use	†Mean soil organic C, g C m^{-2}		
	1900s	2000s	Difference between (2000s–1900s)
Croplands	4282	7765	3483
Temperate broadleaf deciduous forest	8554	10710	2156
Temperate broadleaf evergreen forest	22249	23161	912
Temperate needle-leaf deciduous forest	15214	16123	909
Temperate needle-leaf evergreen forest	25669	26190	521
Tropical broadleaf deciduous forest	12730	13625	895
Tropical broadleaf evergreen forest	20205	21507	1302
Deciduous shrubs	2097	3851	1754
Evergreen shrubs	4223	6447	2224
C3 grass	3929	5165	1236
C4 grass	5812	6425	613

†1900s is the mean of 1901–1910; 2000s is the mean of 2001–2010.

Table 5.3 Dynamic Land Ecosystem Model (DLEM)-estimated soil organic C density in different land cover and land use types in the 1900s and 2010s.

Chapter 6. Net Exchange of CO_2, CH_4, and N_2O between atmosphere and terrestrial ecosystems of tropical Asia

Abstract

Recently, it has been suggested that tropical Asia is a net carbon sink; however emission of nitrous oxide (N_2O) and methane (CH_4) can offset the carbon uptake by the terrestrial biosphere. In order to conclude net cooling or warming effects of terrestrial biosphere to global climate, it is important to simultaneous quantify three GHGs together using a modeling framework. One of the major constraints in accurately estimating GHGs emissions from tropical ecosystems is the lack of phosphorus (P) cycling in the modeling framework. In this study, we have incorporated the P cycle in the modeling framework of the Dynamic Land Ecosystem (DLEM), and applied it to estimate the magnitude and spatial pattern of CO_2, CH_4, and N_2O emissions from terrestrial ecosystems of tropical Asia during 1901–2010. During the study period, tropical Asia was a net carbon source (13±12 Tg C $year^{-1}$); however it was a net carbon source till 1950s and became a carbon sink afterwards. A total of 20.4± 3.6 Tg C $year^{-1}$ of CH_4 and 0.70 ±0.09 Tg N $year^{-1}$ of N_2O emissions have occurred which had significant increasing trends during 1901–2010. The global warming potential (GWP) showed that tropical Asia had a strong warming feedback (1063 Tg CO2-equivalents $year^{-1}$), which did not show any significant trend since the increase in carbon uptake was offset by the increases in the CH_4 and N_2O emissions for which LCLUC was the primary factor in tropical Asia. Phosphorus (P) limitation has strongly affected the carbon uptake while the reduction is significantly greater in South-East than South Asia, thereby suggesting that P limitation is stronger in the high precipitation areas of South-

East Asia. Our results have suggested that CH_4 and N_2O emissions can strongly offset the carbon uptake in the tropical Asia. Also, the P can become a significant factor for reducing carbon uptake in the future; therefore research should focus on designing experiments on P fertilizer response in the tropical forests.

6.1 Introduction

The atmospheric concentrations of three greenhouse gases (GHGs) such as carbon dioxide (CO_2), methane (CH_4), and nitrous oxide (N_2O) have increased significantly since Industrial revolution which have been considered as important drivers for climate warming (Forster et al., 2007). Of three GHGs, CO_2 is released from fossil fuel consumption, cement production, and land use changes (Boden et al., 2010; Peters et al., 2012; Houghton, 2002), which contributes to 65% of the global warming. The global warming potential (GWP) is substantially higher for CH_4 (25-fold CO_2-equivalents) and N_2O (298-fold CO_2-equivalents) as compared to CO_2 at 100-year time scale (Forster et al., 2007), which contribue to one quarter of the anthropogenic climate warming. Recent studies suggest that CH_4 and N_2O emissions from terrestrial biosphere can largely offset or even overturn the climate cooling effects (Tian et al., 2015; Tian et al., 2011). Therefore, quantification of three GHGs together is critical for scientific community to estimate GWP (Lu and Tian, 2013) which may help policy makers to formulate climate mitigation strategies (Bonan, 1995).

Several efforts have been made to estimate terrestrial GHGs emissions in North America, Europe (Pacala et al., 2001; Janssens et al., 2003; Schulze et al., 2010), and China (Piao et al., 2010; Tian et al., 2009) but it is relatively unknown in tropical Asia (Patra et al., 2012), which is home of one quarter of the global population. Terrestrial

ecosystems in tropical Asia (South and Southeast Asia) play crucial roles in the regional and global carbon cycling (Flint and Richards, 1991; Richards and Flint, 1994; Tian et al., 2003; Zhang et al., 2014). In the 20th century, tropical Asia has experienced substantial increase in the human population, which coupled with economic growth has resulted in significant land cover and land use changes (Tian et al., 2014; Tao et al., 2013; Richards and Flint, 1994). For example, the cropland expansion rate was highest (Millennium Ecosystem Assessment, 2005) and had the highest deforestation rate (Achard et al., 2002) across the globe. A number of studies have reported that terrestrial ecosystems in tropical Asia have acted net carbon sinks (Zhang et al., 2014); however, it remains uncertain if terrestrial ecosystems have cooling or warming effect after considering CH_4 and N_2O. Thus, a comprehensive study which simultaneously examines the exchanges of CO_2, CH_4, andN_2O between atmosphere and tropical Asia is greatly needed.

To estimate GHGs from tropical ecosystems, one of the biggest constraints is the lack of phosphorus (P) cycling in the modeling framework (Yang et al., 2014). Unlike temperate, the tropical ecosystems are strongly limited by P availability (Yang et al., 2014), which can provide significant uncertainties in the GHGs estimations (Goll et al., 2012). Since P supplied primarily by the weathering of the fresh minerals, therefore P availability is high relatively early in soil development which decrease over time due to leaching, occlusion by secondary minerals, and the formation of recalcitrant soil organic matter (Walker and Syers, 1976). In ten Amazonian sites, Aragao et al. (2009) suggested that terrestrial NPP increased with the availability of soil P, which has also been revealed by others that P fertilizers stimulated forest NPP in tropics (Quesada et

al., 2012; Wright et al., 2011). Despite the importance of the P in regulating terrestrial carbon uptake in the tropical ecosystems, P cycle is lacking in the majority of the ecosystem modeling mechanisms with the exception of CASA (Carnegie– Ames–Stanford Approach)-CNP and JSBACH-CNP (Jena Scheme for Biosphere–Atmosphere Coupling) (Wang et al., 2007, 2009; Goll et al., 2012). Lack of P limitation could overestimate the carbon sink as well as the contribution of different environmental factors on carbon cycling. Recently, using JSBACH-CNP, Goll et al., (2012) have reported that global carbon uptake was 16% lower with P limitation as compared to simulations without P limitation in the tropical ecosystems. Therefore, lack of P limitation in the ecosystem models can produce significant uncertainties in the carbon budgets of the tropical Asia.

Here, we incorporated P pools and fluxes with the carbon and nitrogen cycles in the modeling framework on the Dynamic Land Ecosystem Model (DLEM). We applied the improved version of the DLEM driven by land cover and land use change, climate, CO_2 concentration, and atmospheric nutrient deposition to estimate the NCE in the tropical Asia at 0.25 degree resolution during 1900–2010.

6.2 Methods

Tropical Asia includes the South and Southeast Asia, which extends from 38° N to 16° S latitude and from 60° to 140° E longitude, encompassing a land area of approximately 5.0×10^6 km^2 and 4.7×10^6 km^2, respectively (Figure 1.1). In general, South Asia is agricultural and Southeast Asia is the world's third largest tropical rainforest (UNEP, 2009) forest area dominated region (Tao et al., 2013). South Asia includes the countries of Afghanistan, Bangladesh, Bhutan, India, Nepal, Sri Lanka, and

Pakistan, while the Southeast Asia covers Brunei, Burma, Indonesia, Cambodia, Laos, Malaysia, the Philippines, Thailand, and Vietnam. Both the South Asia and Southeast Asia are influenced by monsoons that bring strong seasonal changes in precipitation, and are subject to climate extremes, particularly floods and droughts.

6.3 Input datasets

6.3.1 Land cover and land use data development

In this study, we first generated the cropland and urban datasets in the grid format (0.25°×0.25°) by incorporating our newly developed Indian datasets (Tian et al., 2013) and the datasets from HYDE v3.1 (Klein Goldewijk et al. 2011) during 1900–2010. A potential vegetation map for entire tropical Asia was generated by combining multiple data sources. We first combined the distribution of different plant functional types from MODIS global land cover map (MOD12Q1 V004, http://duckwater.bu. edu/lc/mod12q1.html), which is similar to the classification used by the DLEM (Liu and Tian, 2010; Tian et al., 2011), with the global potential vegetation map developed by Ramankutty and Foley (1998) to derive the potential vegetation map. Both data sets were aggregated using the majority rule and their vegetation classes were regrouped to match the respective plant functional types defined in the DLEM. In the second step, global C4 grassland percentage map developed by Still et al. (2003) was used to determine the distribution of C4 grassland in the tropical Asia. In the final step, we identified the wetland area based on the half degree resolution Global Lakes and Wetlands Database (GLWD) developed by Lehner and Doll (2004). All the land use and land cover datasets were prepared at the annual time step from 1900–2010.

The results have shown that in the tropical Asia, total cropland area was 157 million ha in 1900 that has increased to approximately 291 million ha in 2010 (Figure 6.2). A significant deforestation has occurred in the tropical Asia and the area under forests has decreased from 332 million ha to 270 million ha during 1900–2010. In SE Asia, majority of the deforestation has occurred in Indonesia, Thailand, and Philippines. In Tropical Asia, the cropland area followed a continuous increasing trend during the study period, with a relatively slower rate after the 1960s (Tao et al., 2013). As compared to croplands and forests, a very few changes in the shrubland and grassland areas have occurred in tropical Asia during the study period (Figure 6.2).

6.3.2 Cropping systems datasets

Using inventory (DES, 2010) and remote sensing datasets (Leff et al., 2004), we identified ten crop types including rice (*Oryza sativa* L.), wheat (*Triticum aestivum* L.), cotton (*Gossypium hirsutum* L.), millets, groundnut, sorghum (*Sorghum bicolor* [L.] Moench), soybean (*Glycine max* [L.] Merr.), rapeseed (*Brassica napus)*, corn (*Zea mays* L.), and sugarcane (*Saccharum officinarum* L.). The major cropping systems includes single cropping system (rice only) and double cropping systems (rice–wheat; millet–wheat; soybean–wheat; rice–rapeseed; maize–wheat; cotton–wheat; rice–rice). The rotation type in each grid was developed using phenological characteristics and census data at the national level and state level (DES, 2010; Ren et al., 2011a, 2012). The MODIS 8-day LAI products (MOD15) during 2000–2008 (http://modis.gsfc.nasa.gov/data/dataprod) in conjunction with observation and survey datasets were used to identify rotation type and the contemporary patterns of phenologic metrics. This method has been used in various geographical regions

including Southern United States (Tian et al., 2010a, 2012), North American continent (Tian et al., 2010b; Xu et al., 2010), and China (Ren et al., 2011a, 2012; Tian et al., 2011a,b).

In this study, we have obtained the nitrogen fertilizer datasets at country scale from FAO statistical database (http://faostat.fao.org) and at state level in India from DES, (2010). We then calculated the annual fertilization rate (g N/m2) as the ratio of national fertilizer application amount to total cropland area in each country (Tian et al., 2011b). The irrigation map was based on land use and land cover data, and global irrigated fraction map at 5-arc minute resolution (Leff et al., 2004; Siebert et al., 2007).

6.2.3 Climate data

The climate data (including average, maximum, minimum air temperature, precipitation, relative humidity, and shortwave radiation) were obtained from NCEP/NCAR reanalysis 1 at 0.5 × 0.5 degree resolution (http://www.cdc.noaa.gov/cdc/data.ncep.reanalysis.html) and were linearly downscaled to 0.25 degree resolution (Wei et al., 2014). During the study period, mean annual precipitation showed significant inter-annual variations; however no significant long-term trend was observed (Figure 6.3). On the other hand, mean annual temperature has showed significant increase after 1950s to 2000s during the study period (slope: 0.009 $^{o}C\ year^{-1}$).

The atmospheric CO_2 concentration data was derived from Carbon Dioxide Information Analysis Center (CDIAC, http://cdiac.ornl.gov/; verified 10 Apr. 2015) that has shown that CO_2 concentration increased steadily from 295 ppm in 1900 to 391 ppm in 2010 (Figure 6.3). The information on AOT40 dataset (accumulated hourly O_3

concentrations above a threshold of 40 ppb) was obtained from global datasets from Felzer et al., (2005). The atmospheric nitrogen deposition (NDEP) was extracted from global data set (Dentener, 2006) that was extrapolated at annual time step during 1900–2010.

6.2.3 Soil properties and topographic maps

In the tropical Asia, the spatial maps for soil bulk density, soil pH, and texture(i.e., percentage of clay, sand, and silt content), were obtained from the International Satellite Land Surface Climatology Project (ISLSCP) Initiative II Data Collection distributed by the Oak Ridge National Laboratory Distributed Active Archive Center (http://daac.ornl.gov/). This collection provided spatially-explicit global soil information derived from data and methods developed by the Global Soil Data Task, which was coordinated by the Data and Information System (DIS) of the International Geosphere–Biosphere Programme (IGBP). We assumed that soil texture, soil pH, and bulk density have remained similar from 1900–2010, and therefore only one map has been used as a driving factor for the DLEM.

In the DLEM, topographic maps including elevation, slope and aspect are used as input datasets. We first aggregated the Global 30 Arc Second Elevation Data (GTOPO30) developed by the United States Geological Survey (Bliss and Olsen, 1996) to half degree resolution to develop the digital elevation model. Finally, we derived the 0.25 degree resolution aspect and slope maps from the digital elevation model.

6.2.4 Experimental Design

The implementation of the DLEM simulation includes the following steps: 1) equilibrium run, 2) spin-up run and 3) transient run. The primary purpose of the

equilibrium run is to achieve the equilibrium state when net carbon exchange for 50 consecutive years is <0.5 g C m^{-2}, the net water pool change is <1.0 mm and the net nitrogen change is < 0.5 g N m^{-2} is made. At this step the model is driven by average climate conditions from 1901 to 1930 and land use and land cover data in 1900. After that three thirty-year spin-up runs, driven by random data sequence of de-trended climate during 1901–1930, are conducted to reduce the biases in the simulations. In the transient run, the environmental factors from 1901 to 2010 were used to drive the model to produce transient simulation.

To determine the magnitude and spatial distribution of the NCE, we designed a total of eight simulation experiments (Table 6.1). Two simulation experiments ($Multifactor_{withPlim}$ and $Multifactor_{noPlim}$) were set to quantify the extent of carbon uptake limited by the P limitation in the tropical Asia. In these two simulation experiments, all the environmental factors were dynamic. In addition, six experiments were set up to determine the relative contribution of individual environmental factor (climate, atmospheric CO_2 concentration, NDEP, and LCLUC on NCE during 1901–2010. In the multifactor experiments, all the environmental factors were dynamic during 1901–2010 (Table 6.1). In the other experiments, one factor was kept constant (to the level of 1901) while others were transient. One exception was No-Climate experiment in which climate was the 30-year mean of 1901–1930 (Table 6.1).

6.4 Results

6.4.1 Net Carbon Exchange

The DLEM simulations have shown that NCE varied significantly ranging from –325 Tg C $year^{-1}$ in 1979 to 278 C $year^{-1}$ in 1971 in terrestrial biosphere of tropical Asia

(Figure 6.4). At 110-year time scale, inter-annual variations in the NCE are driven by climatic variability (particularly precipitation) and there is no significant long-term increasing or decreasing trends. Two regions (South and South East Asia) showed a clear distinction in the NCE source/sink strength (Figure 6.4). For example, South Asia was a net carbon source –60±71 Tg C $year^{-1}$ while South-East Asia was a net carbon sink 47±89 Tg C $year^{-1}$ during the 110-years study period.

The DLEM simulations have suggested that the effects of environmental factors on NCE varied both in magnitude and temporal scales (Figure 6.4). For example, P limitation was the major factor, which reduced NCE by 517 Tg C $year^{-1}$ over tropical Asia in 1900s indicating that P is a significant factor for driving carbon cycling in the region. Interestingly, the effects of P were comparatively greater in the South-East Asia than South Asia due to presence of higher proportion of tropical forests in the South-East Asia.

6.4.2 Methane

The annual fluxes of CH_4 emissions over the tropical Asia have increased significantly during 1901–2010 (Figure 6.5). A total CH_4 emission from tropical Asia was approximately 18.5 T g C $year^{-1}$ in the 1900s which increased to 29.3 gC $year^{-1}$ in the 2000s (Figure 6.5). Major sources of CH_4 were located in eastern India, Bangladesh, and South-East Asia primarily due to high proportion of the rice based cropping systems and natural wetlands in the South East Asia. Among biomes, CH_4 flux density was greater in the wetlands (34–49 g C m^{-2} $year^{-1}$) followed by croplands (3.1–4.9 g C m^{-2} $year^{-1}$) and forests (–0.31–0.14 g C m^{-2} $year^{-1}$) while shrublands and grasslands were net CH_4 sinks (–0.12–0.035 g C m^{-2} $year^{-1}$) (Table 6.2).

6.4.3 Nitrous oxide

In the tropical Asia, total N_2O emissions ranged from 0.6 Tg N $year^{-1}$ to 0.96 Tg N $year^{-1}$ during 1901–2010 (Figure 6.6). The strong sources of N_2O emission are in South Asia, where N_2O emission reached as high as 0.2 gNm^{-2} $year^{-1}$. The weakest N_2O sources were observed in the western parts (e. g., Pakistan), where N_2O was released at a rate of <0.05 gNm^{-2} $year^{-1}$. Among the different biome types, the N_2O emission density was higher in croplands (0.09–0.15 g N $year^{-1}$) than natural vegetation types (0.003–0.11 g N $year^{-1}$) during the study period (Table 6.3). This is a proven fact as croplands receive nitrogen fertilizers under various kinds of tillage operations, irrigation (wetting and drying of soils) that stimulate N_2O emission (Drury et al., 2012).

6.4.4 Global Warming Potential

In terms of global warming potential, the tropical Asia had a net warming effect of –1063 ± 436 Tg CO_2eq $year^{-1}$ ranging from –2262Tg CO_2eq $year^{-1}$ in 1979 to –36 Tg CO_2eq $year^{-1}$ in 1971, at a 100-year time horizon (Figure 6.7). In tropical Asia, CH_4 and N_2O emissions contribute to approximately 95% of the GWP thereby suggesting that CH_4 and N_2O provide significant feedbacks to global climate change. Over the past 110-year time period, there has been a substantial inter-annual variation in the annual GWP of the terrestrial ecosystems (Figure 6.7). Though, no-significant long-term trend was identified ($p= 0.82$) in the GWP, the emissions of three GHGs changed substantially during the study period. This suggested that decreasing GWP due to CO_2 emissions were partially neutralized by increasing emissions of CH_4 (–3.5 ± 1.1 Tg CO_2eq $year^{-1}$) and N_2O (–1.2 ± 0.4 Tg CO_2eq $year^{-1}$).

Atmospheric CO_2 concentration stimulated the plant biomass production and therefore increased NCE (i. e., decreased CO_2 emissions) by 203 Tg C $year^{-1}$ in the 2000s over tropical Asia (Figure 6.4). Our results are consistent with others that elevated CO_2 concentration stimulated plant growth resulting higher carbon uptake in the tropical Asia (Bala et al., 2013). Several field scale studies have shown that elevated CO_2 concentration (600 ppm) stimulated the plant biomass in grasslands (from 2.0 g $plant^{-1}$ to 2.87 g $plant^{-1}$), forests (Nataraja et al., 1998), and croplands (Vanaja et al., 2011) in tropical Asia. Using multivariate analysis, Bala et al., (2013) reported that elevated CO_2 concentration was the most important factor in increasing net primary productivity in India during 1982–2006. The LCLUC, which is the combined effect of land conversions and cropland management (Table 1), has released approximately 7–253 Tg C $year^{-1}$ from terrestrial biosphere of tropical Asia. Climate was the second most important factor that emitted carbon by a mean value of 93 Tg C $year^{-1}$ in the 1900s and 211 Tg C $year^{-1}$ in the 2000s indicating especially climate change became important factor after latter half of 20^{th} century. Overall, the DLEM simulations have shown that combined effect of these environmental changes have increases the carbon uptake over the tropical Asia. However, these environmental changes have also increased the CH_4 and N_2O emissions during the study period (Figure 6.3).

6.5 Contribution of different environmental factors on Global Warming Potential

6.5.1 Elevated atmospheric CO_2 concentration

Over the tropical Asia, elevated atmospheric CO_2 concentration has increased CH_4 emissions by 3.4 Tg C $year^{-1}$; thereby partially offsetting the terrestrial cooling effect from higher carbon uptake (Figure 6.5). Using open-top chambers at the International Rice Research Institute (IRRI), Philippines, Ziska et al. (1998) reported that elevation of

300 μL L^{-1} above normal CO_2 concentration has increased the CH_4 emissions by 50% from 142 mg CH_4 m^{-2} day^{-1} to 227 mg CH_4 m^{-2} day^{-1}. In another study, Allen et al. (2003) reported an increase of approximately 50–100% in the net CH_4 flux due to elevated CO_2 concentration rice fields in Florida. In an experiment on elevated CO_2 concentration (355 to 550 μol mol^{-1}) in a mire peatland, Hutchin et al., (1995) reported that CH_4 fluxes have increased by 100% as compared to ambient CO_2 concentration which occurred due to increase in the photosynthesis. However, the response of elevated CO_2 concentration to CH_4 emissions was lower than these studies probably due to two reasons. Firstly, the increase in the CO_2 concentration was comparatively lower (linear increase from 295 μL L^{-1} to approximately 390 μL L^{-1} during 1901–2010) than that used by the field scale studies. These studies were conducted for short time period while in the long term progressive nutrient limitation may occur that can decrease the response of elevated CO_2 concentration on plant biomass.

In our study, the elevated CO_2 concentration has slightly decreased the total N_2O emission in the tropical Asia (Figure 6.4). Previously, both the stimulatory and inhibitory effects of elevated CO_2 concentration on N_2O emission have been reported in the field scale studies (Kammann et al., 2008; Dijkstra et al., 2012). In a meta-analysis, Dijkstra et al., (2012) reported that elevated CO_2 concentration significantly increased N_2O emissions in nitrogen fertilizer studies while the effects were not significant non-fertilized studies thereby indicating interactions between elevated CO_2 concentration and N_2O emissions. If progressive nitrogen limitation occurs due to elevated CO_2 concentration can decrease the N_2O emissions due to higher uptake of nitrogen by plants. This condition usually occurs in the forest and grasslands (Aber and Melillo, 2001; Vitousek

and Farrington, 1997). In this way, the DLEM simulated results have suggested that a progressive nitrogen limitation exits which has decreased N_2O emissions in response to elevated atmospheric CO_2 concentration in the tropical Asia.

6.5.2 Land Cover and Land Use Change

The LCLUC has substantially increased the CH_4 and N_2O emissions from tropical Asia (Figure 6.5 and Figure 6.6) due to cropland expansion that receives nitrogen fertilizers. This was consistent with previous studies (Mosier et al., 1991; Mcswiney and Robertson, 2005; Zhang et al., 2007; Liu and Greaver, (2009) which reported stimulation of N_2O emission by anthropogenic nitrogen inputs. Similarly, expansion of the rice based cropping systems has increased CH_4 flux by 8.7 Tg C $year^{-1}$ in the 2000s during the study period. Various studies have shown that nitrogen fertilizers stimulate crop growth and provide more carbon substrates (via organic root exudates and sloughed-off cells) to the CH_4 producing microbes (Aulakh et al., 2001; Denier van der Gon et al., 2002) and thereby increasing CH_4 emissions from rice fields (Banger et al., 2012; Banik et al., 1996; Shang et al., 2011). Our study has demonstrated that LCLUC is the single most important factor in increasing the CH_4 and N_2O emissions from tropical Asia.

The spatial pattern of the GWP suggested higher warming potential for regions in South Asia than South-East Asia due to higher proportion of the croplands which released significant CH_4 and N_2O emissions.

6.5.3 Climate

Our results have suggested that variability in the NCE were determined by the annual precipitation ($r= +0.27$; $P < 0.0043$) due to its effects on the plant growth (Panigraphy et al., 2005; Singh et al., 2011). Among two regions, South Asia receives

comparatively lower precipitation (700–1100 mm) than South-East Asia (1900–2600 mm) during 1901–2010 (Figure 6.8). Regional scale analysis showed that NCE and regional mean annual precipitation are strongly correlated in the South Asia ($r= +0.43$; $P < 0.0001$) while a weak correlation exists in the South-East Asia ($r= +0.15$; $P < 0.095$) during 1901–2010. Previously, several studies have shown that carbon uptake in the South Asia is strongly linked to the mean annual precipitation (Nayak et al., 2015). Panigraphy et al., (2005) have shown that terrestrial net primary productivity was significantly lower in the drought year of 2002–2003 (1.9 Pg C $year^{-1}$) than normal year of 2004–2005 (2.5 Pg C $year^{-1}$) due to water stress on the vegetation in the drier years.

Using the DLEM simulations, Pan et al., (2014b) reported that precipitation explained approximately 63% of the variation in terrestrial net primary productivity at a global scale. The DLEM simulation results have warned scientific community and policy makers that increased incidences of extreme droughts in future can significantly increase the carbon emissions from tropical Asia.

6.6 Discussion

The DLEM simulations have substantially contributed to our understanding of the magnitude and well as its contributing factors of the GHGs emissions in the tropical Asia. This study has suggested that tropical Asia was a net carbon sink during the study period. However, it has warming effect if CH_4 and N_2O emissions are considered. Among all the factors studied, P limitation has a significant effect in reducing the carbon uptake in the tropical ecosystems.

6.5.1 Comparison with previous estimations

Though tropical Asia is one of the most important regions, a large uncertainty exists in the NCE estimates of the previous studies (Patra et al., 2012, 2013; Zhang et al., 2014). In this study, we compared the DLEM simulated net carbon exchange with inversion studies available South and South East Asia (Zhang et al., 2014; Patra et al., 2011; Niwa et al., (2012). Our results have shown that tropical Asia acted as a net carbon sink (132±107 Tg C $year^{-1}$) in the 2000s. Using CONTRAIL (Comprehensive Observation Network for Trace gases by Airline) observations from 2006–2010, Zhang et al., (2014) have reported that tropical Asia was a carbon sink of 170 Tg C $year^{-1}$ if the impact of fires are excluded. Therefore, our estimations are slightly lower than estimated by Zhang et al., (2014) using inverse methods.

A total of 11 TransCom inversions have shown that a large uncertainty in the terrestrial carbon balance existed in South Asia ranging from a sink of –158 Tg C $year^{-1}$ to a source of 507 Tg C $year^{-1}$, with a median value being a sink of −35.4 Tg C $year^{-1}$ during 2007–2008 (Patra et al., 2013). In the South Asia, the median value of NCE estimated by the 11 inversions techniques is closer to our estimation of –11 Tg C $year^{-1}$ during 2007–2008. However, two regional scale inversions were conducted using CARIBIC and CONTRAIL, which showed greater carbon sink but with larger uncertainty in the estimates in 2006–2008. For example, magnitude of terrestrial carbon uptake estimated by our study (–39 Tg C $year^{-1}$) was an order of magnitude lower than estimated a regional scale inversion (–300 Tg C $year^{-1}$) using CARIBIC aircraft measurements by Patra et al., (2011). The number of CARIBIC aircraft measurement used by Patra et al., (2011) were limited to flights between Frankfurt (Germany) and

Chennai (southern part of India) in conjunction with the surface measurements. The DLEM simulations have shown that majority of the carbon emissions have occurred in the northern parts of India (Figure 5.6). Therefore, it is possible that Patra et al., (2011) overestimated the carbon sink in South Asia. Niwa et al., (2012) used aircraft measurements on various flight routes of CONTRAIL which includes flights over northern India; estimated atleast three folds lower carbon sink estimated by Patra et al., (2011) in the South Asia (88 Tg C year^{-1}) during 2007–2008.

Similar to the inversion estimates, bottom-up studies involving ten land ecosystem models, Patra et al., (2013) reported that South Asia acted as net carbon sink ranging from 80 to 651 Tg C year^{-1} with average value (carbon sink) of 210 Tg C year^{-1} during 1980–2009, which are significantly greater than our estimates. However, ten models estimated net ecosystem productivity (NEP) ignored carbon flux due to land conversions and product decay and therefore might have overestimated carbon sink.

6.5.4 Phosphorus limitation for net carbon exchange

The DLEM simulations have suggested that P limitation has reduced the NCE by 430±130 Tg C year^{-1} in the tropical Asia during the study period. The reduction in the NCE due to P limitation is 3-5 folds greater in the South East Asia than South Asia, suggesting that P limitation is strong in the South East Asia. It has been demonstrated that carbon uptake in the tropical forest is strongly limited by P availability (Cleveland et al. 2011; Vitousek 2012). According to Walker and Syers's model (Walker & Syers 1976), P availability in highly weathered is lower than other soil types, and most P is adsorbed by soil minerals and is not biologically available to plant. Using the Jena Scheme for Biosphere–Atmosphere Coupling in Hamburg (JSBACH), Goll et al., (2012)

have reported that global carbon uptake was 13–16% lower due to P limitation between 1861–2100.

Phosphorus limitation in tropical forest has been verified through fertilization experiments (Kaspari et al. 2008; Wright et al. 2011). Meanwhile, P fertilization experiment also suggested that plant demonstrated positive response to nitrogen addition, which suggested a ‘co-limit’ state of tropical rain forest (Townsend et al. 2011; Wright et al. 2011; Cleveland et al. 2011). Results of this study show that the potential of carbon uptake by biosphere in the tropical Asia is controlled by P availability.

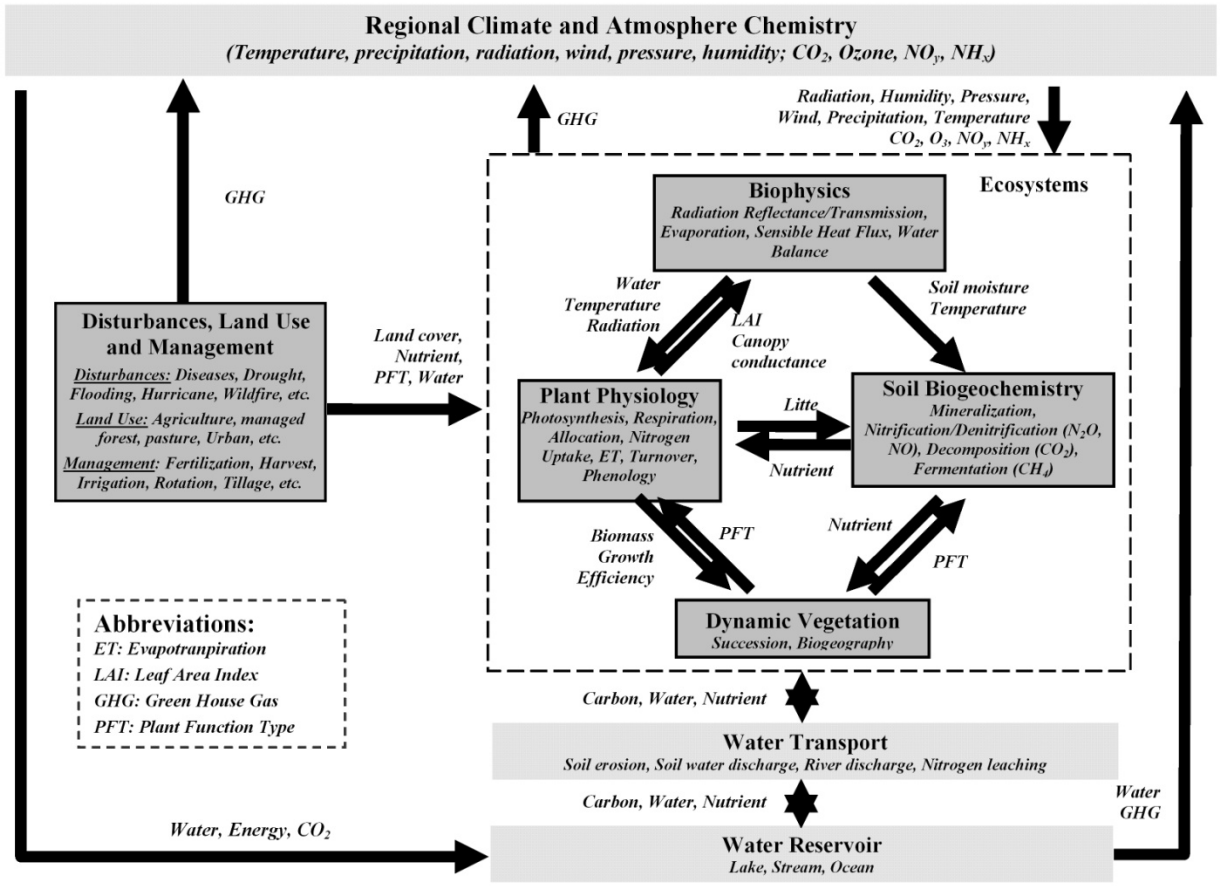

Figure 6.1 Conceptual model of the Dynamic Land Ecosystem Model (DLEM)

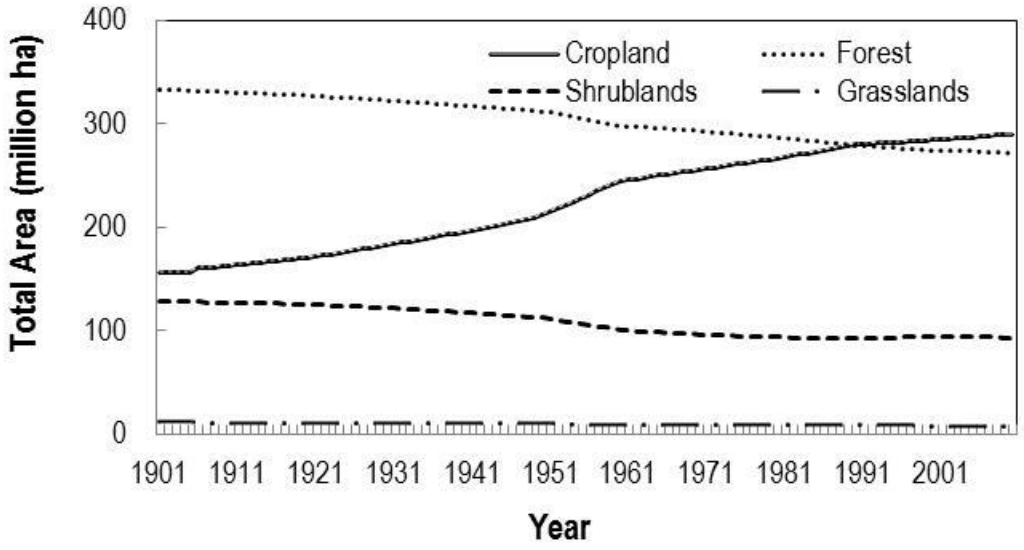

Figure 6.2. Land cover and land use change in tropical Asia during 1901–2010.

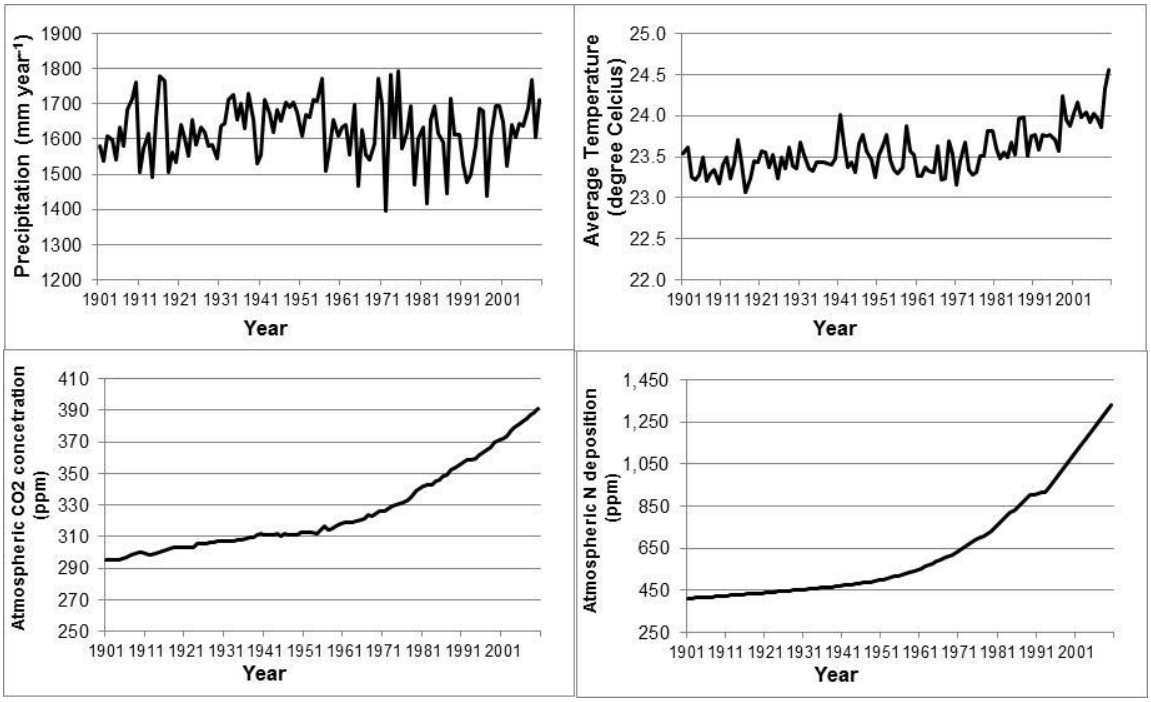

Figure 6.3. Temporal trends in the annual average temperature, precipitation, atmospheric CO_2 concentration, and nitrogen deposition in the tropical Asia during 1901–2010.

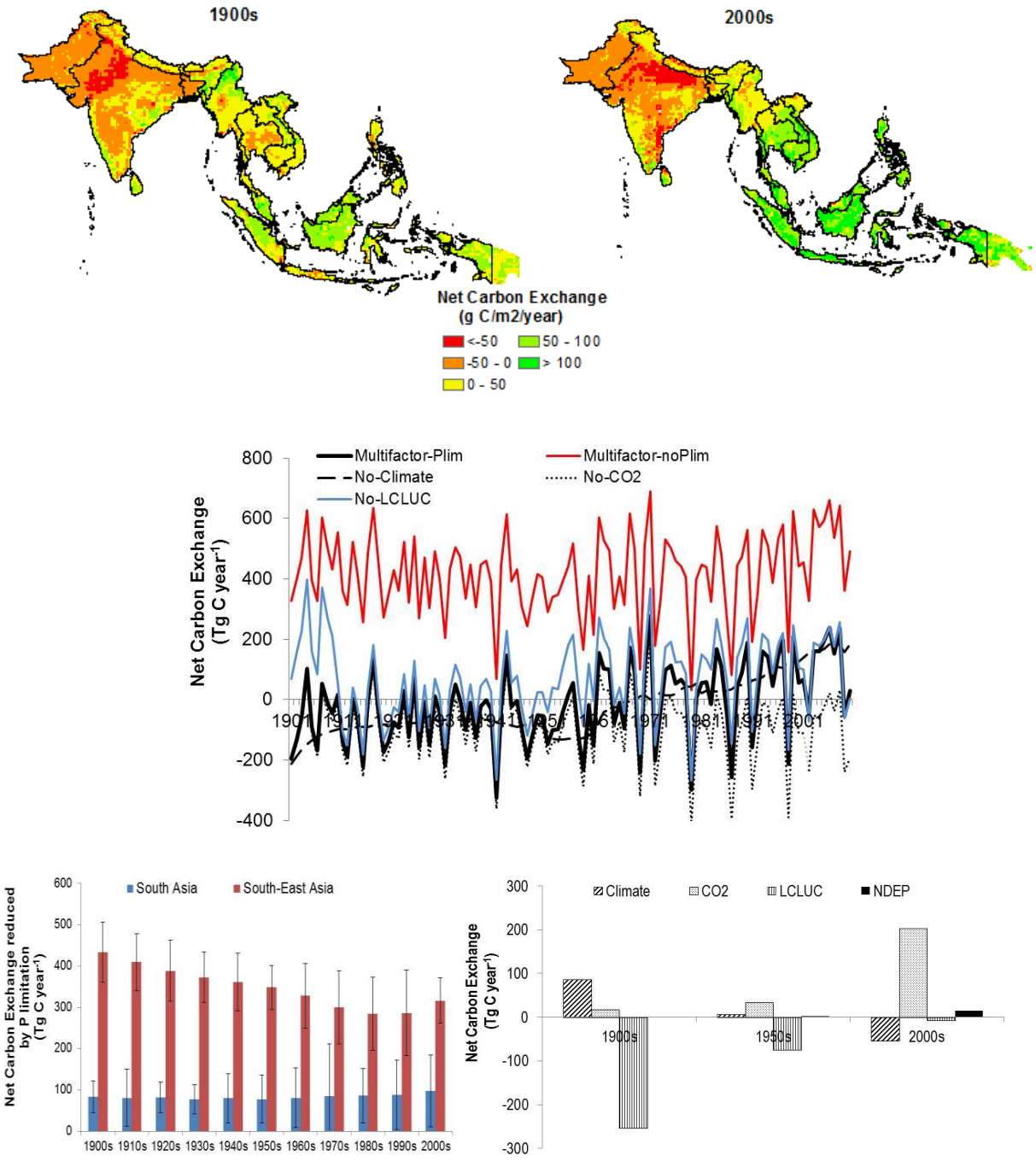

Figure 6.4. Net Carbon Exchange (g C m^{-2} $year^{-1}$) between atmosphere and terrestrial biosphere in the tropical Asia. Positive values indicate carbon sink and negative values indicate carbon source.1900s is the mean of 1901–1910; 2000s is the mean of 2001–2010.

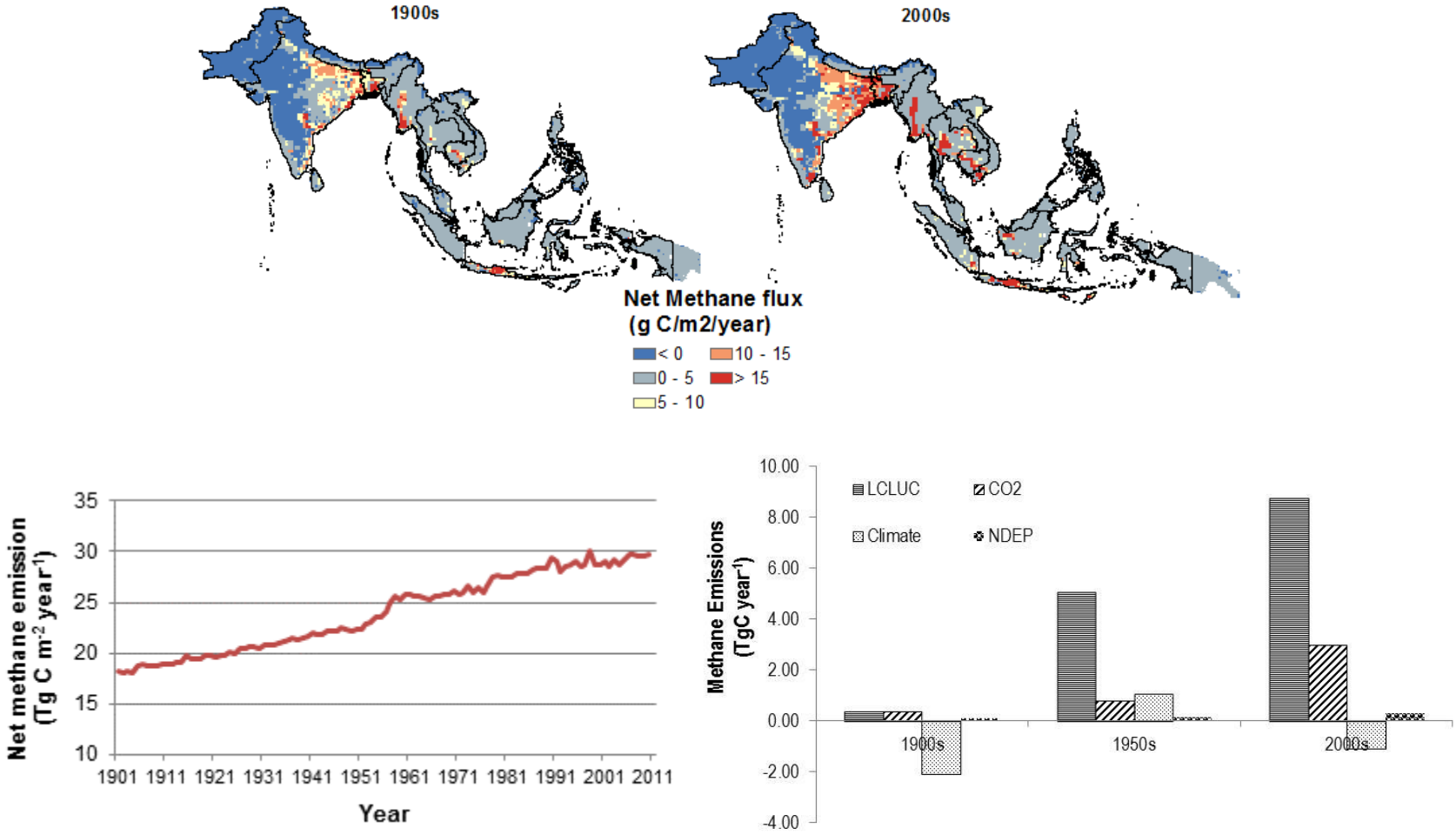

Figure 6.5. Net methane emission (g C m^{-2} $year^{-1}$) from terrestrial biosphere in the tropical Asia.1900s is the mean of 1901–1910; 2000s is the mean of 2001–2010.

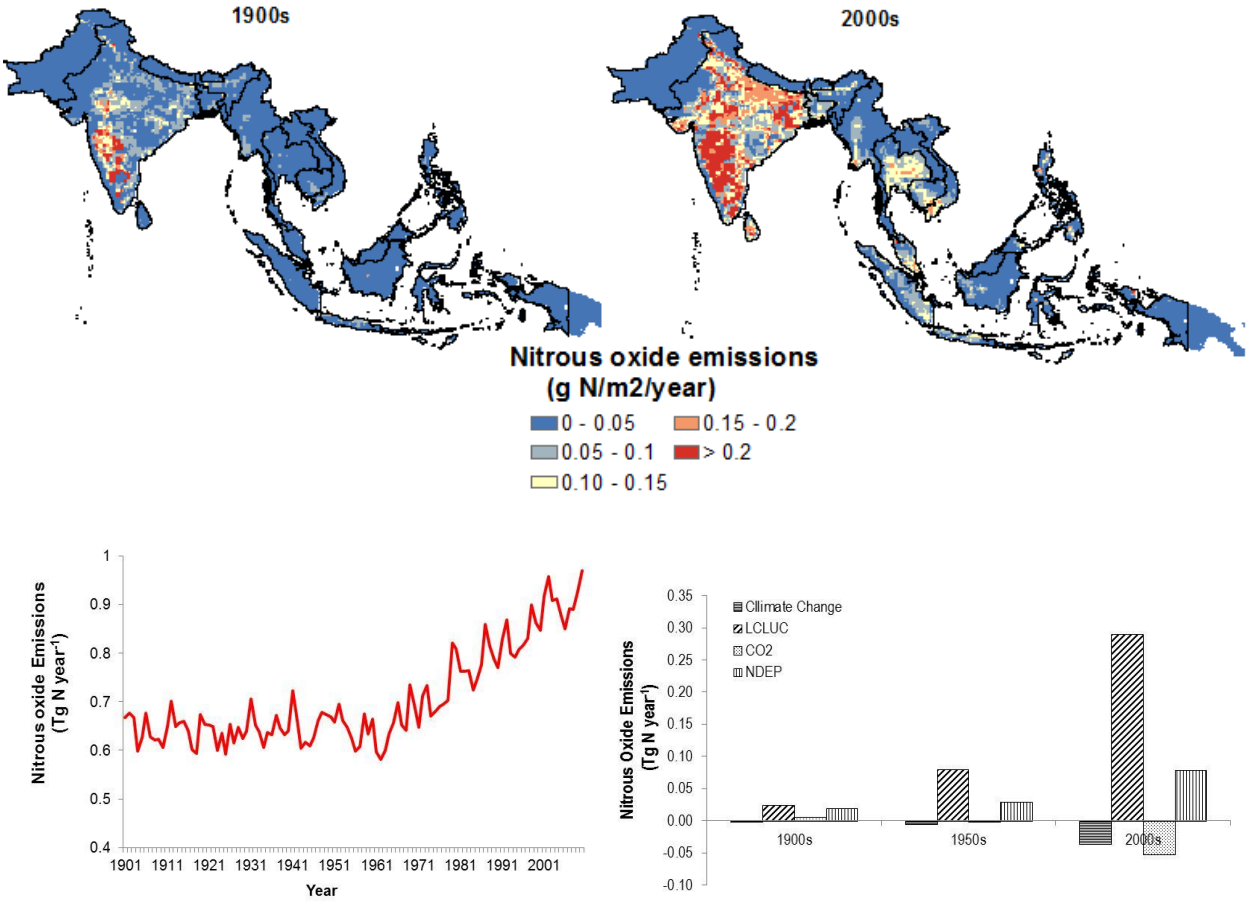

Figure 6.6. Nitrous oxide emissions (g C m^{-2} $year^{-1}$) from terrestrial biosphere in the tropical Asia.1900s is the mean of 1901–1910; 2000s is the mean of 2001–2010.

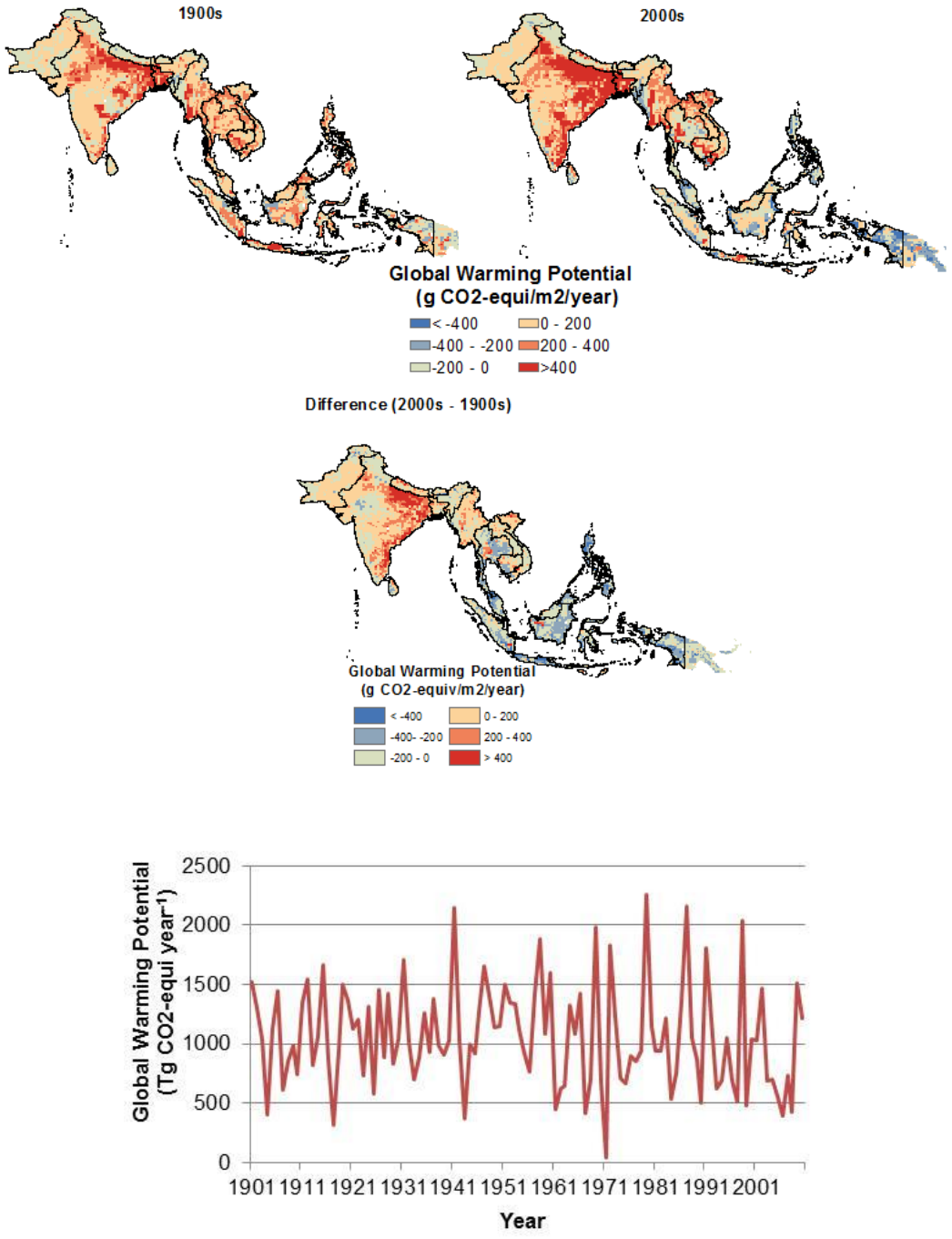

Figure 6.7. Global Warming Potential (Tg CO2-equivalents year^{-1}) of the terrestrial biosphere in the tropical Asia. Positive values indicate net warming and negative values indicate net cooling effect.1900s is the mean of 1901–1910; 2000s is the mean of 2001–2010.

Biome	Methane emission (g C m^{-2} $year^{-1}$)		
	1900s	1950s	2000s
Croplands[£]	3.1±0.16	3.6±0.30	4.8±0.41
Temperate Broadleaf Deciduous Forest	-0.26±0.03	-0.11±0.10	-0.31±0.09
Temperate Broadleaf Evergreen Forest	-0.07±0.004	-0.06±0.007	-0.006±0.009
Temperate Needle leaf Deciduous Forest	0.06±0.06	0.04±0.07	0.09±0.07
Temperate Needle leaf Evergreen Forest	-0.05±0.004	-0.05±0.007	-0.006±0.0007
Tropical Broadleaf Deciduous Forest	0.099±0.03	0.1±0.08	0.07±0.07
Tropical Broadleaf Evergreen Forest	0.11±0.049	0.14±0.06	0.14±0.05
Shrubs	-0.04±0.003	-0.051±0.001	-0.106±0.001
Grass	-0.0353±0.003	-0.0494±0.001	-0.116±0.001
Wetlands	34.6±0.31	37.7±9.5	49.7±5.4
All biomes	3.6±0.08	4.1±0.15	4.9±0.28

Table 6.2 Mean methane emission density (g C m^{-2} $year^{-1}$) from different biomes in tropical Asia.

Biome	Nitrous oxide (g N m^{-2} $year^{-1}$)		
	1900s	1950s	2000s
Croplands	0.09±0.02	0.093±0.007	0.150±0.02
Temperate Broadleaf Deciduous Forest	0.004±0.0003	0.006±0.0006	0.019±0.010
Temperate Broadleaf Evergreen Forest	0.0034±0.0003	0.0044±0.001	0.0066±0.002
Temperate Needle leaf Deciduous Forest	0.006±0.0003	0.007±0.0007	0.009±0.0009
Temperate Needle leaf Evergreen Forest	0.0003±0.0001	0.0004±0.0001	0.0005±0.0002
Tropical Broadleaf Deciduous Forest	0.008±0.001	0.006±0.0011	0.0091±0.0018
Tropical Broadleaf Evergreen Forest	0.005±0.0004	0.008±0.0012	0.0151±0.0016
Shrubs	0.0132±0.003	0.0195±0.007	0.0569±0.0025
Grass	0.0353±0.003	0.0494±0.001	0.11±0.001
All biomes	0.023±0.0013	0.029±0.0002	0.064±0.0112

Table 6.3. Mean nitrous oxide emissions (g N m^{-2} $year^{-1}$) from different biomes in the tropical Asia.

Chapter 7. Uncertainties in the model structure, parameter estimation, and input datasets

We believe that several uncertainties could have arisen from model structure, parameter values, and input datasets in our study. In this chapter, we discussed these uncertainties in the model estimations.

7.1 Model structure

Though, the DLEM is of the only few available models to be able to simulate complex carbon, nitrogen, and phosphorus processes. Currently, the data for validating phosphorus limitation effects on carbon uptake are limited to only few phosphorus fertilizer experiments. In future, modeling mechanisms should be improved to make use of distribution of soil groups for phosphorus limitation. In general, Ultisols and Oxisols have very low phosphorus availability as compared to other soils (such as Inceptisols). To tackle the unavailability of the phosphorus fertilizer experiments in forests, it would be useful to set soil group caveats for phosphorus limitation.

In the future, few mechanisms should be improved. For example, soil may act as a sink of atmospheric N_2O under certain conditions (Chapuis-Lardy et al., 2007). Owing to incomplete understanding of this phenomenon, this mechanism was not incorporated in the modeling framework of the DLEM.

7.2 Parameter estimations

The parameter values estimated during the calibration process from errors in the measurements could be the source of uncertainty. For model calibration, we obtained the field data primarily from croplands, forests, and shrublands. In the future, efforts should be made to quantify the peatland areas using various high resolution remote

sensing and modeling approaches. The field data used for model calibration of CH_4 and N_2O was primarily obtained from croplands. The second major field observation data uncertainty was the methane (CH_4) and nitrous oxide (N_2O) emissions from natural plant functional types.

7.3 Input datasets

Several discrepancies existed in the currently available land use and land cover datasets (Banger et al., 2013), we have used newly developed LULC datasets based on high resolution remote sensing datasets and finer resolution historical archives (Tian et al., 2014). However, uncertainties still existed in the forest cover density and cropping systems which were not reported in the inventory reports (DES, 2010). The distribution of cropping systems should be improved in the historical period using inventory archives. Here, we have used state-wise dataset in India to identify the major cropping system; however district level datasets on cropping systems may improve the area under rice fields. In this study, only two irrigation scenarios (continuous irrigation and no irrigation) are considered in croplands. In reality, irrigation depends on water demand from industries, municipalities, and croplands. Overall, intermitted irrigation which involves drainage of rice fields is followed in Asia; however data in the grid format is not available in the current land use datasets. This intermittent drainage practice has potential to affect CH_4 emissions as well as the can modify the response of different factors on CH_4 emissions (Banger et al., 2012)

Although, we refined the FAO datasets on N fertilizer maps which used one value in India to state level fertilizer information compiled by DES (2010). However, specific information on manures (amount and type of manure) uses is still lacking. We believe

that significant uncertainty may exist in the soil organic carbon (SOC) content of the wetlands and peatlands. In the South-East Asia, peatland distribution, which is important for carbon cycling, is missing in the current land cover and land use datasets.

Chapter 8. Conclusions and Future Research Recommendations

Tropical Asia, including South and Southeast Asia, is a home to one quarter of global population and plays a critical role in the GHGs (carbon dioxide (CO_2), methane (CH_4), and nitrous oxide (N_2O) budgets (Richards and Flint, 1994; Tian et al., 2003; Tao et al., 2013; Houghton, 2002). Previous studies have shown that tropical Asia can act as a carbon sink, which may be partially or completely offset by CH_4 and N_2O emissions. Therefore, it is important to quantify three GHGs together to determine the cooling or warming feedbacks of terrestrial ecosystems to global climate. Using the Dynamic Land Ecosystem Model (DLEM), the GHGs emissions from terrestrial ecosystems of tropical Asia were assessed during 1901–2010, focusing on its responses to LCLUC, elevated CO_2 concentration, climate, atmospheric nitrogen deposition (NDEP), and tropospheric O_3 pollution concentration.

Key conclusions are listed as below:

1. Our newly reconstructed land use and land cover at 5-arc minute resolution have shown that a significant loss of forests (from 89 million ha to 63 million ha) while total cropland area has increased from 92 million ha to 140.1 million ha during 1880–2010. Greater cropland expansion has occurred during 1940–1980s that coincided with the period of farm mechanization, electrification, and introduction of high yielding crop varieties as a result of government policies to achieve self-sufficiency in food production. Using the DLEM simulations, we have shown that the terrestrial NPP ranged from 1.2 Pg C $year^{-1}$ to 1.7 Pg C $year^{-1}$ over India during 1901–2010. Elevated CO_2 concentration stimulated terrestrial NPP by 0.29 Pg C $year^{-1}$ which was partially offset by climate that not only produced inter-annual variations but also decreased

terrestrial NPP by 0.11 Pg C year^{-1}. LCLUC stimulated the terrestrial NPP over the country. In the recent three decades, tropospheric O_3 pollution reduced the terrestrial NPP by 4.2% (0.06 Pg C year^{-1}) and the effect is slightly higher croplands (7.4%) than other biomes in the 2000s thereby suggesting that tropospheric O_3 pollution is a threat to Indian food security.

2. In India, the SOC stock has increased by 2.9 Pg C from 20.5 to 23.4 Pg C during 1901–2010. Of the environmental factors studied, elevated atmospheric CO_2 concentration that stimulates plant biomass production has increased SOC stocks over the country by 1.28 Pg C during 1901–2010. Land cover and land-use change has increased SOC stocks by 1.7 Pg C primarily in the croplands where N fertilizer and irrigation management have increased crop growth resulting in SOC sequestration. Climate was the single most important factor that decreased SOC stocks by 0.78 Pg C due to increase in heterotrophic respiration as well as due to frequent occurrence of drought years that reduced biomass production over the country.

3. Tropical Asia was a net carbon source (13±12 Tg C year^{-1}), while South Asia was a net source (61±7Tg C year^{-1}) and South-East Asia was a sink (47±9 Tg C year^{-1}) during 1901–2010. Over the 110 year time period, carbon uptake has increased significantly and tropical Asia became a net sink after 1950s onwards due to elevated CO_2 concentration and NDEP while climate and LCLUC had negative effects.

4. Tropical Asia emitted a total of 20.4± 3.6 Tg C year^{-1} CH_4 and 0.70 ±0.09 Tg N year^{-1} N_2O emissions during 1901–2010. Major sources of CH_4 were located in eastern India, Bangladesh, and South-East Asia primarily due to high proportion of the rice based cropping systems and natural wetlands in the South East Asia. On the other

hand, N_2O emission sources were more scattered in the tropical Asia. The weakest N_2O sources were observed in the western parts (e. g., Pakistan), where N_2O was released at a rate of <0.05 gNm^{-2} $year^{-1}$. Elevated atmospheric CO_2 concentration has increased CH_4 emissions by 3.4 Tg C $year^{-1}$ but had not effect on N2O emissions. The LCLUC has substantially increased the CH_4 and N_2O emissions from tropical Asia due to cropland expansion which also included rice based cropping systems that receives nitrogen fertilizers.

5. In terms of global warming potential (GWP), tropical Asia provided a strong warming feedback (1063±43 Tg CO_2-equivalents $year^{-1}$) to the global climate warming. During the study period, GWP has not shown any significant increasing or decreasing trends ($p< 0.82$) despite increases in the terrestrial carbon uptake over the tropical Asia. This has suggested that CH_4 and N_2O have offset the benefits from carbon uptake in tropical Asia.

6. Phosphorus limitation significantly reduced carbon uptake by 430±130 Tg C $year^{-1}$ in the tropical Asia during 1901–2010. The reduction in the carbon uptake due to P limitation is 3-5 folds greater in the South-East Asia than South Asia, suggesting that P limitation is stronger in the South-East Asia due to high precipitation and presence of tropical forests. This is the preliminary attempt to incorporate P cycle in the DLEM framework and future efforts.

7. Meanwhile, I identified several uncertainty sources in tropical Asia which need to be addressed in the future. Firstly, I have improved the currently available LCLUC datasets. However, distribution of peatlands is still missing, which play a significant role in the regional and global cycle. Current datasets don’t have finer resolution peatland

datasets, which could be improved in future. Secondly, magnitude of carbon uptake limited by P is highly uncertain in the tropical Asia. There is a clear knowledge gap on how much carbon uptake can be limited by P availability in the future. Therefore, we should collaborative programs involving ecosystem modelers and field's scientists should be encouraged to design P fertilizer experiments.

References

Aber, J. D. and Melillo, J. M., 2001. Terrestrial Ecosystems, Academic Press, New York.

Achard, F., Eva, H.D., Stibig, H.J., Mayaux, P., Gallego, J., Richards, T., Malingreau, J.P., 2002. Determination of deforestation rates of the world's humid tropical forests. Science 297, 999–1002.

Aerts, R., and F. S. Chapin III. 2000. The mineral nutrition of wild plants revisited: a reevaluation of processes and patterns. Advances in Ecological Research 30:1–67.

Aggarwal, A.K. & Goyal, A. K. 1987. Effect of grazing on net primary production and system transfer function in a western Himalayan grassland community. Tropical Grasslands, 21 (4), 155–158.

Ajtay, G.L., P. Ketner, and P. Duvigneaud. 1979. Terrestrial primary production and phytomass In: B. Bolin et al., editors, The Global Carbon Cycle (SCOPE 13). Wiley, Chichester. UK, p. 129-182.

All India Coordinated Research Project on Long-Term Fertilizer Experiments (AICRP-LTFE) to Study Changes in Soil Quality, Crop Productivity, and Sustainability. Annual Report, Indian Council of Agricultural Research, 2006–2007.

Ambasht, N.K., and M. Agrawal. 2003. Effects of enhanced UV-B radiation and tropospheric ozone on physiological and biochemical characteristics of field grown wheat. Biol. Plant. 47:625–628. doi:10.1023/B:BIOP.0000041076.95209.c3

Ambasht, R. S., Maurya, A. N. and Singh, U. N. 1972. Primary production and turnover in certain protected grasslands of Varanasi, India. In: Tropical Ecology with an emphasis on organic production, F.B. Golley (Eds.), University Georgia, Athens, USA, pp. 43 - 50.

Ambus, P. and Robertson, G. P., 1999. Fluxes of CH4 and N2O in aspenstands grown under ambient and twice-ambient CO2. *Plant Soil,* 209, 1–8.

Aragão, L. E. O. C., Malhi, Y., Metcalfe, D. B., Silva-Espejo, J. E.,Jiménez, E., Navarrete, D., Almeida, S., Costa, A. C. L., Salinas, N., Phillips, O. L., Anderson, L. O., Alvarez, E., Baker, T. R., Goncalvez, P. H., Huamán-Ovalle, J., Mamani-Solórzano, M., Meir, P., Monteagudo, A., Patiño, S., Peñuela, M. C., Prieto, A., Quesada, C. A., Rozas-Dávila, A., Rudas, A., Silva Jr., J. A., and Vásquez, R. 2009. Above- and below-ground net primary productivity across ten Amazonian

forests on contrasting soils, Biogeosciences, 6, 2759–2778, doi:10.5194/bg-6-2759-2009.

Arino, O., Bicheron, P., Achard, F., Latham, J., Witt, R., Weber, J.L., 2008. GLOBCOVER The most detailed portrait of Earth. ESA Bulletin-European Space Agency (136), 24-31.

Arora, V. and Boer, G.J.,2010. Uncertainties in the 20th century carbon budget associated with land use change. Global Change Biology, 16, 3327–3348.

Aulakh, M.S., Wassmann, R., Bueno, C., Rennenberg, H. 2001. Impact of root exudates of different cultivars and plant development stages of rice (Oryza sativa L.) on methane production in a paddy soil. Plant and Soil, 230, 77–86.

Babu, Y.J., Li C.S., Frolking, S., Nayak, D.R., and Adhya, T.K., 2006. Field validation of DNDC model for methane and nitrous oxide emissions from rice-based production systems of India. *Nutr Cycl Agroecosys,* 74: 157–174.

Baishya, R. & Barik, S. K. 2011. Estimation of tree biomass, carbon pool and net primary production of an old-growth Pinus kesiya Royle ex. Gordon forest in north-eastern India. Annals of Forest Science, 68:727–736.

Bala, G., Gopalakrishnan, R., Jayaraman, M., Nemani, R., Ravindranath, N.H. 2011. CO_2-fertilization and potential future terrestrial carbon uptake in India. Mitig. Adapt. Strat., 16, 143–160.

Bala, G., J. Joshi, R. Chaturvedi, H. Gangamani, H. Hashimoto, and R. Neman. 2013. Variability of AVHRR-derived NPP in India. Remote Sensing, 5:810-829. doi:103390/rs5020810.

Balagopalan, M. and Jose, A.I. 1986. Distribution of organic carbon and different forms of nitrogen in a natural forest and adjacent eucalypt plantation at Arippa, Kerala. In: Eucalyptus in India: Past, Present and Future, 112–119.

Banger K., Toor G.S., Biswas A., Sidhu S.S. and Sudhir K. 2010. Soil organic carbon fractions after 16-years of applications of fertilizers and organic manure in a Typic Rhodalfs in semi-arid tropics. Nutrient Cycling in Agroecosystems 86: 391-399.

Banger, K., H.Q. Tian, and C.Q. Lu. 2012. Do nitrogen fertilizers stimulate or inhibit methane emissions from rice fields? Glob. Change Biol. 18:3259–3267. doi:10.1111/j.1365-2486.2012.02762.x

Banger, K., Kukal, S.S., Toor,G., Sudhir, K., and Hanumanthraju, T.H. 2009. Impact of long-term additions of chemical fertilizers and farm yard manure on carbon and

nitrogen sequestration under rice-cowpea cropping system in semiarid tropics. Plant Soil 318:27–35

Banger, K., Tian, H.Q. and B. Tao., 2013. Contemporary land cover and land use patterns estimated by different regional and global datasets in India. J. Land Use Sci. 10:95–107. doi:10.1080/1747423X.2013.858786.

Banger, K., Tian, H.Q., Tao, B., Lu, C., Ren, W., Yang, J. 2015. Magnitude, spatiotemporal patterns, and controls for soil organic carbon stocks in India during 1901–2010. In press, Soil Science Society of America Journal, doi:10.2136/sssaj2014.11.0456.

Banik, A., Sen, M., and Sen, S.P. 1996. Effects of inorganic fertilizers and micronutrients on methane production from wetland rice (Oryza sativa L). Biology and Fertility of Soils, 21, 319–322.

Bartholome, E. and Belward, A.S. 2005. GLC2000: A new approach to global land cover mapping from Earth observation data. International Journal of Remote Sensing, 26(9), 1959-1977.

Batjes N.H. 2009. Harmonized soil profile data for applications at global and 537 continental scales: updates to the WISE database. Soil Use and Management, 25, 538 124-127.

Batjes, N.H., 2006. ISRIC-WISE derive soil properties on a 5 by 5 arc-minutes global grid (version 1.1). Report 2006/02. Accessed http://www.isric.org.

Behera, B. K. 1994. Community structure, primary production and energetic of a grassland community of Boudh-Kandhamal (Dist-Phulbani) in Orissa,Ph.D. Thesis, Berhampur University, Berhampur, Orissa.

Beig, G., Ghude, S. D., Polade, S. D., and B. Tyagi, 2008. Threshold exceedances and cumulative ozone exposure indices at tropical suburban site, Geophys. Res. Lett., 35, L02802. doi:10.1029/2007GL031434.

Bhat, D. Murali, M., K. S., and Ravindranath, N. H., 2001. Formation and Recovery of Secondary Forests in India: A Particular Reference to Western Ghats in South India. Journal of Tropical Forest Science 13(4): 601–620.

Bhatia, A., Pathak, H., Aggarwal, P.K., (2004). Inventory of methane and nitrous oxide emissions from agricultural soils of India and their global warming potential. *Current Science,* 87(3), 317-324.

Bhattacharyya, T., Chandran, P., Ray, S.K., Mandal, C., Pal, D.K., Venugopalan, M.V., Durge, S.L., Srivastava, P., Dubey, P.N., Kamble, G.K., Sharma, R.P., Wani,

S.P., Rego, T.J., Ramesh, V. and Manna, M.C. 2006. Estimation of carbon stocks in red and black soils of selected benchmark spots in semi-arid tropics of India. Global Theme on Agroecosytems Report no. 28. Patancheru 502324, Andhra Pradesh, India: International Crops Research Institute for the Semi-Arid Tropics (ICRISAT). p. 86.

Bhattacharyya, T., D.K. Pal, C. Mandal, and M. Velayutham. 2000. Organic carbon stock in Indian soils and their geographical distribution. Curr. Sci. 79:655–660.

Bhattacharyya, T., D.K. Pal, M. Easter, N.H. Batjes, E. Milne, K.S. Gajbhiye, P. Chandran, S.K. Ray, C. Mandal, K. Paustian, S. Williams, K. Killian, K. Coleman, P. Falloon, D.S. Powlsone, 2007. Modeled soil organic carbon stocks and changes in the Indo-Gangetic Plains, India from 1980 to 2030. Agric. Ecosyst. Environ. 122:84–94. doi:10.1016/j.agee.2007.01.010

Billings, S. A., Richter, D. D. and Yarie J. 2000. Sensitivity of soil methane fluxes to reduced precipitation in boreal forest soils, Soil Biol. Biochem., 32, 1431–1441, doi:10.1016/S0038-0717(00)00061-4

Billore, S. K. and Mall, L. P. 1977. Dry matter structure and its dynamics in Sehima community II. Dry matter dynamics, Trop. Ecol. 18: 29 - 35.

Bliss, N.B., Olsen, L.M., 1996. Development of a 30-arcsecond digital elevation model of South America. Pecora Thirteen, Human Interactions with the Environment—Perspectives from Space, Sioux Falls, South Dakota, August, pp. 20–22.

Boden, T. A., Marland, G., and Andres, R. J. 2010. Global CO2 Emissions from Fossil-Fuel Burning, Cement Manufacture, and Gas Flaring: 1751–2006, Carbon Dioxide Inf. Anal. Cent., Oak Ridge Natl. Lab., Oak Ridge, Tenn.

Bonan, G.B., Levis, S., Sitch, S., Vertenstein, M., Oleson, K.W., 2003. A dynamic global vegetation model for use with climate models: concepts and description of simulated vegetation dynamics. Global Change Biology 9, 1543–1566.

Bond-Lamberty, B.P. and A.M. Thomson. 2010. A Global Database of Soil Respiration Data, Version 1.0. Data set. Available on-line [http://daac.ornl.gov] from Oak Ridge National Laboratory Distributed Active Archive Center, Oak Ridge, Tennessee, U.S.A. doi:10.3334/ORNLDAAC/984.

Booker F., Muntifering R., McGrath M. et al. 2009. The ozone component of global change: potential effects on agricultural and horticultural plant yield, product quality and interactions with invasive species. Journal of Integrative Plant Biology, 51, 337–351.

Bosse, U., and Frenzel, P. 1997. Activity and distribution of methane-oxidizing bacteria in flooded rice soil microcosms and in rice plants (Oryza sativa). Applied and Environmental Microbiology, 63, 1199–1207.

Bousquet, P, Ciais, P, Miller, J.B. et al. 2006. Contribution of anthropogenic and natural sources to atmospheric methane variability. Nature, 443, 439–443.

Bouwman, A.F., 1996. Direct emission of nitrous oxide from agricultural soils. *Nutrient Cycling in Agroecosystems,* 46, 53-70.

Bouwman, A.F., Boumans, L.J.M., Batjes, N.H., 2002. Modeling global annual N2O and NO emissions from fertilized fields. *Global Biogeochem Cycles,* 16(4):28.1–28.8.

Center for International Earth Science Information Network – CIESIN, 2011. http://sedac.ciesin.columbia.edu/data/set/grump-v1-population-count/metadata accessed November 2013.

Chapin F.S., III, Woodwell G.M., Randerson J.T., Rastetter E.B., Lovett G.M., Baldocchi D.D., Clark D.A., Harmon M.E., Schimel D.S., Valentini R., Wirth C., Aber J.D., Cole J.J., Goulden M.L., Harden J.W., Heimann M., Howarth R.W., Matson P.A., McGuire A.D., Melillo J.M., Mooney H.A., Neff J.C., Houghton R.A., Pace M.L., Ryan M.G., Running S.W., Sala O.E., Schlesinger W.H. and Schulze E.D. 2006. Reconciling carbon-cycle concepts, terminology, and methods. Ecosystems 9: 1041-1050.

Chapin, F. S. 1980. The mineral nutrition of wild plants. Annual Review of Ecology and Systematics, 11:233–260.

Chapin, F. S., K. Autumn, and F. Pugnaire. 1993. Evolution of traits in response to environmental stress. American Naturalist, 142:S78–S92.

Chapuis-Lardy, L., Wrage, N., Metay, A., Chotte, J. L., and Bernoux, M., 2007. Soils, a sink for N2O? A review. *Glob. Change Biol.,* 13, 1–17, doi:10.1111/j.1365-2486.2006.01280.x.

Chaubey, I., Migliaccio, K. Green, C. Arnold, J. and Srinivasan., R. 2006. Phosphorus Modeling in Soil and Water Assessment Tool (SWAT) Model. In Book Modeling Phosphorus in the Environment. Radcliff,D., M.Cabrera. CRC Press: Flordia, U.S., 2006, 163-187.

Chhabra A. and Dadhwal V.K. 2004a. Assessment of major pools and fluxes of carbon in Indian forests. Climatic Change 64: 341-360.

Chhabra A. and Dadhwal V.K. 2004b. Estimating terrestrial net primary productivity over India using satellite data. Current Science 86: 269-271.

Chhabra, A., S. Palria, and V.K. Dadhwal. 2003. Soil organic carbon pool in Indian forests. For. Ecol. Manage. 173:187–199. doi:10.1016/S0378-1127(02)00016-6

Cleveland ,C.C., Townsend, A.R., Taylor, P., et al. 2011. Relationships among net primary productivity, nutrients and climate in tropical rain forest: a pan-tropical analysis. Ecology letters, 14, 939–47.

Conrad, R. 1996.Soil Microorganisms as controllers of atmospheric trace gases (H2, CO, CH4, N2O and NO). *Microbiological reviews* 60, 4, 609-640.

Cramer, W., R. J. Olson, S. D. Prince, and J. M. O. Scurlock. and members of the Global Primary Production Data Initiative (GPPDI). 2001. Global productivity: determining present patterns. Pages 429–448 in J. Roy, B. Saugier, and H. Mooney, editors. Terrestrial global productivity: past, present, future. Academic Press, San Diego, California, USA.

Crutzen, P.J., 1970. The influence of nitrogen oxides on the atmospheric ozone content. *Quarterly Journal of Royal Meteorology Society,* 96, 320-325.

Crutzen, P.J., 1979. The role of NO and NO2 in the chemistry of the troposphere and stratosphere. *Annual Review of Earth Planet Science,* 7, 443-472.

Dadhwal VK, Nayak SR. 1993. A preliminary estimate of biogeochemical cycle of carbon for India. Science and Culture 59(1): 9–13.

Dadhwal, V.K. and Chhabra, A., 2002. Landuse/ landcover change in Indo-Gangetic plains: cropping pattern and agroecosystem carbon cycle. In: Abrol, Y.P., Sangwan, S., and Tiwari, M.K. (eds.), Landuse Change Historical Perspectives: Focus on Indo-Gangetic Plains, Allied Publishers Pvt. Ltd., pp. 249-276.

Dadhwal, V.K., N. Shukla, and A.B. Vora. 1998. Carbon cycle for Indian Forest ecosystem: A preliminary estimate In: B.H. Subbaraya et al., editors, Global change studies: Scientific Results from ISRO-GBP. ISRO, Bangalore. p. 411-430.

Dan, L., J. Ji, and He, Y. 2007. Use of ISLSCP II data to intercompare and validate the terrestrial net primary production in a land surface model coupled to a general circulation model, J. Geophys. Res., 112, D02S90, doi:10.1029/2006JD007721.

Das, A., Lal, R., Patel, D., Idapuganti, R., Layek, J., Ngachan, S., Ghosh, P., Bordoloi, J., Kumar, M., 2014. Effects of tillage and biomass on soil quality and productivity of lowland rice cultivation by small scale farmers in North Eastern India. Soil Till. Res. 143, 50–58.

Davidson E.A. and Ackerman I.L. 1993. Changes in soil carbon inventories following cultivation of previously untilled soils. Biogeochemistry 20: 161-193.

Davidson, E. A., Keller, M., Erickson, H. E., Verchot, L. V., and Veldkamp, E. 2000. Testing a conceptual model of soil emissions of nitrous and nitric oxides, Bioscience, 50, 667–680.

Davidson, E.A., and I.A. Janssens. 2006. Temperature sensitivity of soil carbon decomposition and feedbacks to climate change. Nature 440:165–173. doi:10.1038/nature04514

de Graaff, M.A., K.J. van Groenigen, J. Six, B. Hungate, and C. van Kessel. 2006. Interactions between plant growth and soil nutrient cycling under elevated CO2: A meta-analysis. Glob. Change Biol. 12:2077–2091. doi:10.1111/j.1365-2486.2006.01240.x

Deevey, E. S. 1970. Mineral cycles. Scientific American, 223: 149–158.

Del Campillo, M.C., van der Zee, S.E.A.T.M. and Torrent, J. 1999. Modelling long term phosphorus leaching and changes in phosphorus fertility in excessively fertilized acid sandy soils. European Journal of Soil Science, 50, 391-399.

Denier van der Gon, H.A.C., N. van Breemen, H.U. Neue, R.S. Lantin, J.B. Aduna, M.C.K. Alberto, and R. Wassmann. 1996. Release of entrapped methane from wetland rice fields upon soil drying. Global Biogeochem. Cycles 10:1–7. doi:10.1029/95GB03460

Denman, K.L., Brasseur, G., Chidthaisong, A, et al., 2007. Couplings between changes in the climate system and biogeochemistry. In: Solomon S, Qin D, Manning M, et al. (Eds). Climate change 2007: the physical science basis. Contribution of Working Group I to the Fourth Assessment Report of the Intergovernmental Panel on Climate Change. Cambridge, UK: Cambridge University Press.

Dentener F., Drevet J., Lamarque J.F., Bey I., Eickhout B., Fiore A.M., Hauglustaine D., Horowitz L.W., Krol M., Kulshrestha U.C., Lawrence M., Galy-Lacaux C., Rast S., Shindell D., Stevenson D., Van Noije T., Atherton C., Bell N., Bergman D., Butler T., Cofala J., Collins B., Doherty R., Ellingsen K., Galloway J., Gauss M., Montanaro V., Muller J.F., Pitari G., Rodriguez J., Sanderson M., Solmon F., Strahan S., Schultz M., Sudo K., Szopa S. and Wild O. 2006. Nitrogen and sulfur deposition on regional and global scales: A multimodel evaluation. Global Biogeochemical Cycles 20.

Dentener, F., Stevenson, D., Cofala, J., Mechler, J., Amann, R., Bergamashi, P., Raes, F., and Derwent, R. 2005. The impact of air pollutant and methane emission controls on tropospheric ozone and radiative forcing: CTM calculations, Atmos. Chem. Phys., 5, 1731–1755.

DES (Department of Economics and Statistics, Government of India), 2010. http://eands.dacnet.nic.in (accessed April, 2014).

Devi, S. L. & Yadava, P. S. 2009. Aboveground biomass and net primary production of semi-evergreen tropical forest of Manipur, north-eastern India. Journal of Forestry Research, 20(2): 151−155.

Dijkstra, F. A., S. A. Prior, G. B. Runion, H. A. Torbert, H. Tian, C. Lu, and R. T. Venterea. 2012. Effects of elevated carbon dioxide and increased temperature on methane and nitrous oxide fluxes: evidence from field experiments. Frontiers in Ecology and the Environment 10(10):520–527.

Ding, W. X., Cai, Z. C., and Tsuruta, H. 2004. Cultivation, nitrogen fertilization, and set-aside effects on methane uptake in a drained marsh soil in Northeast China, Glob. Change Biol., 10, 1801-1809.

Dlugokencky, E.J., Walter, B.P., Masarie, K.A., Lang, P.M., Kasischke, E.S. 2001. Measurements of an anomalous global methane increase during 1998. Geophysical Research Letters, 28, 499–502.

Don, A., Schumacher, J., and Freibauer, A. 2011. Impact of tropical land-use change on soil organic carbon stocks - a meta-analysis. Global Change Biology, 17, 1658–1670.

Elser, J. J., Bracken, M. E. S., Cleland, E. E., Gruner, D. S., Harpole, W. S., Hillebrand, H., Ngai, J. T., Seabloom, E.W., Shurin, J. B., and Smith, J. E. 2007.Global analysis of nitrogen and phosphorus limitation of primary producers in freshwater, marine and terrestrial ecosystems, Ecol. Lett., 10, 1135–1142.

Entry, J.A., Sojka, R.E. and G. Shewmaker, 2002. Managment of irrigated agriculture to increase carbon storage in soils. Soil Sci. Soc. Am. J. 66, 1957–1964.

FAO (Food and Agriculture Organization of the United Nations), 2013. http://www.fao.org/corp/statistics/en/ accessed April, 2013.

Farquhar, G. D., Caemmerer, S. and Berry, J. A. 1980. A biochemical model of photosynthetic CO2 assimilation in leaves of C3 species. Planta 149, 78–90.

Feddema, J.J. et al., 2005. The importance of land-cover change in simulating future climates. Science, 310(5754), 1674-1678.

Felzer B., Reilly J., Melillo J., Kicklighter D., Sarofim M., Wang C., Prinn R. and Zhuang Q. 2005. Future effects of ozone on carbon sequestration and climate change policy using a global biogeochemical model. Climatic Change 73: 345-373.

Feng Z., Kobayashi K. and Ainsworth E.A. 2008. Impact of elevated ozone concentration on growth, physiology, and yield of wheat (Triticum aestivum L.): a meta-analysis. Global Change Biology 14: 2696-2708.

Filippelli, G.M. 2008. The Global Phosphorus Cycle: Past, Present, and Future. Elements, 4, 89–95.

Firestone, M.K., Davidson, E.A., (1989). Microbiological basis of NO and N2O production and consumption in soil. In: Exchange of Trace Gases Between Terrestrial Ecosystems and the Atmosphere (eds Andreae MO, Schimel DS), pp. 7-21. John Wiley and Sons, New York.

Flint, E.P., 1994. Changes in land-use in South and Southeast-Asia from 1880 to 1980 - A data-base prepared as part of a coordinated research-program on carbon fluxes in the tropics. Chemosphere, 29(5), 1015-1062.

Forest Survey of India, 1999. India State of Forest Report 1999. Ministry of Environment and Forest.Government of India, Dehra Dun.

Forest Survey of India, 2012. India State of Forest Report 2011. Ministry of Environment and Forest. Government of India. Dehra Dun.

Forster, P., Ramaswamy, V., Artaxo, P., et al., 2007. Changes in atmospheric constituents and in radiative forcing. In: Solomon S, Qin D, Manning M, et al. (Eds). Climate change 2007: the physical science basis. Contribution of Working Group I to the Fourth Assessment Report of the Intergovernmental Panel on Climate Change. Cambridge, UK: Cambridge University Press.

Fuchs, R., Herold, M., Verburg, P. H., and Clevers, J. G. P. W. 2003. A high-resolution and harmonized model approach for reconstructing and analysing historic land changes in Europe, Biogeosciences, 10, 1543-1559, doi:10.5194/bg-10-1543-2013, 2013.

Gadgil, M., and R. Guha. 1995. Ecology and equity. The use and abuse of nature in contemporary India. Penguin Books India, New Delhi.

Ganeshmurthy, A.N., Mongia, A.D. and Singh, N.T. 1989. Forms of sulphur in soil profiles of Andaman and Nicobar Islands. J. Indian Soc. Soil Sci., 37 (4), 825–829

Ganeshmurthy, A.N., Mongia, A.D. and Singh, N.T. 1989. Forms of sulphur in soil profiles of Andaman and Nicobar Islands. J. Indian Soc. Soil Sci., 37 (4), 825–829

Garkoti, S.C. & Singh, S.P. (1995). Variation in net primary productivity and biomass of forests in the high mountains of Central Himalaya. Journal of Vegetation Science 6: 23-28.

Garkoti, S.C. & Singh, S.P. (1995). Variation in net primary productivity and biomass of forests in the high mountains of Central Himalaya. Journal of Vegetation Science 6: 23-28.

Ghosh, P.K., A. Das, R. Saha, Khakrang, A.K. Tripathi, G.C. Munda, and S.V. Ngachan. 2009. Long-term effect on soil quality in acid soil of North-East India. Soil Res. 47:372–379. doi:10.1071/SR08169

Ghosh, S., Wilson, B., Ghoshal, S., Senapati, N. and Mandal, B. 2012. Organic amendments influence soil quality and carbon sequestration in the Indo-Gangetic plans of India. Agric. Ecosystems Env., 156: 134–41.

Ghude, S. D., C. Jena, D. M. Chate, G. Beig, G. G. Pfister, R. Kumar, and V. Ramanathan 2014. Reductions in India's crop yield due to ozone, Geophys. Res. Lett., 41, doi:10.1002/2014GL060930.

Goldberg, S. D., and Gebauer, G. 2009. Drought turns a Central European Norway spruce forest soil from an N2O source to a transient N2O sink, Glob. Change Biol., 15, 850-860, DOI 10.1111/j.1365-2486.2008.01752.x.

Goll, D. S., Brovkin, V., Parida, B. R., Reick, C. H., Kattge, J., Reich, P. B., van Bodegom, P. M., and Niinemets, Ü. 2012. Nutrient limitation reduces land carbon uptake in simulations with a model of combined carbon, nitrogen and phosphorus cycling, Biogeosciences, 9, 3547–3569, doi:10.5194/bg-9-3547-2012.

Government of India, 1894, 'Forest Policy, 1894'.

Government of India, 1952, 'National Forest Policy, 1952'.

Government of India, 1988, 'National Forest Policy, 1988'.

Grant RF, Hutyra LR, Oliveira RC De, Munger IW, Saleska SR, Wofsy SC (2009) Modeling the carbon balance of Amazonian rain forests : ecological controls on net ecosystem productivity resolving. ecological monographs, 79, 445–463.

Guidry, M.W., and Mackenzie, F.T. 2000. Apatite weathering and the Phanerozoic phosphorus cycle. Geology, 28: 631-634.

Gupta, R.K., and D.L.N. Rao. 1994. Potential of wastelands for sequestering carbon by reforestation. Curr. Sci. 66:378–380.

Hakanson, L. 2003. Propagation and analysis of uncertainty in ecosystem models, in: Models in ecosystem science, edited by: Canham, C. D., Cole, J. J., and Lauenroth, W. K., Princeton University Press, Princeton.

Hansen, M.C. and Reed, B., 2000. A comparison of the IGBP DISCover and University of Maryland 1km global land cover products. International Journal of Remote Sensing, 21(6-7), 1365-1373.

Hati, K.K., A. Swarup, A.K. Dwivedi, et al. 2007. Changes in soil physical properties and organic carbon status at the topsoil horizon of a Vertisol of central India after 28 years of continuous cropping, fertilization and manuring. Agric. Ecosyst. Environ. 119:127–134. doi:10.1016/j.agee.2006.06.017

Heimann, M., and Reichstein, M. 2008. Terrestrial ecosystem carbon dynamics and climate feedbacks. Nature, 451, 289-292, 10.1038/nature06591.

Hein, R., Crutzen, P., and Heimann, M. 1997. An inverse modeling approach to investigate the global atmospheric methane cycle, Global Biogeochem. Cy., 11, 43-76.

Hingane, L.S. 1991. Some aspects of carbon-dioxide exchange between atmosphere and Indian plant biota. Clim. Change, 18, 425–435.

Hooda, R. S., Dye, D. G. and Shibasaki, R., 1996 . Estimation of Indian agricultural productivity using Production Efficiency Model. Inter. Archives of Photogrammetry and Remote Sensing, Vol. XXXI, Part B7, pp. 298-303.

Houghton, R.A. and Hackler, J.L., 1999. Emissions of carbon from forestry and land-use change in tropical Asia. Global Change Biology, 5(4), 481-492.

Houghton, R.A. and Hackler, J.L., 2003. Sources and sinks of carbon from land-use change in China. Global Biogeochemical Cycles, 17(2).

Houghton, R.A. et al., 2012. Carbon emissions from land use and land-cover change. Biogeosciences, 9(12), 5125-5142.

Houghton, R.A., 2002. Temporal patterns of land-use change and carbon storage in China and tropical Asia. Science in China (Series C) 45, 10–17 (Suppl.).

Huang, Y., Sun, W., Zhang, W., Yu, Y., Su, Y., and Song, C. 2010. Marshland conversion to cropland in northeast China from 1950 to 2000 reduced the greenhouse effect, Glob. Change Biol., 16, 680-695, doi:10.1111/j.1365-2486.2009.01976.x.

Hurtt, G.C. et al., 2006. The underpinnings of land-use history: three centuries of global gridded land-use transitions, wood-harvest activity, and resulting secondary lands. Global Change Biology, 12(7), 1208-1229.

Hutchin, P. R., Press, M. C., Lee, J. A., and Ashenden, T. W. 1995. Elevated concentrations of CO2 may double methane emissions from mires, Glob. Change Biol., 1, 125-128.

IPCC. 2007. The physical science basis. Contribution of workgroup I to the fourth assessment report of the Intergovernmental Panel on Climate Change, Cambridge University Press, Cambridge, United Kingdom and New York, NY, USA.

Jagadeesh Babu, Y., C. Li, S. Frolking, D.R. Nayak, and Adhya. T.K. 2006. Field validation of DNDC model for methane and nitrous oxide emissions from rice-based production systems of India. *Nutrient Cycling in Agroecosystems,* 74:157-174. doi:10.1007/s10705-005-6111-5.

Jain, A. K., and Yang, X. 2005. Modeling the effects of two different land cover change data sets on the carbon stocks of plants and soils in concert with CO2 and climate change. Global Biogeochem Cycles, 19(2): GB2015

Janssens, I. A., Freibauer, A., Ciais, P., Smith, P., Nabuurs, G.-J., Folberth, G., Schlamadinger, B., Hutjes, R. W. A., Ceulemans, R., Schulze, E.-D., Valentini, R., and Dolman, A. J. 2003. Europe's terrestrial biosphere absorbs 7 to 12% of European Anthropogenic CO2 emissions, Science, 300, 1538–1542.

Jastrow, J. D., Miller, R. M., Matamala, R., Norby, R. J., Boutton, T. W., Rice, C. W. and Owensby, C. E. 2005. Elevated atmospheric carbon dioxide increases soil carbon. Glob. Change Biol., 11, 2057–2064. doi:10.1111/j.1365-2486.2005.01077.x.

Jastrow, J.D., R.M. Miller, and C.E. Owensby. 2000. Long-term effects of elevated atmospheric CO2 on below-ground biomass and transformations to soil organic matter in grassland. Plant Soil 224:85–97. doi:10.1023/A:1004771805022.

Jeganathan, C., Dadhwal, V.K., Gupta, K. and Raju, P.L.N., 2009. Comparison of MODIS vegetation continuous field - based forest density maps with IRS-LISS III derived maps. Journal of the Indian Society of Remote Sensing, 37(4), 539-549.

Jenny, H. and Raychaudhuri. S.P. 1960. Effect of climate and cultivation on nitrogen and organic matter reserves in Indian soils. Indian Council of Agricultural Research, New Delhi, pp. 126.

Johnston, C.A., P. Groffman, D.D. Breshears, Z.G. Cardon, W. Currie, W. Emanuel, J. Gaudinski, R.B. Jackson, K. Lajtha, K. Nadelhoffer, D. Nelson, Jr., W.M. Post, G.

Retallack, and L. Wielopolski. 2004. Carbon cycling in soil. Front. Ecol. Environ 2:522–528. doi:10.1890/1540-9295(2004)002[0522:CCIS]2.0.CO;2

Joshi, A.K., Pant, P., Kumar, P., Giriraj, A. and Joshi, P.K., 2011. National Forest Policy in India: Critique of Targets and Implementation. Small-Scale Forestry, 10(1), 83-96.

Joshi, B. & Pant, S. C. 2012. Monthly variation in plant biomass and net primary productivity of a mixed deciduous forest at foothills of Kumaun Himalaya. International journal of Conservation Science, 3 (1), 41–50.

Joshi, P.K.K., Roy, P.S., Singh, S., Agrawal, S. and Yadav, D., 2006. Vegetation cover mapping in India using multi-temporal IRS Wide Field Sensor (WiFS) data. Remote Sensing of Environment, 103(2), 190-202.

Kai, F.M., Tyler, S.C., Randerson, J.T., Blake, D.R., 2011. Reduced methane growth rate explained by decreased Northern Hemisphere microbial sources. Nature 476, 194-197

Kammann C, Muller C, Grunhage L, Jager HJ. 2008. Elevated CO2 stimulates N2O emissions in permanent grassland. Soil Biology & Biochemistry 40: 2194–2205.

Kaplan, J. O., Krunhardt, K. M., and Zimmermann, N., 2009. The prehistoric and preindustrial deforestation of Europe. Quatern Science Reviews 28(27–28):3016–3034

Kaspari, M., Garcia, M.N., Harms, K.E., Santana, M., Wright, S.J., Yavitt, J.B. 2008. Multiple nutrients limit litterfall and decomposition in a tropical forest. Ecology letters, 11, 35–43.

Keeling, R.F., Piper, S.C., Heimann, M. 1996. Global and hemispheric CO2 sinks deduced from changes in atmospheric O2 concentration. Nature 381:218–221

Khalil, M.A.K., and Butenhoff, C.L. 2008. Spatial variability of methane emissions from rice fields and implications for experimental design. Journal of Geophysical Research-Biogeosciences, 113, G00A09, doi: 10.1029/2007JG000517.

Kirschke, S., et al. 2013. Three decades of global methane sources and sinks. Nature Geoscience 6(10):813–823.

Klein Goldewijk, K. and Verburg, P. H., 2013. Uncertainties in global-scale reconstructions of historical land use: an illustration using the HYDE data set. Landscape Ecology, 28:861–877, DOI 10.1007/s10980-013-9877-x.

Klein Goldewijk, K., 2001. Estimating global land use change over the past 300 years: The HYDE Database. Global Biogeochemical Cycles, 15(2), 417-433.

Klein Goldewijk, K., 2007. ISLSCP II Historical Land Cover and Land Use, 1700-1990. In Hall, Forest G., G. Collatz, B. Meeson, S. Los, E. Brown de Colstoun, and D. Landis (eds.). ISLSCP Initiative II Collection. Data set. Available on-line [http://daac.ornl.gov/] from Oak Ridge National Laboratory Distributed Active Archive Center, Oak Ridge, Tennessee, U.S.A. doi:10.3334/ORNLDAAC/967.

Klein Goldewijk,K., Beusen, A., van Drecht, G. and de Vos, M., 2011. The HYDE 3.1 spatially explicit database of human-induced global land-use change over the past 12,000 years. Global Ecology and Biogeography, 20(1), 73-86.

Knisel, W. G. 1993. GLEAMS: Groundwater Loading Effects of Agricultural Management Systems. UGA-CPES-BAED Publication no. 5.

Krausmann F., Erb K.-H., Gingrich S., Haberl H., Bondeau A., Gaube V., Lauk C., Plutzar C. and Searchinger T.D. 2013. Global human appropriation of net primary production doubled in the 20th century. Proceedings of the National Academy of Sciences of the United States of America 110: 10324-10329.

Kroeze, C., Mosier, A., Bouwman, L., 1999. Closing the N2O Budget: a retrospective analysis. *Global Biogeochemistry Cycles,* 13, 1-8.

Kukal, S.S., Rehana, R. and D.K. Benbi, 2009. Soil organic carbon sequestration in relation to organic and inorganic fertilization in rice-wheat and maize-wheat systems. Soil and Tillage Research, 102(1): 87-92.

Kumar, N. J.I., Sajish, P.R., Kumar, R.N., & Patel, K. (2011). Biomass and Net Primary Productivity in three different Aged Butea Forest Ecosystems in Western India, Rajasthan. Our Nature, 9: 73-82.

Kundu, S., R. Bhattacharyya, V. Prakash, et al. 2007. Carbon sequestration and relationship between carbon addition and storage under rainfed soybean–wheat rotation in a sandy loam soil of the Indian Himalayas. Soil Tillage Res. 92:87–95. doi:10.1016/j.still.2006.01.009

Le Quere, C., Raupach, M. R., Canadell, J. G., Marland, G., Bopp, L., Ciais, P., Conway, T. J., Doney, S. C., Feely, R. A., Foster, P., Friedlingstein, P., Gurney, K., Houghton, R. A., House, J. I., Huntingford, C., Levy, P. E., Lomas, M. R., Majkut, J., Metzl, N., Ometto, J. P., Peters, G. P., Prentice, I. C., Randerson, J. T., Running, S. W., Sarmiento, J. L., Schuster, U., Sitch, S., Takahashi, T., Viovy, N., van der Werf, G. R., and Woodward, F. I. 2009. Trends in the sources and sinks of carbon dioxide, Nat. Geosci., 2, 831–836.

Leff B., Ramankutty N. and Foley J.A. 2004. Geographic distribution of major crops across the world. Global Biogeochemical Cycles 18.

Lehner, B., Döll, P., 2004. Development and validation of a global database of lakes, reservoirs and wetlands. Journal of Hydrology 296 (1–4), 1–22.

Leonard, R.A., Knisel,W.G., Still, D.A.1987. Cleams:Groundwater Loading Effects of Agricultural Management Systems. American Society of Agricultural Engineers, 30, 1403–1418.

Lewis, D.R, and McGechan, M.B. 2002. A Review of Field Scale Phosphorus Dynamics Models. Biosystems Engineering, 82, 359–380.

Lin, B., Sakoda, A., Shibasaki, R., Goto, N., and Suzuki, M. 2000. Modeling a global biogeochemical nitrogen cycle in terrestrial ecosystems. *Ecol. Model.,* 135, 89–110.

Liu, J., H.Q. Tian, M. Liu, D. Zhuang, J.M. Melillo and Z. Zhang. 2005. China's changing landscape during the 1990s: Large-scale land transformation estimated with satellite data. *Geophysical Research Letters*, *32*, L02405, doi:10.1029/2004GL021649.

Liu, J., M. Liu, H.Q. Tian, D. Zhuang, Z. Zhang, W. Zhang and X. Tang, X. Deng. 2005. Spatial and temporal patterns of China's cropland during 1990-2000: An analysis based on Landsat TM data. Remote Sensing of Environment 98: 442-456.

Liu, L. L , and Greaver T.L. 2009. A review of nitrogen enrichment effects on three biogenic GHGs: the CO2 sink may be largely offset by stimulated N2O and CH4 emission. *Ecology Letters,* 12, 1103–1117.

Liu, M., H. Tian, G. Chen, W. Ren, C. Zhang, and J. Liu, 2008. Effects of land-use and land-cover change on evapotranspiration and water yield in China during 1900-2000, *Journal of the American Water Resources Association*, *44*(5), 1193-1207, doi:10.1111/j.1752-1688.2008.00243.x.

Liu, M.L. and Tian, H.Q., 2010. China's land cover and land use change from 1700 to 2005: Estimations from high-resolution satellite data and historical archives. Global Biogeochemical Cycles, 24.

Lo Seen, D., B.R. Ramesh, K.M. Nair, M. Martin, D. Arrouays, and G. Bourgeon. 2010. Soil carbon stocks, deforestation and land-cover changes in the western ghats biodiversity hotspot (India). Glob. Change Biol. 16:1777–1792. doi:10.1111/j.1365-2486.2009.02127.x

Lobell, D.B., Sibley, A, Ortiz-Monasterio, J.I. 2012. Extreme heat effects on wheat senescence in India. Nature Climate Change 2: 186–189. doi: 10.1038/nclimate1356.

Loveland, T.R. and Belward, A.S. 1997. The IGBP-DIS global 1 km land cover data set, DISCover: first results. International Journal of Remote Sensing, 18(15), 3291-3295.

Lu, C. and Tian, H., 2012. Net greenhouse gas balance in response to nitrogen enrichment: Perspectives from a coupled biogeochemical model. Global Change Biology, doi:10.1111/gcb.12049.

Lu, C., H. Tian, M. Liu, W. Ren, X. Xu, G. Chen, and C. Zhang. 2012. Effect of nitrogen deposition on China's terrestrial carbon uptake in the context of multifactor environmental changes. Ecol. Appl. 22:53–75. doi:10.1890/10-1685.1

Lu, D., Xu, X., Tian, H., Moran, E., Zhao, M., and Running, S., 2010. The Effects of Urbanization on Net Primary Productivity in Southeastern China. Environmental Management, 46(3), 404-410, DOI: 10.1007/s00267-010-9542-y.

Majumder, B., B. Mandal, and P. Bandyopadhyay. 2008. Soil organic carbon pools and productivity in relation to nutrient management in a 20-year-old rice–berseem agroecosystem. Biol. Fertil. Soils 44:451–461. doi:10.1007/s00374-007-0226-6

Mandal, B., B. Majumder, P.K. Bandyopadhyay, G.C. Hazra, A. Gangopadhyay, R.N. Samantaray, A.K. Mishra, J. Chaudhury, M.N. Saha, and S. Kundu. 2007. The potential of cropping systems and soil amendments for carbon sequestration in soils under long-term experiments in subtropical India. Glob. Change Biol. 13:357–369. doi:10.1111/j.1365-2486.2006.01309.x

Mandal, B., Majumder, B., Adhya, T.K., Bandyopadhyay, P. K., Gangopadhyay, A., Sarkar, D., Kundu M.C., Choudhury, S.G., Hazra, G.C., Kundu, S., Samantaray, R.N. and Misra, A.K. 2008. Potential of double-cropped rice ecology to conserve organic carbon under subtropical climate. Glob. Change Biol. 14:2139–2151. doi:10.1111/j.1365-2486.2008.01627.x

Manna, M.C., A. Swarup, R.H. Wanjari, H.N. Ravankar, B. Mishra, M.N. Saha, Y.V. Singh, D.K. Sahi, P.A. Sarap. 2005. Long-term effect of fertilizer and manure application on soil organic carbon storage, soil quality and yield sustainability under sub-humid and semi-arid tropical India. Field Crops Res. 93:264–280. doi:10.1016/j.fcr.2004.10.006

Matson, P.A., Billow, C.R., Hall, S.J. and Zachariassen, J.1996. Nitrogen trace gas responses to fertilization in sugar cane ecosystems. J. Geophys. Res. 101(D13): 18522–18545

McGroddy, M. E., Daufresne, T. and Hedin, L. O. 2004. Scaling of C:N:P stoichiometry in forests worldwide: implications of terrestrial Redfield-type ratios. Ecology, 85, 2390–2401.

McSwiney, C.P., and Robertson, G.P., 2005. Nonlinear response ofN20 flux to incremental fertilizer addition in a continuous maize (Zea mays L.) cropping system. *Global Change Biol.*, 11: 1712-1719.

Melton, J. R., et al. 2013. Present state of global wetland extent and wetland methane modeling: conclusions from a model Intercomparison project (WETCHIMP. Biogeosciences 10(2):753–788.

Millennium Ecosystem Assessment, 2005. Ecosystems and Human Well-being: Current State and Trends. The Millennium Ecosystem Assessment Series, 1, Island Press, Washington, D.C., USA.

Ministry of Environment and Forests, 1980. Forest Conservation Act 1980. Government of India.

Mishra, V., 2002. Population growth and intensification of land use in India. International Journal of Population Geography 8(5): 365–383.

Misra, C. M. 1973. Primary productivity of a grassland ecosystem at Ujjain, Ph. D. Thesis. Vikram Univ. Ujjain.

Misra, M. K. 1978. Phytosociology and primary production of a grassland community at Berhampur, Orissa, India. Ph. D. Thesis, Berhampur University, Berhampur.

Mitra, A.P., Sharma, Subodh, K., Bhattacharya, S., Garg, A., Devotta, S., Sen, Kalyan, (Eds.), (2004). Climate Change and India: Uncertainty Reduction in GHG Inventories. Universities Press (India) Pvt. Ltd., Hyderabad.

Mittal, M.L., Hess, P.G., Jain, S.L., Arya, B.C. and Sharma, C. 2007. Surface ozone in the Indian region. Atmospheric Environment 41: 6572-6584.

Morgan, J.A., A.R. Mosier, D.G. Milchunas, D.R. LeCain, J.A. Nelson, and W.J. Parton. 2004. CO2 enhances productivity, alters species composition, and reduces digestibility of short-grass steppe vegetation. Ecol. Appl. 14(1):208–219. doi:10.1890/02-5213

Morsky, S., Haapala, J. K., Rinnan, R. A., Tiiva, P., Saarnio, S., Silvola, J., Holopalinen, T., and P.J., M. 2008. Long-term ozone effects on vegetation, microbial community and methane dyanmics of boreal peatland microcosms in open-field conditions, Glob. Change Biol., 14, 1891-1903, 10.1111/j.1365-2486,2008.01615.x.

Mosier A, Kroeze C, Nevison C *et al.,* 1998. Closing the global N2O budget: nitrous oxide emissions through the agricultural nitrogen cycle - 0ECD/IPCC/IEA phase II development of IPCC guidelines for national greenhouse gas inventory methdology. *Nutrient Cycling in Agroecosystems,* 52, 225-248.

Mosier, A., Schimel, D., Valentine, D., Bronson, K., and Parton, W. 1991. Methane and nitrous oxide fluxes in native, fertilized and cultivated grasslands. *Nature,* 350, 330–332, 1991.

Nair, K.M., Chamuah, G.S. and Deshmukh, S.N. 1989. Forest soils of Meghalaya, their characterisation, classification and constraints to productivity. Van Vigyan, 27 (1), 34–41

Nayak R.K., Patel N.R. and Dadhwal V.K. 2010. Estimation and analysis of terrestrial net primary productivity over India by remote-sensing-driven terrestrial biosphere model. Environmental Monitoring and Assessment 170: 195-213.

Nayak R.K., Patel N.R. and Dadhwal V.K. 2013. Inter-annual variability and climate control of terrestrial net primary productivity over India. International Journal of Climatology 33: 132-142.

Nayak R.K., Patel N.R. and Dadhwal V.K. 2015. Spatio-temporal variability of net ecosystem productivity over India and its relationship to climatic variables. Environ Earth Science, DOI 10.1007/s12665-015-4182-4.

Nayak, P., D. Patel, B. Ramakrishnan, et al. 2009. Long-term application effects of chemical fertilizer and compost on soil carbon under intensive rice–rice cultivation. Nutr. Cycling Agroecosyst. 83:259–269. doi:10.1007/s10705-008-9217-8

Negi S.S., 1986. Forest Policy and Five Year Plan. In A Hand Book of Forestry. IBH, Dehradun. P 102-120.

Nemani R.R., Keeling C.D., Hashimoto H., Jolly W.M., Piper S.C., Tucker C.J., Myneni R.B. and Running S.W. 2003. Climate-driven increases in global terrestrial net primary production from 1982 to 1999. Science 300: 1560-1563.

Niwa, Y., Machida, T., Sawa, Y., Matsueda, H., Schuck, T. J., Brenninkmeijer, C. A. M., Imasu, R., and Satoh, M. 2012. Imposing strong constraints on tropical terrestrial CO2 fluxes using passenger aircraft based measurements, J. Geophys. Res.-Atmos., 117, D11303, doi::10.1029/2012JD01747.

Norby, R.J., J. Ledford. C.D. Reilly et al. 2004. Fine-root production dominates response of a deciduous forest to atmospheric CO2 enrichment. Proc. Nat. Acad. Sci. USA, 101: 9689–9693.

NRSA (National Remote Sensing Agency), 2007. Natural resources census: national land use and land cover mapping using multi-temporal AWiFS data, Project Report. Publication No. NRSA/LULC/1:250 K/2007-1. National Remote Sensing Agency, Hyderabad, India

Ollinger, S.V., Aber, J.D., Reich, P.B.,1997. Simulating ozone effects on forest productivity: interactions among leaf-, canopy-, and stand-level processes. Ecological Applications, 7, 1237–1251.

Pacala, S.W., Hurtt, G.C., Houghton, R.A., Birdsey, R.A., Heath, L., Sundquist, E.T., Stallard, R.F., Baker, D., Peylin, P., Moorcroft, P., Caspersen, J., Shevliakova, E., Harmon, M.E., Fan, S.M., Sarmiento, J.L., Goodale, C., Field, C.B., Gloor, M., Schimel, D. 2001. Consistent Land- and Atmosphere-Based U.S. Carbon Sink Estimates. Science 292 , 2316–2320.

Pan, S., H. Tian, S.R. Dangal, C. Zhang, J. Yang, B. Tao, Z. Ouyang, X. Wang, C. Lu, and W. Ren. 2014a. Complex spatiotemporal responses of global terrestrial primary production to climate change and increasing atmospheric CO2 in the 21st century. PLoS ONE 9:E112810. doi:10.1371/journal.pone.0112810

Pan, S., H. Tian, S.R. Dangal, Q. Yang, J. Yang, C. Lu, B. Tao, W. Ren, and Z. Ouyang. 2015. Responses of global terrestrial evapotranspiration to climate change and increasing atmospheric CO2 in the 21st century. Earth's Future 3:15–35. doi:10.1002/2014EF000263

Pan, S., Tian H., Dangal S., Ouyang Z., Lu C.,Yang J., Ren W.,Tao B.,Banger K., Yang Q., and Zhang B. (2014b). Interannual and spatial variations of net primary production in the global terrestrial ecosystem during 2000-2009. Journal of Geographical Sciences. (Accepted).

Pan, S., Tian H., Dangal S., Ouyang Z., Tao B., Ren W., Lu C., Wang X. and Running S. 2014c. Modeling and monitoring terrestrial primary production in a changing global environment: Toward a multi-scale synthesis of observation and simulation. Advances in Meteorology doi: 10.1155/2014/965936.

Pande, P. K. 2005. Biomass and productivity in some disturbed tropical dry deciduous teak forests of Satpura plateau, Madhya Pradesh. Tropical Ecology, 46(2): 229–239.

Panigrahy, R. K., Panigrahy, S., Parihar, J. S. 2004. Spatiotemporal pattern of agro ecosystem net primary productivity of India: A preliminary analysis using spot Vgt data. Int. Symp. on Geospatial Databases for Sustainable Development, Goa 36(4): 724–729.

Panigrahy, S., Murthy, T.V.R., Patel, J.G., and Singh, T.S. 2012. Wetlands of India: inventory and assessment at 1:50,000 scale using geospatial techniques. Current Science, 102(6):852-856

Parashar, D.C., Kushrestha, U.C., Sharma, C., 1998. Anthropogenic emissions of NOx, NH3 and N2O in India. *Nutrient Cycl. Agroecosyst.* 52, 255–259.

Parton, W.J., Scurlock, J.M.O., Ojima, D.S., Gilmanov, T.G., Scholes, R.J., Schimel, D.S., Kirchner, T., Menaut, J-C., Seastedt, T., Garcia Moya, E., Apinan Kamnalrut, and J.L. Kinyamario. 1993. Observations and modeling of biomass and soil organic matter dynamics for the grassland biome worldwide. Global Biogeochemical Cycles, 7:785-809.

Parton, W.J., Stewart, J.W.B., Cole, C.V., 1988. Dynamics of C, N, P, and S in grassland soils: a model. Biogeochemistry 5, 109–131.

Patel N.R, Dadhwal V.K Saha S.K, Garg A and Sharma N, 2010. Evaluating the potential of MODIS data to infer water stress scalar for estimating cropland NPP. Tropical Ecology, 51(1): pp. 93-105.

Pathak, H., N. Jain, A. Bhatia, S. Mohanty, and N Gupta. 2009. Global warming mitigation potential of biogas plants in India. Environ. Monit. Assess. 157:407–418. doi:10.1007/s10661-008-0545-6

Patra, P. K., Canadell, J. G., Houghton, R. A., Piao, S. L., Oh, N.-H., Ciais, P., Manjunath, K. R., Chhabra, A.,Wang, T., Bhattacharya, T., Bousquet, P., Hartman, J., Ito, A., Mayorga, E., Niwa, Y., Raymond, P. A., Sarma, V. V. S. S., and Lasco, R. 2013. The carbon budget of South Asia, Biogeosciences, 10, 513–527, doi:10.5194/bg-10- 513-2013.

Patra, P. K., Niwa, Y., Schuck, T. J., Brenninkmeijer, C. A. M., Machida, T., Matsueda, H., and Sawa, Y. 2011. Carbon balance of South Asia constrained by passenger aircraft CO2 measurements, Atmos. Chem. Phys., 11, 4163–4175, doi:10.5194/acp-11-4163-2011.

Patra, P.K., Canadell, J.G., Houghton, R.A. et al. 2013. The carbon budget of South Asia. Biogeosciences, 10, 513–527.

Petersen, B.M., Jensen, L.S., Hansen, S., Pedersen, A., Henriksen, T.M., Sorensen, P., Trinsoutrot-Gattin, I. & Berntsen, J. 2005. CN-SIM: a model for the turnover of soil organic matter. II. Short-term carbon and nitrogen development. Soil Biology & Biochemistry, 37, 375–393.

Peylin, P., Law, R. M., Gurney, K. R., Chevallier, F., Jacobson, A. R., Maki, T., Niwa, Y., Patra, P. K., Peters, W., Rayner, P. J., Rödenbeck, C., and Zhang, X. 2013. Global atmospheric carbon budget: results from an ensemble of atmospheric

CO2 inversions, Biogeosciences Discuss., 10, 5301–5360, doi:10.5194/bgd-10-5301-2013

Piao, S. L., Fang, J., Ciais, P., Peylin, P., Huang, Y., Sitch, S., and Wang, T. 2009. The carbon balance of terrestrial ecosystems in China, Nature, 458, 1009–1013.

Post, W. M., and Kwon, K. C. 2000. Soil carbon sequestration and land-use change: processes and potential, Global Change Biology, 6, 317–327.

Potere, D., Schneider, A., 2007. A critical look at representations of urban areas in global maps GeoJournal 69, 55–80.

Potter, C. S., Matson, P. A., Vitousek, P. M., and Davidson, E. A. 1996. Process modeling of controls on nitrogen trace gas emissions from soils worldwide*. J. Geophys. Res.,* 101, 1361–1377.

Powers, J.S., Corre, M.D., Twine, T.E. and E. Veldkamp. 2011. Geographic bias of field observations of soil carbon stocks with tropical land-use changes precludes spatial extrapolation. Proceedings of the National Academy of Sciences, 108:6318–22.

Pradhan, D. 1994. Primary production and phytosociology of a grassland community of Bhubaneswar. Ph.D. Thesis, Berhampur University, Berhampur, Orissa.

Prasad, A.K., Sarkar, S., Singh, R.P. and Kafatos, M., 2007a. Inter-annual variability of vegetation cover and rainfall over India. Advances in Space Research, 39(1), 79-87.

Prasad, B. and Sinha, S. K. 2000. Long-Term Effects of Fertil- izers and Organic Manures on Crop Yields, Nutrient Balance, and Soil Properties in Rice-Wheat Cropping System in Bihar. In: I. P. Abrol, K. F. Bronson, J. M. Duxbury and R. K. Gupta, Eds., Long-Term Soil Fertility Experiments in Rice-Wheat Cropping Systems. Rice-Wheat Consortium Paper Series 6, Rice-Wheat Consortium for the Indo-Gangetic Plains, New Delhi, 2000, pp. 105-119.

Prasad, K.G., Singh, S.B., Gupta, G.N. and George, M. 1985. Studies on changes in soil properties under different vegetations. Indian Forester, 111 (10), 794–801

Prasad, V.K., K.V.S. Badarinath, and A. Eaturu. 2007b. Spatial patterns of vegetation phenology metrics and related climatic controls of eight contrasting forest types in India—Analysis from remote sensing datasets. Theor. Appl. Climatol. 89:95–107. doi:10.1007/s00704-006-0255-3

Prinn, R., D. Cunnold, R. Rasmussen, P. Simmonds, F. Alyea, A. Crawford, P. Fraser, and R. Rosen. 1990. Atmospheric emissions and trends of nitrous oxide deduced

from 10 years of ALE–GAGE data. Journal of Geophysical Research—Atmospheres 95(11):18369–18385.

Raina, A.K., Jha, M.N. and Pharsi, S.C. 1999. Morphology, mineralogy, genesis and classification of soils of Garhwal Himalayas developed on different parent materials. Annu. For., 7 (2), 269–276

Ramankutty, N. and Foley, J.A., 1999. Estimating historical changes in global land cover: Croplands from 1700 to 1992. Global Biogeochemical Cycles, 13(4), 997-1027.

Ramankutty, N., Evan, A.T., Monfreda C, and Foley, J.A. 2008. Farming the planet: 1. Geographic distribution of global agricultural lands in the year 2000. Global Biogeochemical Cycles, 22, GB1003. doi:10.1029/2007GB002952.

Ravindranath, N.H. Somashekhar, B.S. and M. Gadgil, 1997. Carbon flows in Indian forests Climatic Change, 35: 297–320.

Reddy, C.S., Jha, C.S., and Dadhwal, V.K., 2013. Assessment and monitoring of long-term forest cover changes in Odisha, India using remote sensing and GIS. Environment Monitoring and Assessment, 185(5): 4399-4415.

Reddy, K.S., Singh, M. and Swarup, A. 2002. Sulfur mineralization in two soils amended with organic manures, crop residues, and green manures. J. Plant Nutr. Soil Sci. 165:167–171. doi:10.1002/1522-2624(200204)165:2<167::AID-JPLN167>3.0.CO;2-1

Regmi, A.P., J.K. Ladha, H. Pathak, E. Pasuquin, C. Bueno, D. Dawe, P. R. Hobbs, D. Joshy, S. L. Maskey and S. P. Pandey . 2002. Analyses of yield and soil fertility trends in a 20-year rice–rice–wheat experiment in Nepal. Soil Sci. Soc. Am. J. 66:857–867. doi:10.2136/sssaj2002.8570

Regnier, P., P. Friedlingstein, P. Ciais, F.T. Mackenzie, et al. 2013. Anthropogenic perturbation of the carbon fluxes from land to ocean. Nat. Geosci. 6:597–607. doi:10.1038/ngeo1830

Reich P.B. 1987. Quantifying plant response to ozone: a unifying theory. Tree Physiology, 3, 63–91.

Reich, P. B., M. B. Walters, and D. S. Ellsworth. 1997. From tropics to tundra: global convergence in plant functioning. Proceedings of the National Academy of Sciences (USA), 94: 13730–13734.

Reich, P.B. & Oleksyn, J. 2004. Global patterns of plant leaf N and P in relation to temperature and latitude. Proceedings of the National Academy of Sciences of the United States of America, 101, 11001–11006

Ren W., Tian H.Q., Tao B., Huang Y. and Pan S.F. 2012. China's crop productivity and soil carbon storage as influenced by multifactor global change. Global Change Biology 18: 2945-2957.

Ren, W., Tian, H., Tao, B., Chappelka, A., Sun, G., Lu, C., Liu, M., Chen, G. and Xu, X. 2011. Impacts of tropospheric ozone and climate change on net primary productivity and net carbon exchange of China's forest ecosystems. Global Ecology and Biogeography 20: 391-406.

Richards, J. F. and Flint, E. P., 1994. Historic Land Use and Carbon Estimates for South and Southeast Asia 1880-1980, in Daniel, R. C. (ed.), ORNL/CDIAC-61, NDP-046, Oak Ridge National Laboratory, Tennessee, U.S.A., 326 pp

Ridgwell, A. J., Marshall, S. J., and Gregson, K. 1999. Consumption of atmospheric methane by soils: a process-based model, Global Biogeochem. Cy., 13, 59-70.

Rigby, M., et al. 2008. Renewed growth of atmospheric methane, Geophys. Res. Lett., 35, L22805, doi:10.1029/2008GL036037

Rudrappa, L., T.J. Purakayastha, D. Singh, et al. 2006. Long-term manuring and fertilization effects on soil organic carbon pools in a Typic Haplustept of semi-arid sub-tropical India. Soil Tillage Res. 88:180–192. doi:10.1016/j.still.2005.05.008

Saikawa, E., C. A. Schlosser, and R. G. Prinn. 2013.Global modeling of soil nitrous oxide emissions from natural processes. Global Biogeochemical Cycles 27(3):972–989.

Samra, J.S., Banerjee, S.P. and Singhal, R.M. 1985. Classification of soil biosequences in relation to vegetation I Bijnor plantation division (UP). Indian Forester, 111 (7), 525–531

Scharlemann, J.P.W., E.V.J. Tanner, H. Roland, and K. Valerie. 2014. Global soil carbon: Understanding and managing the largest terrestrial carbon pool. Carbon Management 5:81–91. doi:10.4155/cmt.13.77

Schlesinger, W.H. 1983. The world carbon pool in soil organic matter: A source of atmospheric carbon dioxide In: G.M. Woodwell, editor, The role of terrestrial vegetation in the global carbon cycle measurements by remote sensing. SCOPE, John Wiley & Sons, New York. p. 111–127.

Schulze, E. D., Ciais, P., Luyssaert, S., Schrumpf, M., Janssens, I. A., Thiruchittampalam, B., Theloke, J., Saurat, M., Bringeze, S., Lelieveld, J., Lohila, A., Rebmann, C., Jung, M., Bastviken, D., Abril, G., Grassi, G., Leip, A., Freibauer, A., Kutsch, W., Don, A., Nieschulze, J., Borner, A., Gash, J. H., and

Dolman, A. J. 2010. The European carbon balance, Part 4: Integration of carbon and other trace-gas fluxes, Glob. Change Biol., 16, 1451–1469.

Scurlock, J. M. O., W. Cramer, R. J. Olson, W. J. Parton, and S. D. Prince. 1999. Terrestrial NPP: toward a consistent data set for global model evaluation. Ecological Applications 9: 913–919.

Shang, Q.Y., Yang, X.X., Gao, C.M. et al. 2011. Net annual global warming potential and greenhouse gas intensity in Chinese double rice-cropping systems: a 3-year field measurement in long-term fertilizer experiments. Global Change Biology, 17, 2196– 2210.

Shankar, U., Pandey, H.N., & Tripathi, R. S. 1993. Phytomass dynamics and primary productivity in human grasslands along altitudinal and rainfall gradients. Acta Ecologica, 14 (2), 197–209.

Sharma SK, Choudhury A, Sarkar P, Biswas S, Singh A, Dadhich PK, *et al.,* 2011. Greenhouse gas inventory estimates for India. *Current Science*, 101(3):405.

Sharma, K.L., U.K. Mandal, K. Srinivasa, et al. 2005. Long-term soil management effects on crop yields and soil quality in a dryland Alfisol. Soil Tillage Res. 83:246–259. doi:10.1016/j.still.2004.08.002

Singh R.P., Rovshan S., Goroshi S.K., Panigrahy S. and Parihar J.S. 2011. Spatial and Temporal Variability of Net Primary Productivity (NPP) over Terrestrial Biosphere of India Using NOAA-AVHRR Based GloPEM Model. Journal of the Indian Society of Remote Sensing 39: 345-353.

Singh, J. and Borah, I.P. 1995. A Boruah Soil characteristics under three different plant communities of northeast India. Indian Forester, 121 (12), 1130–1134.

Singh, J. S. and Yadava, P. S. 1974. Seasonal variation in composition, plant biomass and net primary productivity of a tropical grassland at kurukshetra, India. Ecol. Monogr. 44: 351 - 376.

Singh, J., Borah, I.P. and A. Baruah, 1995. A Boruah Soil characteristics under three different plant communities of northeast India. Indian Forester, 121 (12), 1130–1134.

Singh, O.P. and Datta, B. 1983. Characteristics of some hill soils of Mizoram in relation to altitude. J. Indian Soc. Soil Sci., 31, 657–661.

Singh, O.P., Datta, B. and Rao, C.N. 1991. Pedochemical characterisation and genesis of soils in relation to altitude in Mizoram. J. Indian Soc. Soil Sci., 39, 739–750

Six, J., R.T. Conant, E.A. Paul, and K. Paustian. 2002. Stabilization mechanisms of soil organic matter: Implications for C-saturation of soils. Plant Soil 241:155–176. doi:10.1023/A:1016125726789

Srivastava, R. Gaikwad, S.T. Ram, J. 1991. Characteristics and classification of some forest soils of Chandrapur district of Maharashtra. Van Vigyan, 29 (4), 234–238

Stehfest, E., and Bouwman, L., (2006). N2O and NO emission from agricultural fields and soils under natural vegetation: Summarizing available measurement data and modeling of global annual emissions. *Nutrient Cycling in Agroecosystems*, 74(3):207–228.

Sterner, R. W., and J. J. Elser. 2003. Ecological stoichiometry: the biology of elements from molecules to the biosphere. Princeton University Press, Princeton, New Jersey, USA.

Still, C.J., Berry, J.A., Collatz, G.J., DeFries, R.S., 2003. Global distribution of C3 and C4 vegetation: carbon cycle implications. Global Biogeochemical Cycles 17. http://dx.doi.org/10.1029/2001GB001807.

Sudhira, H.S. and Gururaja, K.V., 2012. Population crunch in India: is it urban or still rural? Current Science, 103(1), 37-40.

Tamgadge, D.B., Gaikwad, S.T., Gajbhiye, K.S. and Gaikwad, M.S. 2000. Soil landform relationship of granite/gneissic terrain in Deccan plateau, Satpura range, Madhya Pradesh. J. Indian Soc. Soil Sci., 48 (3), 567–571.

Tao, B., H. Tian, G. Chen, W. Ren, C. Lu, K.D. Alley, X. Xu, M. Liu, S. Pan, and H. Virji. 2013. Terrestrial carbon balance in tropical Asia: Contribution from cropland expansion and land management. Global Planet. Change 100:85–98. doi:10.1016/j.gloplacha.2012.09.006

Thornley J.H.M. and Cannell M.G.R. 2000. Modelling the components of plant respiration: representation and realism. Annals of Botany, 85, 55–67.

Thornton P.E. and Rosenbloom N.A. 2005. Ecosystem model spin-up: Estimating steady state conditions in a coupled terrestrial carbon and nitrogen cycle model. Ecological Modelling 189: 25-48.

Tian H, Melillo J, Lu C, et al. 2011b. China's terrestrial carbon balance: Contributions from multiple global change factors. Global Biogeochemical Cycles, 25, GB1007.

Tian, H., C. Lu, J. Melillo, et al. 2012. Food benefit and climate warming potential induced by nitrogen fertilizer uses in China. Environ. Res. Lett. 10.1088/1748-9326/7/4/044020.

Tian, H., G. Chen, C. Lu, X. Xu, W. Ren, B. Zhang, K. Banger, B. Tao, S. Pan, M. Liu, C. Zhang, L. Bruhwiler, and S. Wofsy. 2015. Global methane and nitrous oxide emissions from terrestrial ecosystems due to multiple environmental changes. Ecosystem Health and Sustainability 1:art4. doi:10.1890/EHS14-0015.1

Tian, H., G. Chen, C. Lu, X. Xu, W. Ren, K. Banger, B. Zhang, B. Tao, S. Pan, M. Liu, and C. Zhang. 2013. Global land-atmosphere exchange of methane and nitrous oxide: magnitude and spatiotemporal patterns. Biogeosciences Discussion 10: 19811-19865, doi:10.5194/bgd-10-19811-2013

Tian, H., J. M. Melillo, D. W. Kicklighter, A. D. McGuire, J. V. K. Helfrich III, B. Moore III and C. J. Vörösmarty CJ 1998. Effect of interannual climate variability on carbon storage in Amazonian ecosystems. Nature 396(6712), 664-667, doi: 10.1038/25328.

Tian, H., J. Melillo, D. Kicklighter, S. Pan, J. Liu, A.D. McGuire, and B. Moore, III. 2003. Regional carbon dynamics in monsoon Asia and its implications to the global carbon cycle. Global Planet. Change 37:201–217.

Tian, H., Lu, C., Chen, G., Xu, X., Liu, M., Ren, W., Tao, B., Sun, G., Pan, S., and Liu, J. 2011. Climate and land use controls over terrestrial water use efficiency in Monsoon Asia, Ecohydrology, 4, 322–340.

Tian, H., Melillo, J.M., Kicklighter, D.W., McGuire, A.D., Helfrich, J., Moore, B., Vorosmarty, C.J. 2000. Climatic and biotic controls on annual carbon storage in Amazonian ecosystems. Global Ecology and Biogeography, 9, 315–335.

Tian, H.Q. et al., 2012a. Century-Scale Responses of Ecosystem Carbon Storage and Flux to Multiple Environmental Changes in the Southern United States. Ecosystems, 15(4), 674-694.

Tian, H.Q., K. Banger, B. Tao, and V.K. Dadhwal. 2014. History of land use in India during 1880–2010: Large-scale land transformations reconstructed from satellite data and historical archives. Global Planet. Change 10.1016/j.gloplacha.2014.07.005.

Tian, H.Q., Xu, X.F., Liu, M.L., *et al.,* 2010. Spatial and temporal patterns of CH4 and N2O fluxes in terrestrial ecosystems of North America during 1979–2008: application of a global biogeochemistry model. *Biogeosciences,* 7: 2673–94.

Tian, H.Q., Xu, X.F., Lu, C.Q., Liu, M.L., Ren, W., Chen, G.S., Melillo, J., and Liu, J.Y., 2011a. Net exchanges of CO(2), CH(4), and N(2)O between China's terrestrial ecosystems and the atmosphere and their contributions to global climate warming. J. Geophys. Res. 116: G02011. doi:10.1029/2010JG001393.

Tjoelker M.G., Volin J.C., Oleksyn J., Reich P.B. 1995. Interaction of ozone pollution and light effects on photosynthesis in a forest canopy experiment. Plant Cell and Environment, 18, 895–905.

Totey, N.G., Singh, A.K., Bhowmik, A.K. and Khatri, P.K. 1986. Effect of forest covers on physico-chemical properties of soils developed on sandstone. Indian Forester, 112 (4), 314–327

Townsend ,A.R., Cleveland, C.C., Houlton, B.Z., Alden, C.B., White, J.W. 2011. Multi-element regulation of the tropical forest carbon cycle. Frontiers in Ecology and the Environment, 9, 9–17.

Townsend, A.R., Cleveland, C.C., Asner, G.P., and Bustamante, M.M.C. 2007. Controls over foliar N:P ratios in tropical rain forests. Ecology 88: 107–18.

Tripathi S.C. 2010. Behavior of spring wheat genotypes under late and very late situations in northwestern India. Annual Wheat Newsletter, 56, 65-67.

Turner, D.P., Ritts, W.D., Cohen, W.B., Gower, S.T., Running, S.W., Zhao, M., Costa, M.H., Kirschbaum, A.A., Ham, J.M., Saleska, S.R. & Ahl, D.E. 2006. Evaluation of MODIS NPP and GPP products across multiple biomes. Remote Sensing of Environment, 102, 282–292.

U.S. EPA. 2010. Methane and nitrous oxide emissions from natural sources. U.S. Environmental Protection Agency, Washington, D.C., USA. http://www.epa.gov/methane/sources.html.

UNEP, 2009. The forest in Southeast Asia. Vital forest graphics, p. 42.

Vanaja M, Yadav SK, Archana G et al. 2011. Response of C4 (Maize) and C3 (sunflower) crop plants to drought stress and enhanced carbon dioxide concentration.Plant Soil and Environment, 57, 207–215.

Varshney, C. K. 1972. Productivity of Delhi grasslands. In : Tropical Ecology with an emphasis on organic production, P. M. Golley and F.B. Golley (Eds.), Univ. of Georgia, Athens. pp. 27- 42.

Velayutham, M., D.K. Pal, and T. Bhattacharyya. 2000. Organic carbon stock in soils of India In: Global climate change and tropical ecosystems. CRC/Lewis Publishers, Boca Raton, FL. pp. 71-95.

Velmurugan, A., S. Kumar, V.K. Dadhwal, and M.K. Gupta. 2014. Soil organic carbon status of Indian Forests. The Indian Forester 140:468–477.

Verburg, P.H., Newmann, K. and Nol, L., 2011. Challenges in using land use and land cover data for global change studies. Global Change Biology, 17, 974–989.

Verburg, P.H., Veldkamp, A. and Fresco, L.O., 1999. Simulation of changes in the spatial pattern of land use in China. Applied Geography, 19(3), 211-233.

Verma, K.S. Shyampura, R.L. and Jain, S.P. 1990. Characterisation of Soils under forest of Kashmir Valley. J. Indian Soc. Soil Sci., 38, 107–115

Vineela, C., S.P. Wani, C. Srinivasarao, et al. 2008. Microbial properties of soils as affected by cropping and nutrient management practices in several long term manural experiments in the semi-arid tropics of India. Appl. Soil Ecol. 40:165–173. doi:10.1016/j.apsoil.2008.04.001

Vingarzan R. 2004. A review of surface ozone background levels and trends. Atmospheric Environment 38: 3431-3442.

Vitousek, P. and Farrington, H. 1997. Nutrient limitation and soil development: experimental test of a biogeochemical theory. *Biogeochemistry,* 37, 63–75.

Vitousek, P. M. 1984. Litterfall, nutrient cycling, and nutrient limitations in tropical forests. Ecology 65:285–298.

Vitousek, P.M. & Howarth, R.W. 1991. Nitrogen limitation on land and in the sea – how can it occur? Biogeochemistry, 13, 87–115.

Vitousek, P.M. 2012. Litterfall, Nutrient Cycling , and Nutrient Limitation in Tropical Forests Author (s): Peter M . Vitousek Reviewed work (s): Published by : Ecological Society of America Stable URL : http://www.jstor.org/stable/1939481 . LITTERFALL , NUTRIENT CYCLING. 65, 285–298.

Walker, T.W., and Syers, J.K.1976. The fate of phosphorus during pedogenesis. Geoderma, 15, 1–19.

Wang, Y. P, and Houlton B.Z. 2009. Nitrogen constraints on terrestrial carbon uptake: Implications for the global carbon-climate feedback. Geophysical Research Letters, 36, L24403.

Wang, Y. P., Houlton, B. Z., and Field, C. B. 2007. A model of biogeochemical cycles of carbon, nitrogen, and phosphorus including symbiotic nitrogen fixation and phosphatase production, Global Biogeochem. Cy., 21, GB1018, doi:10.1029/2006gb002797.

Wei, Y., S. Liu, D.N. Huntzinger, A.M. Michalak, N. Viovy, W.M. Post, C.R. Schwalm, K. Schaefer, A. R. Jacobson, C. Lu, H. Tian, D. M. Ricciuto, R. B. Cook, J. Mao, and X. Shi. 2014. The North American Carbon Program Multi-scale Synthesis and Terrestrial Model Intercomparison Project—Part 2: Environmental driver data. Geoscientific Model Develop. 7:2875–2893. doi:10.5194/gmd-7-2875-2014

Williams, J.R, and Berndt, H.D. 1977. Sediment Yield Prediction Based on Watershed Hydrology. American Society of Agricultural Engineers, 20, 1100–1104.

Williams, M.A., Rice, C.W., C.E. Owensby, 2000. Carbon dynamics and microbial activity in tallgrass prairie exposed to elevated CO2 for 8 years. Plant and Soil, 227, 127–137.

Willison, T. W., Coulding, K. W. T., and Powlson, D. S. 1995. Effect of land-use change and methane mixing ratio on methane uptake from United Kingdom soil, Glob. Change Biol., 1, 209-212.

Wright SJ (2005) Tropical forests in a changing environment. Trends in ecology & evolution, 20, 553–60.

Wright, S. J., Yavitt, J. B., Wurzburger, N., Turner, B. L., Tanner, E. V., Sayer, E. J., Santiago, L. S., Kaspari, M., Hedin, L. O., and Harms, K. E. 2011. Potassium, phosphorus, or nitrogen limit root allocation, tree growth, or litter production in a lowland tropical forest, Ecology, 92, 1616–1625.

Xu, X., H. Tian, M. Liu, W. Ren, G. Chen, C. Lu and C. Zhang. 2012. Multiple-factor controls on terrestrial N2O flux over North America. *Biogeosciences,* 9, 1351-1366. doi:10.5194/bg-9-1351-2012

Xu, X., Tian, H., and Hui, D. 2008. Convergence in the relationship of CO2 and N2O exchanges between soil and atmosphere within terrestrial ecosystems, Glob. Change Biol., 14, 1651-1660, DOI10.1111/j.1365-2486.2008.01595.x.

Yadav, J.S.P. and Sharma, D.R. 1968. A soil investigation with reference to sal and teak in Madhya Pradesh. Indian Forester, 94, 890–897

Yadav, R.L., B.S. Dwivedi, K. Prasad,O.K Tomar, N.J Shurpali, and P.S Pandey. 2000. Yield trends, and changes in soil organic-C and available NPK in a long-term rice–wheat system under integrate use of manures and fertilisers. Field Crops Res. 68:219–246. doi:10.1016/S0378-4290(00)00126-X

Yaduvanshi, N.P.S., and A. Swarup. 2005. Effect of continuous use of sodic irrigation water with and without gypsum, farmyard manure, press mud and fertilizer on soil properties and yields of rice and wheat in a long term experiment. Nutr. Cycling Agroecosyst. 73:111–118. doi:10.1007/s10705-005-3361-1

Yan, X., H. Akimoto, and Ohara, T. 2003. Estimation of nitrous oxide, nitric oxide and ammonia emissions from croplands in East, Southeast and South Asia. *Global Change Biol.,* 9, 1080 – 1096.

Yan, X.Y., Yagi, K., Akiyama, H. and Akimoto, H. 2005. Statistical analysis of the major variables controlling methane emission from rice fields. Global Change Biology, 11, 1131–1141.

Yang, X. and Post, W.M. 2011. Phosphorus transformations as a function of pedogenesis: a synthesis of soil phosphorus data using Hedley fractionation method. Biogeosciences Discussions, 8, 5907–5934.

Yang, X. Thornton, P. E. Ricciuto, D. M. and Post, W. M. 2014. The role of phosphorus dynamics in tropical forests – a modeling study using CLM-CNP. Biogeosciences, 11, 1667–1681. doi:10.5194/bg-11-1667-2014.

Zaidi P.H. and Singh N.N. 2005. Directorate of Maize Research, New Delhi, pp. 1-145.

Zee, V. D., and Riemsdijk, W.H. V. 1988. Model for Long-term Phosphate Reaction Kinetics in Soil. Journal of Environment Quality, 17, 35–41.

Zhang, H. F., Chen, B. Z., van der Laan-Luijk, I. T., Machida, T., Matsueda, H., Sawa, Y., Fukuyama, Y., Langenfelds, R., van der Schoot, M., Xu, G., Yan, J. W., Cheng, M. L., Zhou, L. X., Tans, P. P., and Peters, W. 2014. Estimating Asian terrestrial carbon fluxes from CONTRAIL aircraft and surface CO2 observations for the period 2006–2010. Atmos. Chem. Phys., 14, 5807-5824, doi:10.5194/acp-14-5807-2014.

Zhang, L. H., Song, C. C., Zheng, X. H., Wang, D. X., and Wang, Y. Y. 2007. Effects of nitrogen on the ecosystem respiration, CH4 and N2O emissions to the atmosphere from the freshwater marshes in northeast China. *Environ. Geol.,* 52, 529–539, doi:10.1007/s00254-006-0485-9.

Zhu, Q. Riley, W. J. Tang, J. and Koven, C. D. 2015. Multiple soil nutrient competition between plants, microbes, and mineral surfaces: model development, parameterization, and example applications in several tropical forests. Biogeosciences Discuss., 12, 4057–4106. doi:10.5194/bgd-12-4057-2015.

Ziska, L.H., J.A. Bunce, and F.A. Caulfield. 1998. Intraspecific variation in seed yield of soybean (Glycine max) in response to increased atmospheric carbon dioxide. Aust. J. Plant Physiol. 25:801–807.